EVALUATION OF THE CO-IMMOBILIZATION OF L-LYSINE α-OXIDASE AND CATALASE IN A HOLLOW FIBER REACTOR SYSTEM

By

Steven R. Reiken

A THESIS

Submitted to
Michigan State University
in partial fulfilment of the requirements
for the degree of

MASTER OF SCIENCE

DEPARTMENT OF CHEMICAL ENGINEERING

1988

ABSTRACT

EVALUATION OF THE CO-IMMOBILIZATION OF
L-LYSINE α-OXIDASE AND CATALASE IN A
HOLLOW FIBER REACTOR SYSTEM

By

Steven R. Reiken

This work was undertaken to evaluate the use of L-lysine α-oxidase in a hollow fiber reactor as a clinical technique for the treatment of leukemia. The basis of the technique is the enzymatic removal of amino acids required for tumor cell metabolism from leukemic blood. Catalase was co-immobilized with the oxidase to remove the reaction product hydrogen peroxide. The enzymes were backflush loaded into single fiber reactors (SFRs) constructed of polyamide asymmetric ultrafiltration fibers. Under optimum conditions of flow rate, enzyme loading, and reactor length, the effectiveness factor observed indicated approach to a diffusion controlled regime. To counteract this, pulsatile flow was tested and yielded a 15 to 30% increase in conversion over that of normal flow. Almost 85% of the lysine could be converted using a hollow fiber cartridge under pulsatile flow conditions. The intrinsic immobilized kinetic parameters for L-lysine α-oxidase were determined to be K_m = 7.0 mM and k = 320.0 min^{-1}. These kinetics were used to successfully scale up to the bench scale from SFR performance data.

To my parents and grandparents for their unrelenting support which make my accomplishments possible.

ACKNOWLEDGEMENTS

I thank Dr. Daina Briedis for her guidance and support in my research and preparation of this thesis.

TABLE OF CONTENTS

LIST OF TABLES

LIST OF FIGURES

CHAPTER 1

INTRODUCTION

The overall objective of the research conducted for this thesis was to develop an immobilized enzyme blood dialyzer/reactor as a clinical tool in cancer therapies. Leukemic blood cells demonstrate high levels of amino acid metabolism relative to that of normal cells. Therefore, short periods of depletion of key amino acids from blood should cause a more significant mortality of leukemic cells. It has been proposed to perform the depletion enzymatically. Injection therapy has the problems of nonrecovery of expensive enzymes and (negative) immune response to the foreign protein in the patient. It was for this reason that an enzyme immobilization technique involving enzyme entrapment within the void space of the porous region of asymmetric hollow fiber membranes was investigated. The specific enzyme/substrate system studied was L-lysine α-oxidase and L-lysine.

The description of the work conducted in this thesis is divided into the following chapters:

Chapter 1- Introduction

Chapter 2- Background

Chapter 3- Analytical Techniques

Chapter 4- Enzyme Kinetics

Chapter 5- Enzyme Retention

Chapter 6- Reactor Operation

Chapter 7- Scale-up

Chapter 8- Conclusions and Recommendations

The background chapter discusses the motivation for the research. A literature review on amino acid metabolism in both healthy and leukemic blood cells is presented. In addition, several enzymes are mentioned for their potential use in cancer therapies, and the reasons for choosing L-lysine α-oxidase are explained. Finally, several models for the hollow fiber reactor are discussed in detail.

Chapter 3 describes the analytical techniques that were necessary to evaluate the performance of the reactor. Methods for the determination of the total protein content, lysine concentration, hydrogen peroxide concentration, and enzyme activity in a given sample are discussed in this section.

In order that the kinetics of the immobilized L-lysine α-oxidase be directly evaluated and compared to the free solution enzyme kinetics given in Chapter 4, single fiber reactors (SFRs) were constructed and tested. SFRs consist of a single hollow fiber encased in a small glass tube with inlet and outlet ports (see Chapter 5). The fiber materials available for testing were polysulfone and polyamide, each at 10,000 and 30,000 molecular weight cutoffs. These hollow fibers consist of an ultrathin inner membrane surrounded by a porous "sponge-like" annular section which is approximately 80 to 90% void (Figure 3, Chapter 2). The ultrathin inner membrane is impermeable to macromolecular species, such as proteins, but not to species below the molecular weight cutoff of the membrane.

Catalase was co-immobilized with L-lysine α-oxidase to remove hydrogen peroxide, a product of the lysine oxidation reaction, from the porous region. Hydrogen peroxide is known to have a cytotoxic effect on blood cells [1] and should therefore be prevented from diffusing into a patient's blood. An additional benefit of the catalase reaction is that

it generates oxygen which may be the limiting reactant for the L-lysine α-oxidase reaction.

The backflush technique for enzyme loading was chosen as the best method for achieving high immobilized enzyme concentrations within the porous region of the hollow fiber. Enzyme retention studies (Chapter 5) indicated that the PA10 (polyamide, 10,000 MW cutoff) fibers were best suited for the immobilization of lysine α-oxidase in the SFR. These fibers were able to retain approximately 85% of the enzyme loaded and had no negative effects on the activity of the enzyme. In addition, the fiber demonstrated no enzyme leakage across the membrane under pressurized flow.

As described in Chapter 2, the basis of SFR operation is to pump substrate solution through the lumen (Figure 3, Chapter 2); the substrate then diffuses through the ultrathin memebrane into the porous region where it reacts to form products, which diffuse back into the lumen. Factorial design logic was used to determine which variables were important in the performance of the single fiber reactor. Factorial design is a statistical technique that allows differentiation between random changes in the performance variable (lysine conversion) and changes caused by specific operating parameters. It was found from this method that the most significant effects on conversion were due to changes in flow rate, the amount of lysine α-oxidase loaded within the hollow fiber, the catalase/oxidase loading ratio, and the reactor length. Further studies showed that the optimum SFR operating conditions were a flow rate of 9 ml/min, 3.97 units of lysine α-oxidase per cm^2 of the fiber's surface area, a catalase to oxidase loading ratio of 2.5:1, and a reactor length of 44.0 cm. Under these conditions, 34.8% of the lysine was converted in four hours of reactor operation.

The diffusion of lysine within the SFR and the intrinsic immobilized kinetics of lysine α-oxidase are discussed in Chapter 6. The evaluation of these kinetics was accomplished by collecting reactor data over a 48 hour period and fitting the unknown kinetic parameters to an appropriate model using the Patern subroutine (see Appendix). These parameters were then used to show that the effectiveness factor (Chapter 6) was approximately 0.65 for the SFR. This indicated that under normal operating conditions, 65% of the enzyme's intrisic immobilized solution kinetics were achieved by the immobilization.

Some limitation in conversion was caused by the diffusion of substrate through the fiber wall to the enzyme. It has been reported that an induced transmembrane pressure drop can be used to force the lysine through the fiber and virtually remove diffusion limitations. The pressure drop, created by a pulsed inlet flow, caused a 15% increase in conversion of lysine under optimum SFR conditions to a final conversion of 40% within four hours.

In Chapter 7, the scale up of SFR results to hollow fiber cartridge design is described. Area was chosen as the design parameter on which to scale up the single fiber reactor. A hollow fiber cartridge consisting of approximately 60 hollow fibers arranged in parallel replaced the SFR in the reactor system. It was found that the cartridge gave slightly lower conversions than predicted using SFR data. This may be due to the SFR model assumption of perfectly distributed enzyme within the fibers of the cartridge. Approximately 85% of the lysine was converted within four hours of cartridge operation. The ability to remove this much lysine from the plasma of patients would have a positive effect in the treatment of leukemia.

As mentioned above, the main objective of this thesis was to develop an immobilized enzyme reactor for clinical use in cancer therapies. The results of the experiments described in the following chapters indicate a good potential for achieving this goal; however, further experiments are needed. The performance of the hollow fiber reactor using whole blood instead of buffer as the substrate solution must be evaluated. It is also hoped that future work may be conducted in conjunction with with the Department of Animal Science of the College of Veterinary Medicine at Michigan State University to allow in vivo testing of the hollow fiber cartridge.

CHAPTER 2

BACKGROUND

Leukocytes and Amino Acid Metabolism

Amino acids serve two major functions in living cells, participation in 1) protein synthesis and 2) intermediary cell metabolism [2]. The relationship between the intra- and extracellular amino acid pool is maintained by transport mechanisms that vary for each individual amino acid and each type of cell. Leukocytes are considered metabolically active cells that possess their own transport mechanisms. These transport mechanisms are particularly important in the various leukemic cells that have an abnormal proliferative capacity and compete actively with the normal cells of the body to maintain their metabolic requirements. Most of the research concerning the relationship between amino acids and leukocytes (normal and leukemic) has focussed on the nutritional requirements of the cells and the content of free amino acids within the cells [2-4]. Exogenous amino acids have been shown to be nutritional requirements for certain types of leukemic cells. This requirement is the result of either a failure of the cell to synthesize the amino acid in an amount needed for the maintenance of normal metabolism [3,4] or an increased demand for certain amino acids necessary for protein synthesis. A higher rate of incorporation of various amino acids into proteins by leukemic or malignant leukocytes than by normal leukocytes has been previously reported [2,5,6]. The content of free amino acids in normal and leukemic leukocytes has also been investigated [7-9], and the concentration of certain amino acids is listed in Table 1.

Table 1
Concentration of Free Amino Acids in Plasma of Normal and Leukemic Patients

Amino acid	Normal concentration(mM)	Leukemic concentration(mM)
Phenylalanine	0.063	0.076
Methionine	0.026	0.026
Threonine	0.186	0.189
Arginine	0.080	0.073
Tyrosine	0.081	0.081
Lysine	0.236	0.247

Since various studies have shown that specific amino acids are required for the optimal growth of malignant versus normal cells [2,7,10], it is believed that the depletion of selected amino acids can abrogate tumor growth. Dietary restrictions that reduce amino acid levels over the long term have proven to be unsuccessful [11]. Recently, several enzymes that degrade essential amino acids have been shown to depress tumor growth. Phenylalanine ammonia-lyase from *Rhodotorula glutinis* inhibits both growth of murine (mouse) and human leukemic cells in vitro [12] and growth of L5178Y mouse leukemia in vivo [13]. Kreis et al. reported that methionine γ-lyase from *Clostridium sporogenes* causes inhibition of the growth of P815 and L1210 cells in vitro [5]. Threonine deaminase from sheep liver, which catalyzes the irreversible α,β-elimination of L-threonine, was shown to inhibit mouse leukemia cells [14]. Finally, Kusakabe et al. [10] found that L-lysine α-oxidase, an enzyme that catalyzes the oxidative deamination of L-lysine, demonstrates growth-inhibitory activity against L5178Y mouse leukemic cells.

Enzyme Selection

The clinical use of L-asparaginase [15] has stimulated the search for other enzymatic therapies for neoplastic diseases. Enzyme therapy is principally based on the higher sensitivity of cancer cells to the deprivation

of essential nutrients than that of normal cells. As mentioned above, several enzymes have demonstrated positive effects in inhibiting growth of leukemic cells. This growth-inhibiting effect is related to the enzyme's ability to catalyze the irreversible degradation of an essential amino acid in plasma. The rate at which an enzyme can perform this task depends on its kinetic parameters. Enzyme kinetics are described in more detail in Chapter 4 in which the Michaelis-Menten model is described. In this model, the Michaelis constant (K_m) is a measure of the strength of the enzyme/substrate complex (a low K_m indicates strong binding) and the turnover number is an indication of the catalytic efficiency of the enzyme. The kinetic parameters for several enzymes are listed in Table 2 [10]:

Table 2
Kinetic Constants of Selected Antitumor Enzymes

Enzyme	K_m (mM)	Turnover # (mol/min-mol-enz)
Phenylalanine ammonia-lyase	.25	300
Methionine γ-lyase	78-90	700
Tyrosine phenol lyase	.28	300
Thronine deaminase	8.0	900
Lysine α-oxidase	.04	7200

It is seen that L-lysine α-oxidase has the lowest Michaelis constant and highest catalytic efficiency of the antitumor enzymes that have been studied. In addition, the enzyme substrate, L-lysine, is one of the more concentrated and highly metabolized amino acids in the plasma of leukemic patients [16]. It was for these reasons that L-lysine α-oxidase was chosen as the enzyme for this investigation.

Kodama et al. [17] were the first to isolate and identify the antitumor activity of L-lysine α-oxidase. These authors reported the identification of

the mold strain *Trichoderma viride* Y244-2 and the conditions necessary for the maximum production of the enzyme. The maximum enzyme production of the mold grown on wheat bran was observed after 10 and 14 days of incubation with and without $NaNO_3$, respectively. The addition of $NaNO_3$ to the medium stimulated the production of the enzyme.

The fungal enzyme was designated as L-lysine α-oxidase. It has a molecular weight of 112,000 and was found to catalyze the α-oxidative deamination of L-lysine as follows:

$$\text{L-lysine} + O_2 + H_2O \text{ -------> } \alpha\text{-keto-}\epsilon\text{-aminocaproate} + NH_3 + H_2O_2 \quad (1)$$

$$\downarrow \quad \uparrow \pm H_2O$$

$$\Delta^1\text{-piperidine-2-carboxylate}$$

The effect of L-lysine α-oxidase on the growth of L5178Y mouse leukemic cells was determined in experiments conducted by Kusakabe et al. [10] in which these cells were grown in RPMI 1640 medium containing 10% calf serum [18] in the absence or presence of the enzyme. L-lysine α-oxidase completely inhibited the growth of L5178Y mouse leukemic cells <u>in vitro</u> when measured by trypan blue exclusion [10]; more than 99% of the cells lost viability when incubated with a L-lysine α-oxidase concentration of 10 milliunits (mu) per ml. A unit is defined as the amount of enzyme required to oxidize one μmol of lysine per minute. Furthermore, 1 mu/ml was sufficient to produce 50% inhibition of cell growth. After the addition of enzyme to the medium, the investigators monitored the lysine concentration present. At the dose that caused complete cell growth inhibition, no lysine was detected. In addition, lysine concentration decreased by about 40% when the enzyme caused 50% inhibition of

growth. The authors also showed that the growth of L5178Y cells was depressed about 70% by preincubation of the medium with lysine α-oxidase, and that growth was fully restored by the addition of lysine. These findings show that the growth-inhibitory effect of the enzyme on the cells is at least in part based on a decrease in lysine concentration in the culture medium.

Kusakabe and his colleagues also examined whether the enzymatic reaction products from lysine participated in the cell growth inhibition. L5178Y cells were incubated with 0.5 mM Δ^1-piperidine-2-carboxylate and ammonia in the RPMI 1640 medium for 72 hr. Cell proliferation was not inhibited by either compound. The other reaction product, H_2O_2, inhibited the growth of these cells in culture at a concentration higher than 0.033 mM, and no growth was exhibited at 0.2 mM. This was to be expected; Freese et al. [1] reported that hydrogen peroxide is a cytotoxic chemical that cleaves the sugar-phosphate backbone of DNA sufficiently to cause the inactivation of cell proliferation. If lysine is completely oxidized, the concentration of H_2O_2 will reach 0.22 mM, which is high enough to inhibit the growth of L5178Y cells. It was thus determined that the *in vitro* cytotoxic effect of L-lysine α-oxidase on L5178Y cells is ascribable to a combination of the deprivation of L-lysine from the medium and the action of formed H_2O_2 on the cells.

In vivo studies on the effect that the oxidase enzyme had on mice bearing L1210 leukemia were also conducted by Kusakabe et al. [10]. L1210 cells were inoculated intraperitonally into mice on day 0. The administration of a dose of 70 units/kg-day of L-lysine α-oxidase intraperitonally on days 1 to 5 resulted in an increase in life-span by 34 to 48% over the control animals. The effect of the enzyme on the lysine level in the plasma of the mice was also determined. A single intravenous injection of 30 units/kg reduced the lysine concentration in the plasma from 0.33 mM to an undetectable level after 1 hr, and this depressed lysine level persisted for 12 hr followed by a

gradual increase. The lysine level was almost fully recovered in 24 hr after the injection. These results suggest that there is a correlation between the theraputic effectiveness of the enzyme and the decrease in the concentration of lysine in the plasma of the mice.

Although the above experiments indicate that injection therapy could be effective in the treatment of certain leukemias, there are two main problems inherent in this technique. First, there is no feasible method for the recovery of the injected enzyme from the body. This is both wasteful and extremely expensive. More importantly, as with any foreign protein, the enzyme should trigger an immune response in the patient which might not only lead to negative side-effects, but could affect the long-term effectiveness of the therapy.

Hollow Fiber Immobilization

Physical entrapment of the enzyme in the matrix of the outer layer of asymmetric hollow ultrafiltration (UF) fibers resolves the problems associated with injection therapy. These fibers (Figure 1) consist of a thin semipermeable inner membrane approximately 0.5 microns thick and an outer supporting macroporous spongy layer (approximately 1.0 mm thick). In normal ultrafiltration operation (Figure 2a), the medium to be filtered is pumped through the lumen under pressure. The solvent and other small molecules cross the membrane relatively unimpeded and are forced out the shell-side ports in the ultrafiltrate stream. Larger molecules cannot pass through the membrane and emerge from the lumen through the downstream port in a more concentrated solution. Nominal molecular weight cutoffs of UF membranes range from 3,000 to 500,000 daltons. Membranes are spun from polymers including polysulfones, polyamides, and acrylics.

Waterland et al. [19] demonstrated that enzymes could be immobilized in

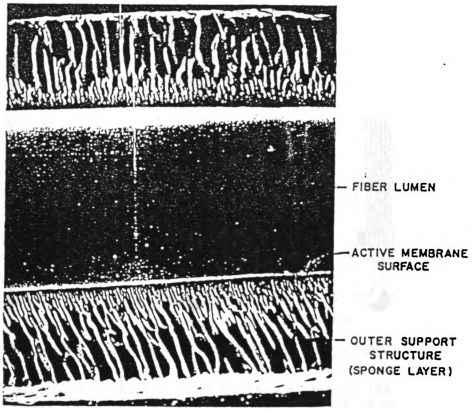

Figure 1: Photomicrographs of a hollow fiber showing the inside active membrane surface and the outer support structure (from [19]).

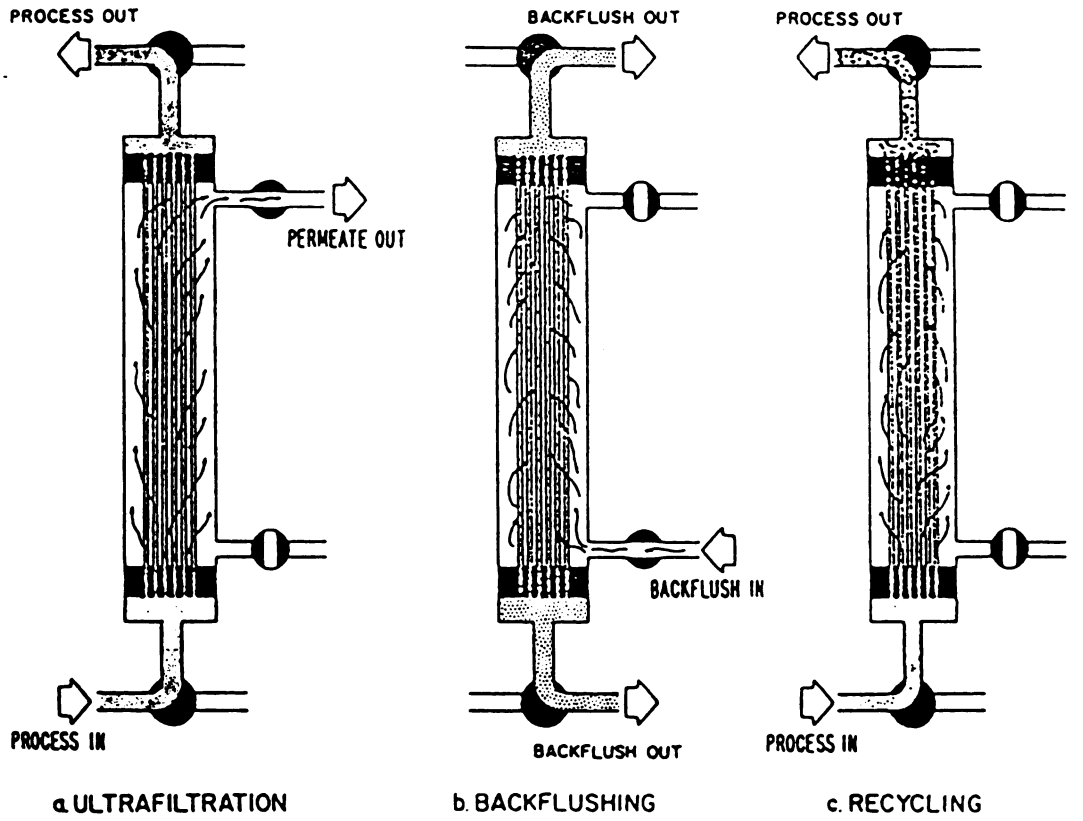

Figure 2: Schematic of hollow fiber cartridge showing the three modes of operation used in system's design (from [19]).

the spongy layer by static loading. In this technique, the shell-side of the cartridge is filled with enzyme solution, and the enzyme diffuses into the spongy layer of the fibers. By repeatedly filling and draining the shell-side with stock enzyme solution, the concentration of enzyme in the spongy layer approaches that of the stock solution.

Breslau and Kilcullen [20] used backflush loading to entrap enzymes within hollow fibers. To backflush load enzyme, pressure is applied to the shell-side, and enzyme stock solution is forced from the shell-side to the lumen-side of the fibers as depicted in Figure 2b. This method achieves significantly higher enzyme concentrations than static loading. After loading, shell-side solutions are drained from the hollow fiber reactor (HFR).

Normal operation of the reactor involves pumping substrate solution through the lumen at low pressure in the recycle mode (Figure 2c). During operation, the shell-side ports are closed, and the shell-side contains no liquid. Substrate is transported from the lumen via diffusion through the membrane and into the spongy layer where it reacts with the enzyme. Products of the reaction then diffuse back across the membrane and exit the reactor in the lumen-side outlet stream.

Advantages of physical immobilization of enzymes in hollow fiber reactors include [21]:

1) quick and easy reactor preparation without chemically altering the enzyme,
2) relatively small effects on the kinetic properties of the enzyme,
3) prevention of microbial access to the enzyme,
4) selectivity of products and substrates through the selectivity of the membrane,
5) large surface area to volume ratio,
6) no enzyme leakage,

7) reuse of the enzyme, and

8) continuous operation at low pressures.

Hollow Fiber Reactor Models

As shown in Figure 3, a hollow fiber is physically divided into three regions; the lumen (region 1), the ultrathin membrane (region 2), and the spongy layer (region 3). Several models have been developed to predict conversions in hollow fiber reactors [22]. The most complete models consider the mass transfer in the three regions, axial flow and radial diffusion in the lumen, radial diffusion across the UF membrane, and radial diffusion and subsequent reaction in the spongy layer. Other mass transport mechanisms including axial diffusion and bulk flow across the membrane due to transmembrane pressure gradients are assumed negligible.

Several investigators have presented models to predict conversions in HFRs using steady state assumptions [23-26]. Using the system conceptualization depicted in Figure 3, it is seen that the mass transfer equation within the lumen can be represented by simple diffusion/convection assuming laminar Newtonian flow and negligible axial diffusion:

Region 1 (lumen):

$$\frac{D_1}{r}\frac{d}{dr}\left[r \frac{dS_1}{dr} \right] = U_0 \left[1 - \frac{r^2}{a^2} \right] \frac{dS_1}{dz} \qquad (2)$$

where the subscripts refer to the particular region of the fiber, D is the substrate diffusivity, S is the substrate concentration, r is the radial dimension, a is the distance from the center of the lumen to the inner surface of the membrane, and z is the axial dimension. $U_z(r)$ is assumed to follow a Poiseuille type radial velocity profile in which U_0 is the center line

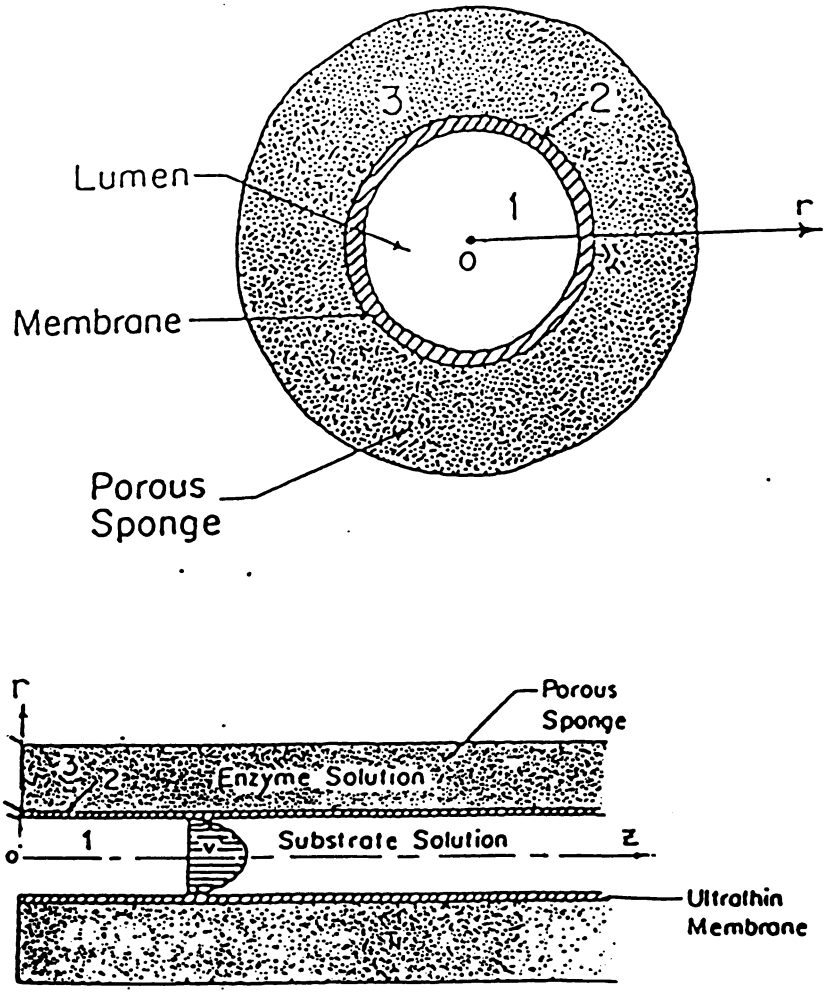

Figure 3: The cylindrical geometry and dimensions of the hollow fiber (from [21]).

velocity. Within the membrane of the hollow fiber, it is assumed that the substrate concentration may be described by a simple diffusion equation:

Region 2 (membrane):

$$\frac{D_2}{r}\frac{d}{dr}\left[r \frac{dS_2}{dr} \right] = 0 \qquad (3)$$

Finally, it is assumed that a simple diffusion/reaction equation governs the substrate concentration within the spongy matrix:

Region 3 (spongy matrix):

$$\frac{D_3}{r}\frac{d}{dr}\left[r \frac{dS_3}{dr} \right] = \frac{V_{max} S_3}{K_m} \qquad (4)$$

where the first-order limit of Michaelis-Menten kinetics have been assumed in which K_m and V_{max} are the Michaelis constant and the maximum attainable reaction rate, respectively.

For hollow fiber reactors, the following initial conditions are usually used:

$$\text{at } t = 0 \qquad \begin{matrix} S_1 = S_0 \\ S_2 = 0 \\ S_3 = 0 \end{matrix} \qquad \text{for all } z \qquad (5)$$

and the boundary conditions are:

$$\text{at } r = o \qquad \frac{dS_1}{dr} = 0 \qquad (6)$$

at r = a
(see Figure 3)

$$D_2 \frac{dS_2}{dr} = D_1 \frac{dS_1}{dr} \tag{7}$$

$$S_1 = \gamma S_2$$

at r = b
(see Figure 3)

$$D_2 \frac{dS_2}{dr} = D_3 \frac{dS_3}{dr} \tag{8}$$

$$S_3 = \gamma S_2$$

at r = d
(see Figure 3)

$$\frac{dS_3}{dr} = 0 \tag{9}$$

The symbol γ represents the membrane partition coefficient.

Solutions to this problem are discussed in a number of sources. Waterland et al. [23] discuss this problem for hollow fiber reactors and present solutions for a variety of conditions. They include nonlinear kinetics in their analysis. Even in the case of linear kinetics, numerical methods must be used to obtain a solution because Equations (2)-(4) are coupled. The results of their solution are presented in terms of the Thiele modulus:

$$\lambda = \frac{V_{max}\, a^2}{K_m D_3} \tag{10}$$

and dimensionless length:

$$Z = \frac{z}{a\alpha} \tag{11}$$

where

$$\alpha = \frac{U_0 a}{D_1} \tag{12}$$

is the peclet number, and concentration is in dimensionless form:

$$S_1 = \frac{S_1}{S_0} \tag{13}$$

Several assumptions that were used in calculating the predictions from Waterland's model are worth noting. The enzyme in the spongy layer was regarded as being evenly distributed. Also, since the solvent in the spongy layer is the same as that in the lumen, and, given the macroporous nature of the spongy layer, the free solution diffusivity of substrate was assumed for this region. Lacking data to describe diffusion across the ultrafiltration layer, Waterland et al. assumed a tenfold higher mass transfer resistance for the membrane than for the free solution.

While the solution to the model presented by Waterland accurately predicts conversion, its calculations are quite cumbersome [24]. The model may also be unnecessarily rigorous in its consideration of the UF membrane since varying the assumed ratio D_1/D_2 between 5 and 20 yielded negligible changes in predicted conversions [23].

Another approach for solving the equations for HFRs is the one presented by Lewis and Middleman [25]. In their analysis they assume slow kinetics (in the sense of a small Thiele modulus) and negligible mass transfer resistance due to the ultrafiltration membrane. These assumptions permit incorporating Equations (2) through (4) and the condition of radial flux continuity into the expression:

$$D_3 \left.\frac{dS_3}{dr}\right|_a = \frac{U_0\ a}{4} \frac{dS_1}{dz} \tag{14}$$

Equations (4) and (14) are then amenable to analytical solution. Using data for static-loaded urease in an HFR, the model was tested at Thiele moduli of 10^{-1} and 4.4×10^{-2}. Experimental conversions conformed with the model's predictions particularly well at the lower Thiele modulus value, and a small but consistent error was observed at the higher value.

Another approach treats hollow fiber reactors as continuous stirred tank reactors (CSTRs) [27-29]. A CSTR model can be used when a recycle loop with a high recirculation rate rate yields nearly constant concentration in the lumen. For such a model, radial concentration gradients in the lumen are eliminated. The governing equations for the lumen, membrane, and spongy matrix are the same as Equations (2), (3), and (4), respectively, where $dS_1/dr = 0$. As above, analytical solution requires simplification to first or zeroeth order kinetics.

The above models use a number of simplifying assumptions to develop the descriptive equations and analytical solutions. Attempting to use such models with data obtained from the experiments conducted in this thesis may be complicated due to the method of lysine α-oxidase immobilization. These models assume evenly distributed catalytic activity in the spongy layer. Backflush loading may, however, yield spongy layer enzyme concentrated around the inner membrane of the spongy layer [30]. The existence of such a layer greatly increases the rate of reaction possible in the region surrounding the lumen and reduces the mean diffusion path required for substrate reaction.

It was therefore necessary to develop a model that accurately predicts the conversion of subtrate in the reactor system being studied. In doing so, the variables that have the greatest effect on the conversion of lysine in the reactor needed to be identified. The statistical method of factorial design was used for this purpose.

Factorial Design

Factorial design is a statistical technique that can be used to evaluate the effect that a given variable has on the observed response of a process [31]. To perform a general factorial design, a fixed number of levels for each of a number of variables is selected and experiments are conducted with all possible combinations. If there are l_1 levels for the first variable, l_2 levels for the second, ..., and l_k levels for the kth, the complete arrangement of $l_1 \times l_2 \times \cdots \times l_k$ experimental runs is called an $l_1 \times l_2 \times \cdots \times l_k$ factorial design. For example, a $2 \times 3 \times 5$ factorial design requires $2 \times 3 \times 5 = 30$ runs, and a $2 \times 2 \times 2 = 2^3$ factorial design requires eight runs. In this thesis, designs in which each variable occurs at only two levels were used. For each variable, a " - " level and a " + " level were designated.

The effect of a variable in a factorial design is defined as the change in the observed response caused by moving from the " - " to the " + " level of that variable. All variables under investigation are of equal interest as is the possibility that these variables interact. If two variables interact then the individual effects cannot be simply added to give the total effect that the variables have on the system.

There are several methods for the analysis of a factorial design. One such method uses Yates's algorithm [31] as a quick way for determining the effects. This algorithm is applied to the observations of the experiments after they have been arranged in what is called standard order. A 2^k factorial design is in standard order when the first column of the design matrix consists of successive minus and plus signs, the second column of successive pairs of minus and plus signs, the third column of four minus signs followed by four plus signs, and so forth. In general, the kth column

consists of 2^{k-1} minus signs followed by 2^{k-1} plus signs. An example of a factorial design in standard order is shown in Table 7 of Chapter 6.

After the design matrix has been arranged in standard order, the results of the experiments are recorded in the observed response column of the algorithm. The Yates calculations consider the responses in successive pairs. The first entries in the first calculated column are obtained by adding the pairs together. The second set of entries are obtained by subtracting the top number from the bottom number of each pair. In the same manner that the first column is obtained from the response column, the second column is derived from the first, and so on.

For a 2^k factorial design, k columns will be generated by adding and subtracting appropriate pairs of numbers. To obtain the effects, the entries of the kth column are divided by the proper divisors. The first divisor will be 2^k, and the remaining divisors will be 2^{k-1}. The first estimate is the grand average of all the observations. The remaining effects are identified by locating the plus signs in the design matrix. Effects that differ greatly from zero are said to be significant. A more detailed description of factorial design is given in Chapter 10 of Box, Hunter, and Hunter [31].

As stated earlier, factorial design logic was used to determine which variables in the reactor system being studied had the greatest effect on the conversion of lysine. Before doing this, however, certain analytical techniques had to be chosen for solution analyses. These techniques are described in the next section.

CHAPTER 3

ANALYTICAL TECHNIQUES

In the following chapters, the free solution and immobilized kinetics, the retention of the enzymes within the spongy layer of asymmetric hollow fibers, and the reactor performance will be discussed. Several analytical techniques are common to the experiments described in these chapters. It was often necessary to determine the total amount of protein, the concentration of lysine, and/or the hydrogen peroxide concentration of a given sample. In addition, the activity of an enzyme in a particular sample was often of interest. The methods used for these analyses are described below.

Lowry Protein Determination

As will be discussed in Chapter 4, it was often necessary to determine the amount of protein in a given sample. The Lowry reaction can be used to perform a protein analysis [32]. The first step in this procedure involves the formation of a copper/protein complex in alkaline solution. This complex then reduces a phosphomolybdic-phosphotungstate to yield an intense blue color. The absorbance of this blue solution can be determined spectroscopically and is directly proportional to the total protein concentration in the sample. This procedure was as follows:

1) Reagent A was prepared by dissolving 100 g Na_2CO_3 in 1 liter (final volume) of 0.5N NaOH.

2) Reagent B was prepared by dissolving 1 g $CuSO_4 \cdot 5H_2O$ in 100 ml (final volume) of distilled water.

3) Reagent C was prepared by dissolving 2 g potassium tartrate in 100 ml (final volume) distilled water. The reagents prepared in steps 1 to 3 may be stored indefinitely.

4) A 0.3 mg/ml protein standard solution was prepared by making the

appropriate dilution to a 10 g/dl solution of bovine albumin obtained from Sigma (catalog No. 690-10).

5) The UV/Vis spectrophotometer (Perkin Elmer Lambda 3A) was then turned on to warm up.

6) Test tubes were numbered and placed in a test tube rack. One of each of the following volumes of the protein standard solution was then carefully pipetted into each tube: 0, 0.1, 0.2, 0.4, 0.6, 0.8, and 1.0 ml.

7) The total volume of each tube was brought up to 1.0 ml by the appropriate addition of distilled water.

8) 15 ml of reagent A, 0.75 ml reagent B, and 0.75 ml reagent C were mixed thoroughly in a 125 ml Erlenmeyer flask.

9) 1.0 ml of the solution made in step 8 was added to each tube. The tubes were vortexed to assure proper mixing.

10) The tubes were incubated for 15 minutes at room temperature.

11) While the tubes were incubating, 5.0 ml of 2N Folin-phenol reagent was diluted to 50 ml with distilled water in a 125 ml Erlenmeyer flask and mixed thoroughly.

12) At the conclusion of the incubation period (step 10), 3.0 ml of the solution prepared in step 11 was forcibly pipetted into each tube. The resulting solution was vortexed immediately. The addition to and mixing of each test tube was completed before proceeding to the next.

13) The absorbance of each sample was determined at a wavelength of 540 nm.

14) The data were plotted as shown in Figure 4 to obtain a standard curve. Samples of unkown protein concentration were assayed using procedures identical to those used for the standard curves.

The major precaution to be observed when performing the Lowry assay concerns the addition of Folin's reagent. This reagent is stable only at acidic pH; however, the reduction described above occurs only at pH 10.0. Therefore, when Folin's reagent is added to the alkaline copper/protein solution, mixing must occur immediately so that the reduction can occur before the phosphomolybdic-phosphotungstate Folin's reagent breaks down. Another concern is Lowry method's sensitivity to foreign ions. Precautions must be taken to keep the samples ion-free.

This assay procedure was very accurate for protein concentrations

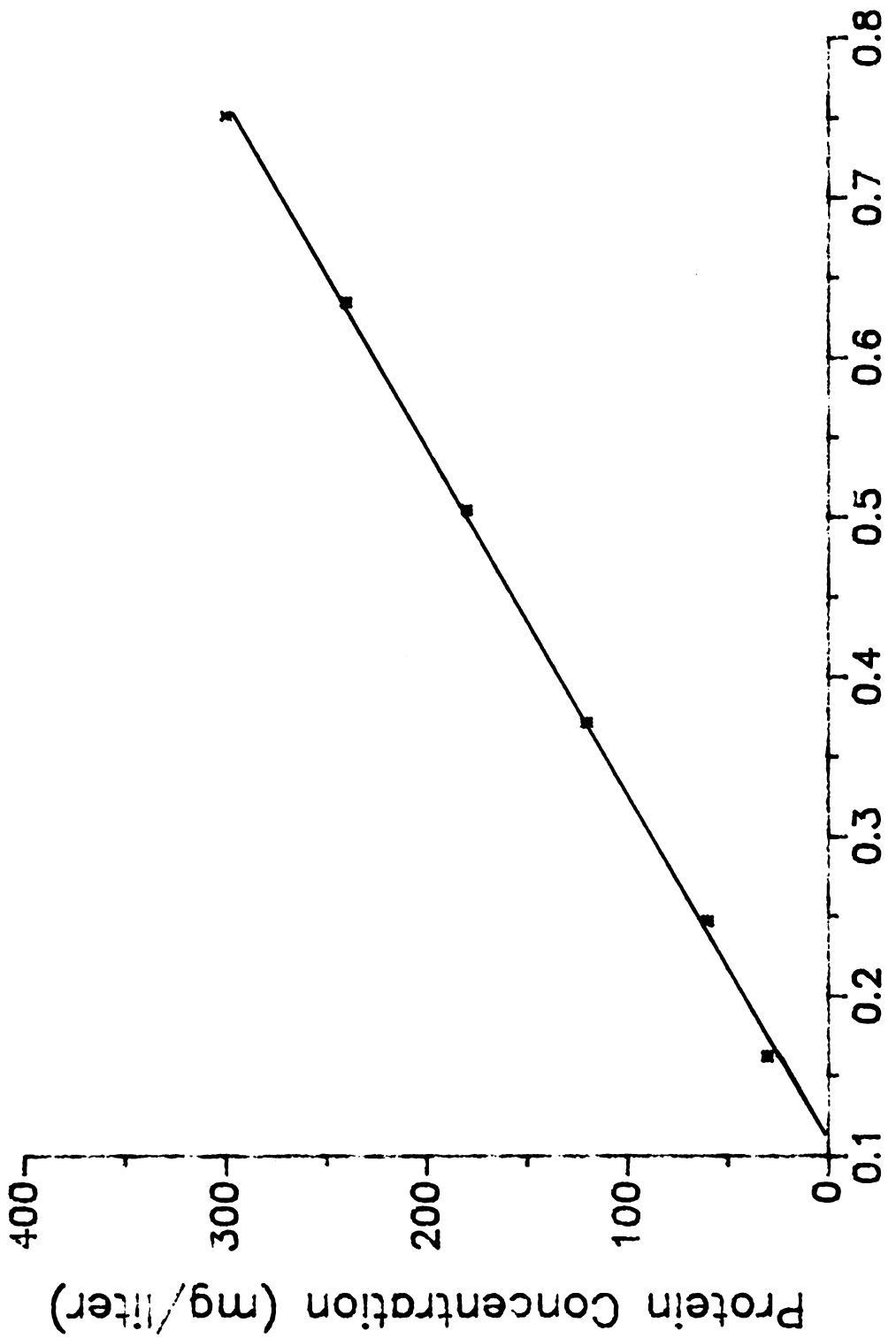

Figure 4-- standard curve for the Lowry method (coefficient of linearity = 0.998)

between 30 and 300 μg/ml. For samples with higher concentrations, a dilution step was required. Samples that were low in protein concentration were "spiked" with protein by adding 0.1 ml of the protein standard prepared in step 4 above to 0.9 ml of the sample before assaying. In addition, it is important to note that this technique only gives the total amount of protein in a sample. For samples where individual enzyme concentrations were needed, a separation step was first performed before using the Lowry method.

Lysine Determination

Lysine concentrations were determined by the method described by Nakatani et al. [33]. This method uses saccharopine dehydrogenase which catalyzes the following reversible reaction:

$$\text{lysine} + \alpha\text{-ketoglutarate} + \text{NADH} + H^+ \rightleftharpoons \text{saccharopine} + NAD^+ + H_2O \quad (15)$$

No structural analogs of L-lysine and α-ketoglutarate are known to serve as substrates for saccharopine dehydrogenase. In addition, the equilibrium of the reaction is greatly in favor of saccharopine formation [34]. By taking advantage of these two facts, it is possible to determine the concentration of lysine in a given sample by simply following the disappearence of NADH caused by reaction (15). Incubation of a small amount of lysine with saccharopine dehydrogenase in the presence of excess α-ketoglutarate and NADH results in a decrease in NADH absorbance at 340 nm that is proportional to the amount of lysine present. This technique is accurate for lysine concentrations up to 0.2 mM. For samples with higher concentrations, a dilution step is required prior to analysis. The lysine (catalog No. L5626), α-ketogluterate (catalog No. K410-2), NADH (catalog No. N8129), and saccharopine dehydrogenase (catalog No. S3633) were all obtained from Sigma.

In order to obtain a standard curve for lysine, lysine solutions at the concentrations listed in Table 3 were prepared by making the appropriate dilutions with buffer to a 10.0 mM lysine stock solution:

Table 3
Concentrations Used to Construct the Lysine Standard Curve

Solution	Lysine Conc. (mM)
1	0.0
2	0.02
3	0.04
4	0.06
5	0.08
6	0.10
7	0.16
8	0.20

One ml of each solution was measured into a test tube. The total volume of each test tube was brought up to 3.0 ml by the addition of 1.0 ml of 0.1 M phosphate buffer (pH 7.0), 0.9 ml of a 0.5 mg/ml NADH solution prepared by diluting the solid into 0.1 M phosphate buffer (pH 7.0), and 0.1 ml of a 0.1 M α-ketoglutarate solution. To initiate reaction, 1.0 ml of saccharopine dehydrogenase stock solution was added to each test tube. The stock solution consisted of 100 units ($\approx$1 mg) of enzyme dissolved in 50 ml of 0.05 M potassium phosphate buffer (pH 6.8). Five mg of bovine serum albumin (obtained from Sigma) was added to the stock solution to increase enzyme stability during storage [35].

After 30 minutes, the absorbance of each solution was measured using 0.1 M phosphate buffer (pH 7.0) as the blank. The change in absorbance of a solution was taken as the difference of absorbance between that solution and the sample with no lysine present (test tube 1). As mentioned earlier, the

amount of lysine that is present in a solution is proportional to the amount of NADH that is consumed by reaction (15) which, in turn, is proportional to the change in absorbance. Therefore a curve of lysine concentration versus change in absorbance at 340 nm can be constructed (Figure 5).

Hydrogen Peroxide Determination

Hydrogen peroxide concentration can be determined directly by using its absorbance at 240 nm. The first step was to prepare H_2O_2 solutions at the concentrations listed in the first column of Table 4 by diluting a 30% (v/v) hydrogen peroxide stock solution with an appropriate amount of 0.1 M potassium phosphate buffer, pH 7.0:

Table 4
Concentrations Used to Construct the H_2O_2 Standard Curve

Solutions	Test tubes
1.5	0.5
3.8	1.267
5.9	1.97
13.5	4.50
17.8	6.90
24.0	8.0
27.3	9.10
44.7	14.90
60.2	20.07
90.3	30.10

One ml of each of these solutions was measured into a test tube and diluted to a total volume of 3 ml with phosphate buffer. This resulted in having ten test tubes with hydrogen peroxide concentrations (Table 4, second column) ranging from 0.5 to 30.1 mM. The absorbance at 240 nm of the solutions in each of the test tubes was measured and recorded. A solution containing a 2:1 ratio (volume basis) of catalase to buffer served as a blank. These data were used to create a standard curve of H_2O_2 concentration versus absorbance (Figure 6).

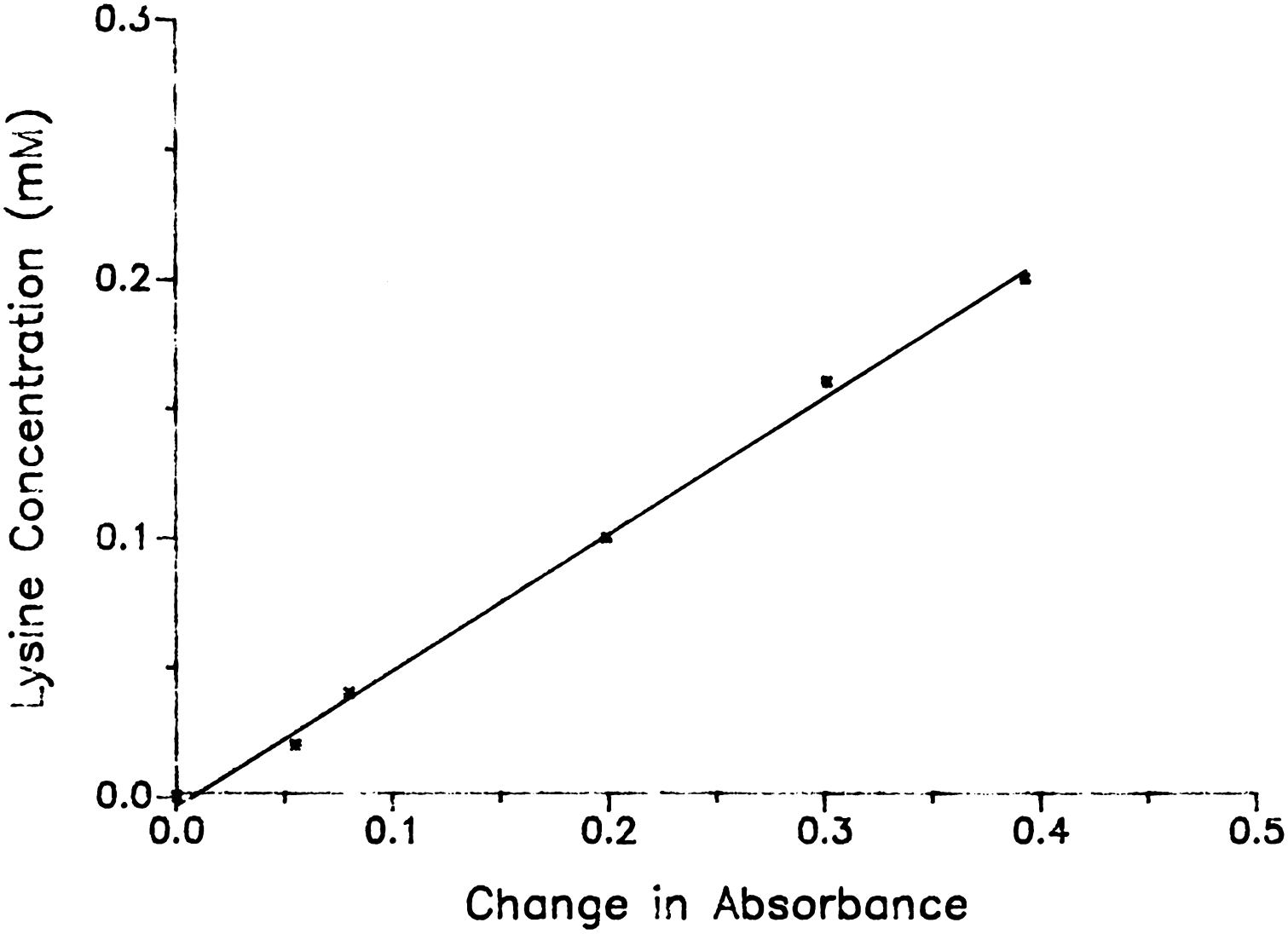

Figure 5— lysine conc. vs. change in absorbance (coefficient of linearity = 0.993)

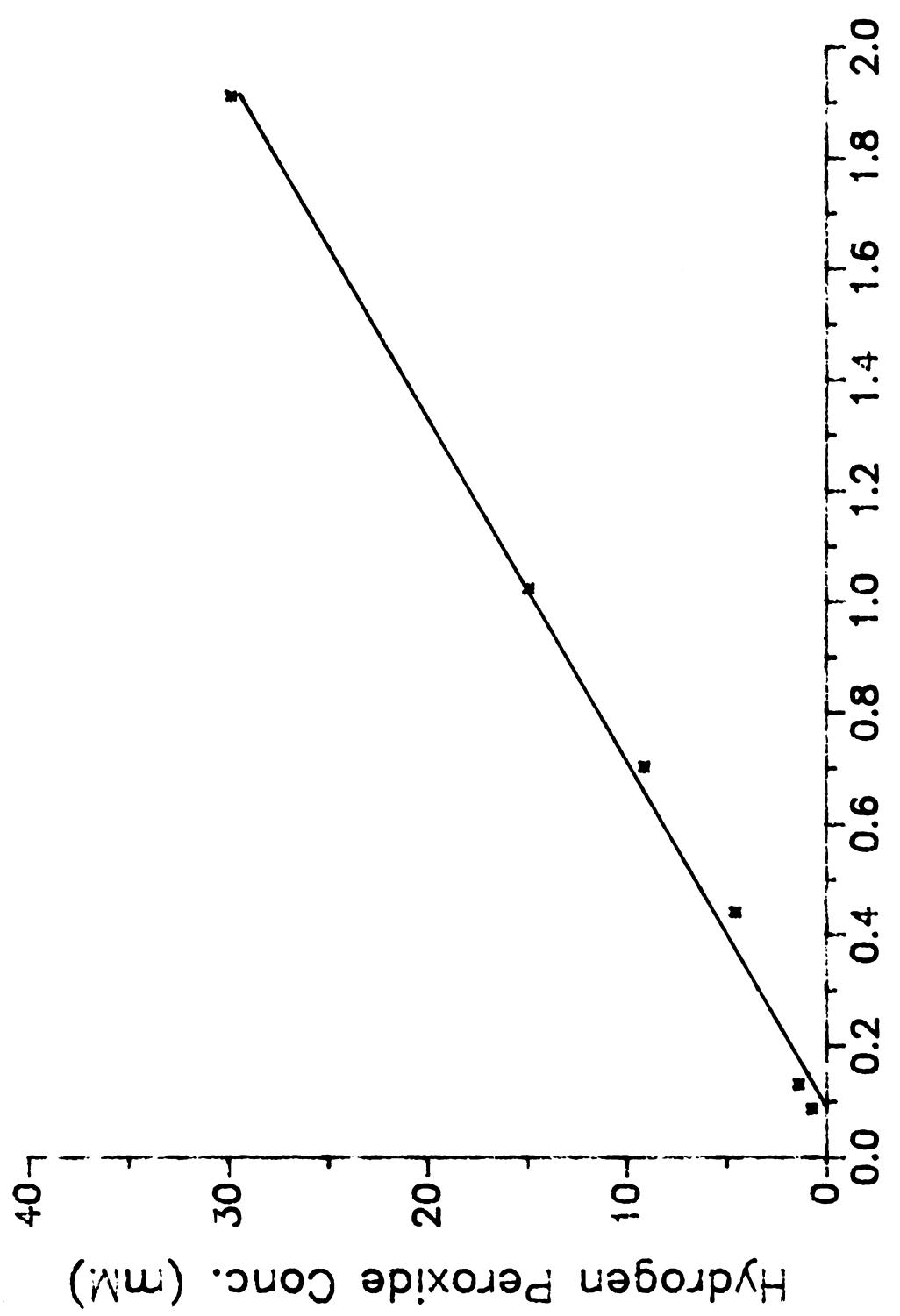

Figure 6— hydrogen peroxide conc. vs. absorbance (coefficient of linearity = 0.997)

Catalase Activity Determination

For the experiments described in Chapter 5, it was necessary to determine whether enzyme activity was affected by the type of hollow fiber material used. The activity of catalase is defined as the amount of substrate converted per mg of enzyme per minute, and was determined by the method of Chance and Herbert [36]. This technique uses the direct measurement of the decrease of light absorbance at a wavelength of 240 nm caused by the decomposition of hydrogen peroxide by catalase. In order to determine the activity of catalase in a given sample, 1.0 ml of the sample was incubated with a 30 mM hydrogen peroxide solution. The absorbance of H_2O_2 at 240 nm was recorded with time using the UV/Vis spectrophotometer in the local mode. From this information and a standard curve of hydrogen peroxide versus absorbance prepared in the manner described above, the amount of H_2O_2 converted per minute was determined. The Lowry method was then used to determine the catalase concentration of the sample which, in turn, was used for the calculation of catalase activity.

L-lysine α-oxidase Activity Determination

The method used for the determination of lysine α-oxidase activity was similar to the one described for catalase. Two ml of a 2.0 mM solution of lysine was pipetted into a test tube which was placed in a water bath (Lab Line,Inc., Model 3540) at 37°C. One ml of the sample being tested was added to the test tube. After one minute, 0.2 ml of 25% trichloroacetic acid (TCA) solution was added to stop the reaction. The amount of lysine remaining in the solution was determined by the saccharopine dehydrogenase method discussed above. From this, the amount of lysine converted was calculated and used with the lysine α-oxidase concentration obtained from the Lowry analysis to determine activity.

The analytical techniques described in this chapter were used extensively in the work described in the sections that follow. A thorough understanding of these methods was necessary as the first step in the development and testing of an immobilized enzyme reactor.

CHAPTER 4

ENZYME KINETICS

Introduction

In order to model the hollow fiber reactor system, knowledge of the intrinsic reaction kinetics is needed. The experiments in this chapter were conducted to determine the free-solution kinetic parameters of both L-lysine α-oxidase and catalase under temperature and pH conditions similar to those of potential medical applications. In addition, the effect that the two enzymes had on each other was investigated.

Enzyme kinetics may often be represented by the Michaelis-Menten equation:

$$V = -\frac{dS}{dt} = \frac{kE_0S}{K_m + S} \tag{16}$$

where V is the reaction rate (the moles of substrate that react per liter per minute), S is the substrate concentration (moles/liter), k is the first order reaction rate constant for the conversion of substrate to product from the enzyme substrate complex which is equal to the moles of substrate converted per mole of enzyme per minute, E_0 is the total amount (moles) of enzyme present, and K_m is the Michaelis constant (mols/liter) [37]. The maximum rate, V_{max}, is attained when the enzyme sites are fully saturated with substrate. This occurs when S is much greater than K_m so that the term $(S / S + K_m)$ approaches unity. Thus

$$V_{max} = V = kE_0 \tag{17}$$

The kinetic constant k is also called the turnover number of the enzyme. It represents the number of substrate molecules converted into product per unit time when the enzyme is saturated with substrate.

Evaluation of Parameters in the Michaelis-Menten Equation

The Michaelis-Menten equation in its original form, Equation (16), is not well suited for the determination of the kinetic parameters K_m and V_{max} from experimental data. However, by rearranging this equation, the following options for plotting of data and graphical parameter evaluation can be derived:

$$\frac{1}{V} = \frac{1}{V_{max}} + \frac{K_m}{V_{max}} \left[\frac{1}{S} \right] \tag{18}$$

$$\frac{S}{V} = \frac{K_m}{V_{max}} + \frac{S}{V_{max}} \tag{19}$$

$$V = V_{max} - K_m \left[\frac{V}{S} \right] \tag{20}$$

Each equation suggests an appropriate linear plot. In using such plots, several points should be noted. Plotting Equation (18) as 1/V vs. 1/S (known as a Lineweaver-Burk plot) cleanly separates the important variables. The most accurately known rate values at high values of S and near V_{max} will tend to be clustered near the origin, while those rate values that are least accurately measured will be far from the origin and will tend most strongly to determine the slope, K_m / V_{max}. Equation (19) tends to spread the data for higher values of V so that the slope $1/V_{max}$ can be determined accurately. The intercept often occurs quite close to

the origin so that the determination of K_m by this method is subject to large errors. The third method uses the Eadie-Hofstee plot of V vs. V/S. Both coordinates contain the measured variable V, which is subject to the largest errors.

These considerations suggest the following strategy for evaluating V_{max} and K_m [38]. First, V_{max} is determined from a plot of Equation (18) (to find the intercept accurately) or Equation (19) (to find slope accurately). Then the graph of velocity versus substrate concentration is used to find $S_{½}$, the substrate concentration where $V = V_{max} / 2$. From Equation (16), it is seen that K_m is equal in magnitude and dimension to $S_{½}$. The K_m value of lysine α-oxidase was too close to the origin to use these techniques, so instead, a statistical analysis of Equation (18) was used to determine the kinetic parameters of the enzyme.

Materials and Methods

Catalase (catalog No. C3155) was obtained from Sigma Chemical Company. The activity of this enzyme was determined by the method of Chance and Herbert [36] described in Chapter 3. The hydrogen peroxide used was analytical grade and was obtained from Mallinckrodt (lot No. 5240 kxly). L-lysine α-oxidase was donated by Yamasa Shoyu Co., LTD. (lot No. 86-u, manufacturers assay of 270 units per ml where one unit hydrolyzes 1 μmol of lysine per minute). Lysine concentrations were determined by the method described by Nakatani et al. [33]. discussed in Chapter 3. This technique is accurate for lysine concentrations up to 0.2 mM. For samples with higher concentrations, a dilution step is required prior to analysis. The lysine, α-ketogluterate, NADH, and saccharopine dehydrogenase were all obtained from Sigma Chemical Company.

Enzyme assays were conducted in 0.1M potassium phosphate buffer (pH 7.0). Hydrogen peroxide solutions were prepared by diluting a 30% by volume stock solution with buffer. Lysine solutions were prepared by diluting a 10.0 mM stock solution with buffer.

Because the reaction that is catalyzed by catalase is very rapid, it is important to be able to quickly obtain the data that are needed to determine the kinetic constants of the enzyme. The first step was to prepare the standard curve for H_2O_2 as described in the previous chapter. Next, ten test tubes with the following hydrogen peroxide concentrations were prepared:

Table 5
Hydrogen Peroxide Concentrations

Test tube	H_2O_2 conc. (mM)
1	1.5
2	3.8
3	5.9
4	13.5
5	17.8
6	24.0
7	27.3
8	44.7
9	60.2
10	90.3

One ml of the solution in test tube 1 was measured into a cuvette. Two ml of catalase solution was added, and the mixture was shaken briskly. The cuvette was placed in the spectrophotometer, and the change in absorbance with time was recorded with a Perkin Elmer R 100A recorder. This information, along with the data presented in Figure 6, was used to determine the rate of the reaction. The method was repeated on the

remaining solutions. Experiments were conducted with enzyme concentrations of 0.4 and 0.8 μg/ml.

Data to determine the kinetic constants of L-lysine α-oxidase were obtained by preparing lysine solutions at concentrations (Table 6) ranging from 0.05 to 10.0 mM:

Table 6
Lysine Concentrations

Test tube	Lysine concentration (mM)
1	0.05
2	0.10
3	0.20
4	0.50
5	1.0
6	2.0
7	4.0
8	6.0
9	8.0
10	10.0

These solutions were measured into test tubes which were placed in a constant temperature water bath shaker (Lab Line Instruments, Inc., Model 3540) at 37°C at least 20 minutes before the addition of enzyme for temperature equilibration. Enzyme was pipetted into each test tube to initiate the reaction. Solutions were immediately vortexed and placed back into the water bath. Experiments were conducted with enzyme concentrations of 0.4 and 0.8 μg/ml. Each treatment was incubated for 20 seconds. Following incubation, the enzyme was inactivated by the addition of 0.2 ml of a 25% trichloroacetic acid solution. The solutions were centrifuged in a bench-top centrifuge (Clay Adams, catalog No. 0521) for five minutes. The saccharopine dehydrogenase method and the data presented on Figure 5 were used to determine the amount of lysine in the supernatant of each sample. From this information, the rates of the reaction were calculated.

Because the reactor system being investigated contained both catalase and oxidase co-immobilized in a hollow fiber reactor, it was important to investigate the effect that the enzymes had on each other's kinetics. The above experiments were repeated using enzyme solutions containing catalase to oxidase ratios of 1:2, 1:1,and 2:1 in place of the pure enzyme stock solutions.

Results

Double reciprocal plots of 1/V vs. 1/S (Lineweaver-Burk) and a plot of reaction rate versus substrate concentration were prepared for both the catalase and L-lysine α-oxidase reactions. These are shown in Figures 7-10. In these figures, the reaction rate was measured in units of mols of substrate reacted per mg of enzyme per minute. To obtain these units, Equation (16) was divided by the enzyme concentration (mg/liter). The Wilkinson method [39] for the regression analysis of these curves gave the following results:

For catalase (no lysine α-oxidase present)

$K_m = 25.3 \pm 2.4$ mM

$k = V_{max} / E_0 = 7.8 \pm 1.8 \times 10^6$ min^{-1}

For lysine α-oxidase (no catalase present)

$K_m = 0.060 \pm 0.010$ mM

$k = 6944.0 \pm 162.4$ min^{-1}

Abe et al. [40] reported K_m and k values for catalase of 25.0 mM and 12.0×10^6 min^{-1}, respectively. There are two main reasons that the turnover number, k, found in these exeriments is slightly lower than the

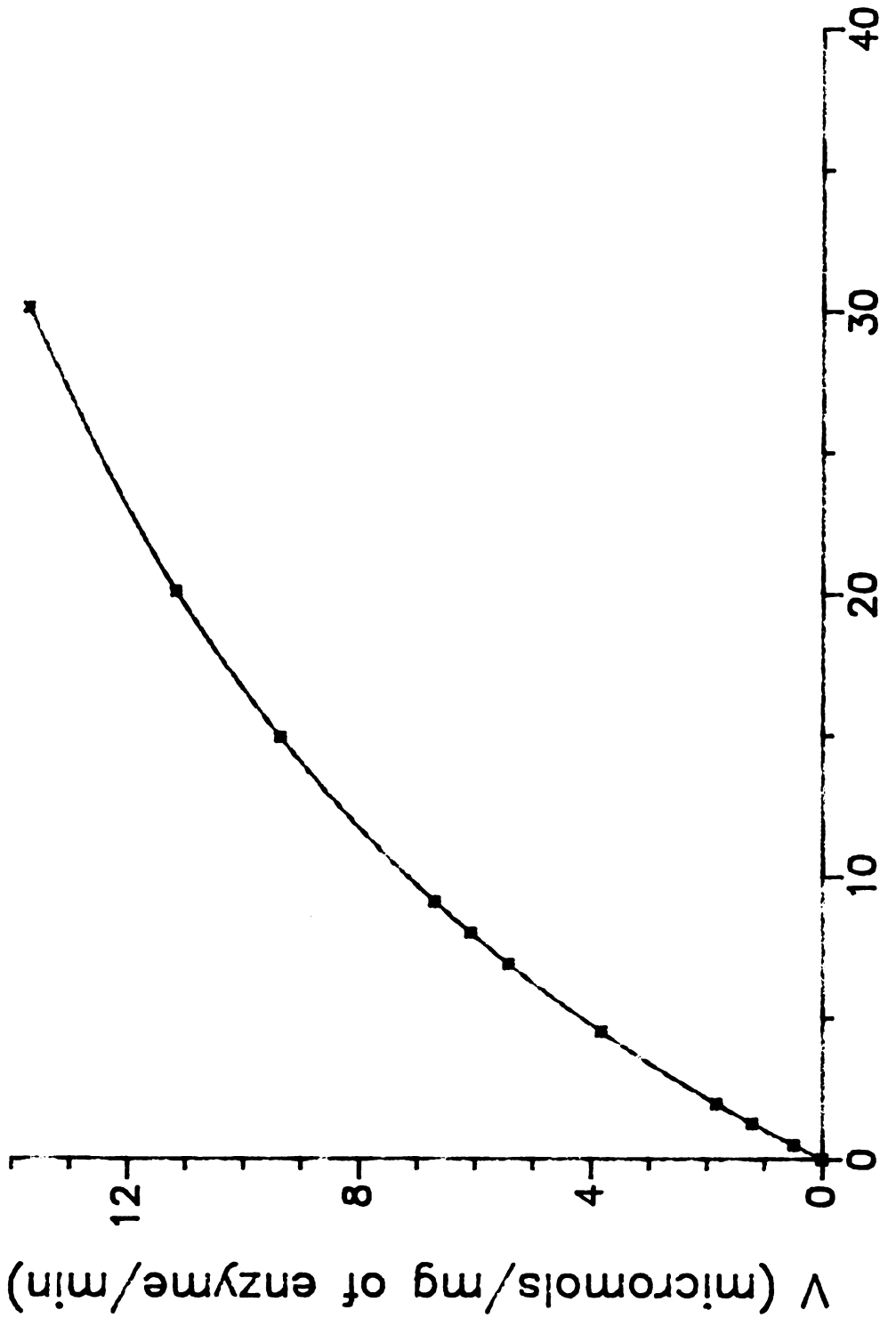

Figure 7— reaction rate vs. substrate concentration for catalase

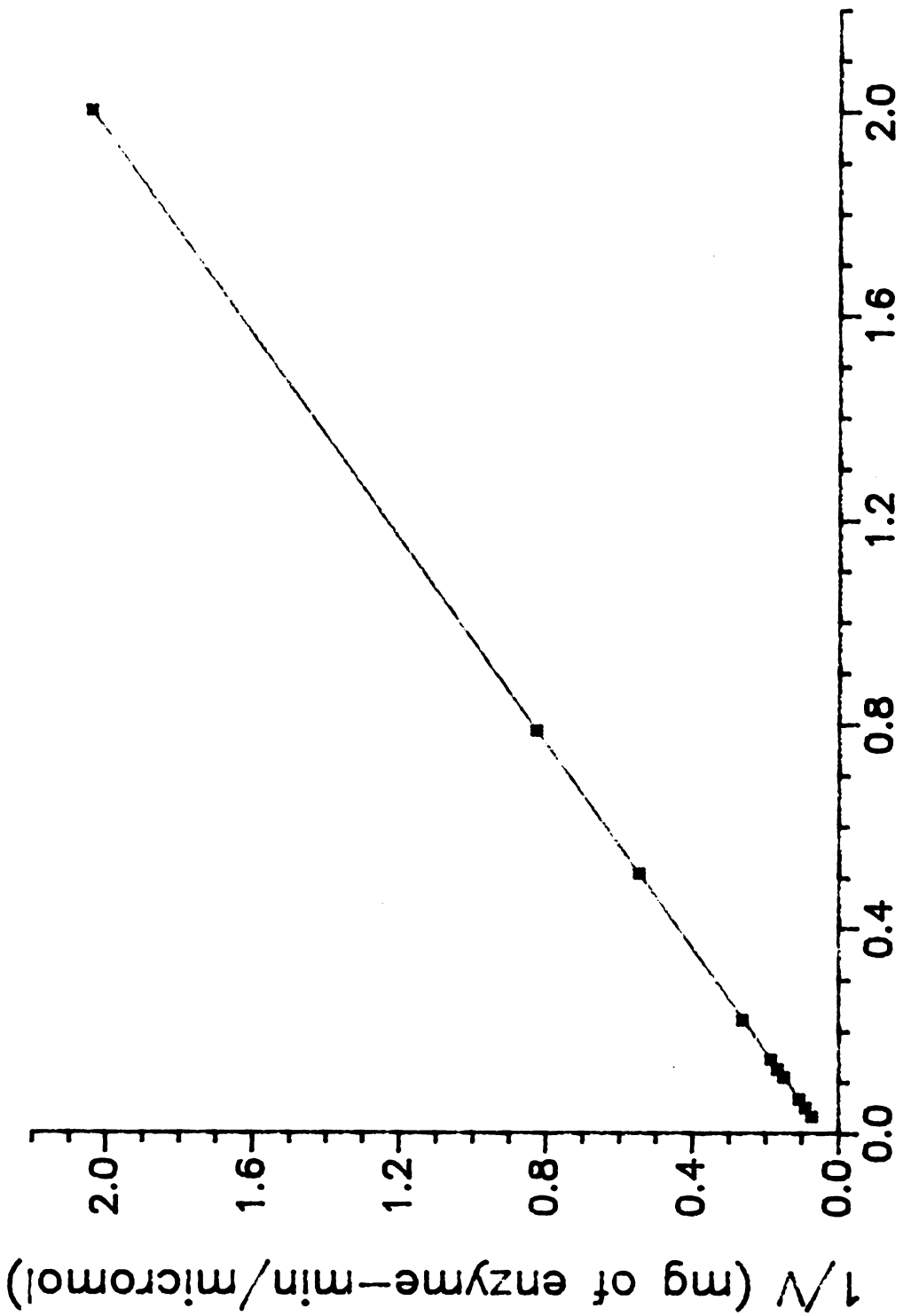

Figure 8– Lineweaver–Burk plot for catalase

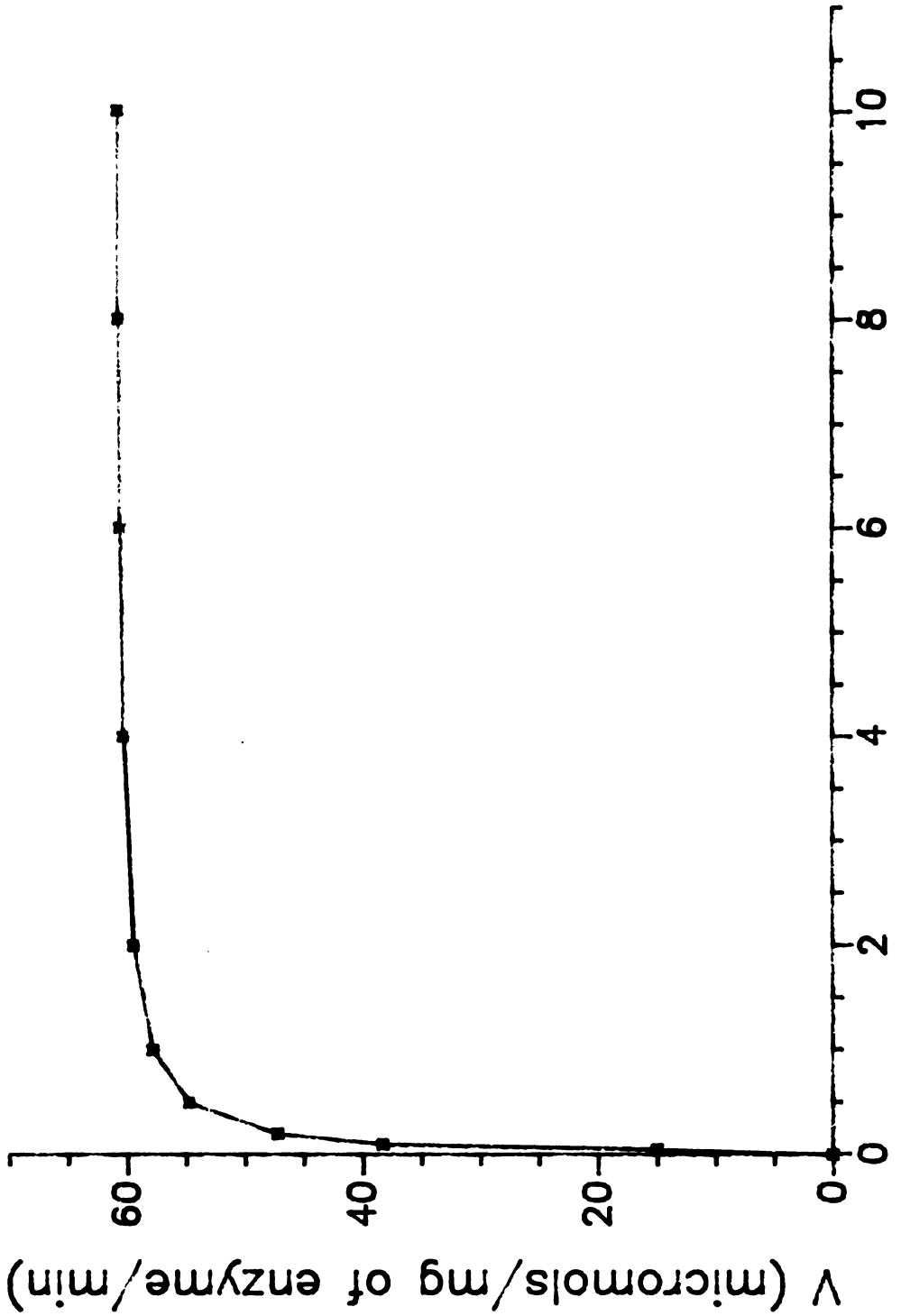

Figure 9— reaction rate vs. substrate conc. for L—lysine α—oxidase

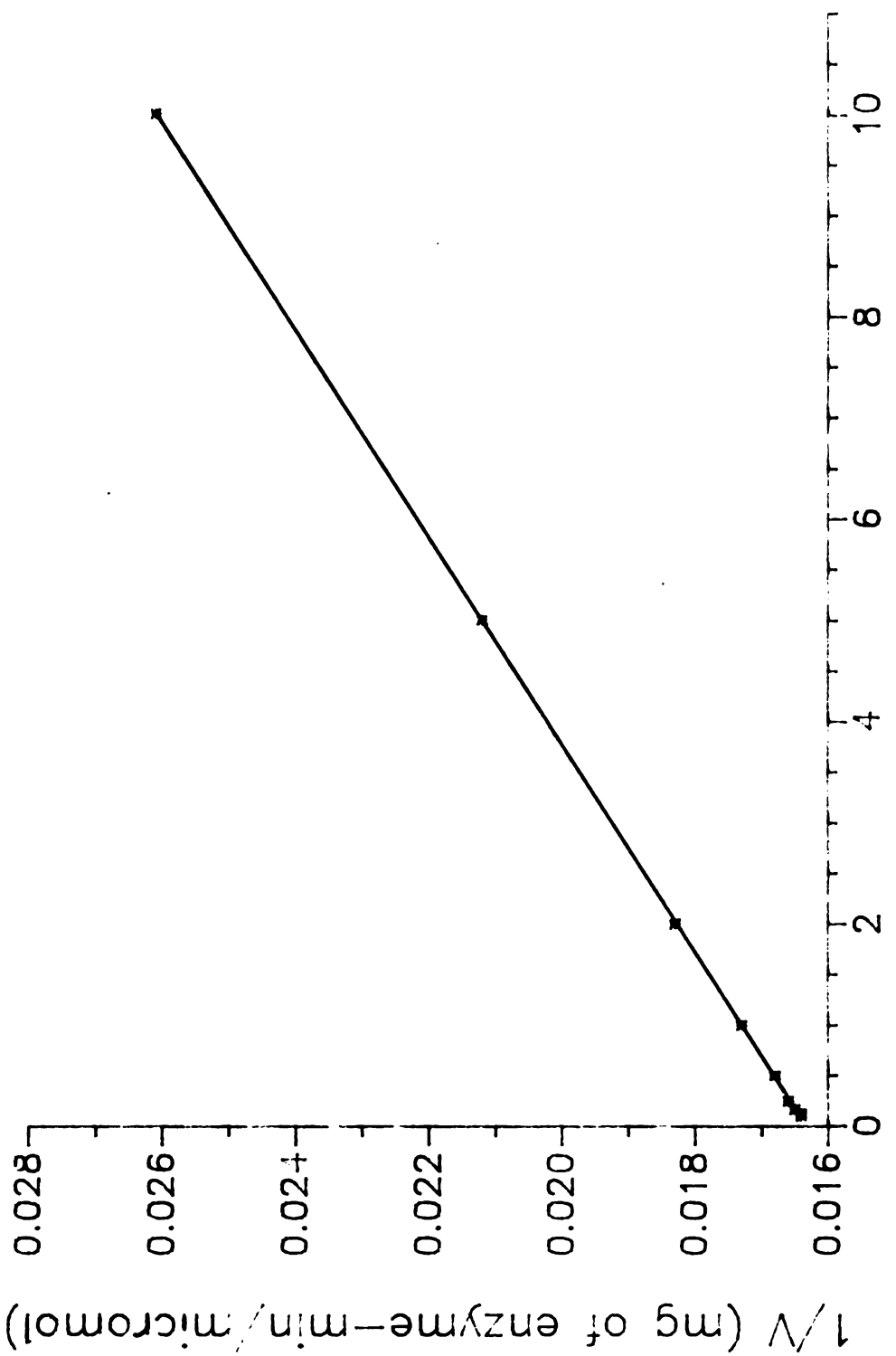

Figure 10— Lineweaver—Burk plot for L—lysine α—oxidase in the absence of catalase

one reported in the literature. The first possibility is due to the difficulty of obtaining initial rate data. Abe states that in determining the kinetic properties of catalase, the first 10 seconds of the reaction are very important. However, in the technique used here, it took a few seconds for the catalase and hydrogen peroxide solutions to mix properly. Therefore, the measured reation rates were most likely lower than the actual rates causing a lower calculated value for the turnover number. The second source of error was introduced by the limitations of spectrophotometry. In general, absorbance readings greater than 2.0 tend to become inaccurate. This limited the hydrogen peroxide concentrations used in this study to values that were of the same magnitude as K_m. Concentrations that are much greater than K_m are usually desired because it is at these concentrations that the veity of the reaction approaches V_{max}.

The Michaelis constant and turnover number for L-lysine α-oxidase in the absence of catalase have been reported to be 0.04 mM and 7200 min^{-1}, respectively [10]. The difference between these values and the ones found from these experiments are within the accuracy of the technique used.

Experiments indicate that the activity of catalase is not affected by the presence of oxidase; however the reverse is not true. Catalase causes an increase in the rate of reaction that is catalyzed by lysine α-oxidase. This effect is shown in Figure 11. Statistical analysis of the Lineweaver-Burk plots (Figure 12) gives the following results for lysine α-oxidase:

No catalase present

$K_m = 0.060 \pm 0.010$ mM

$V_{max} = 62.3 \pm 2.6$ μmols/mg-min

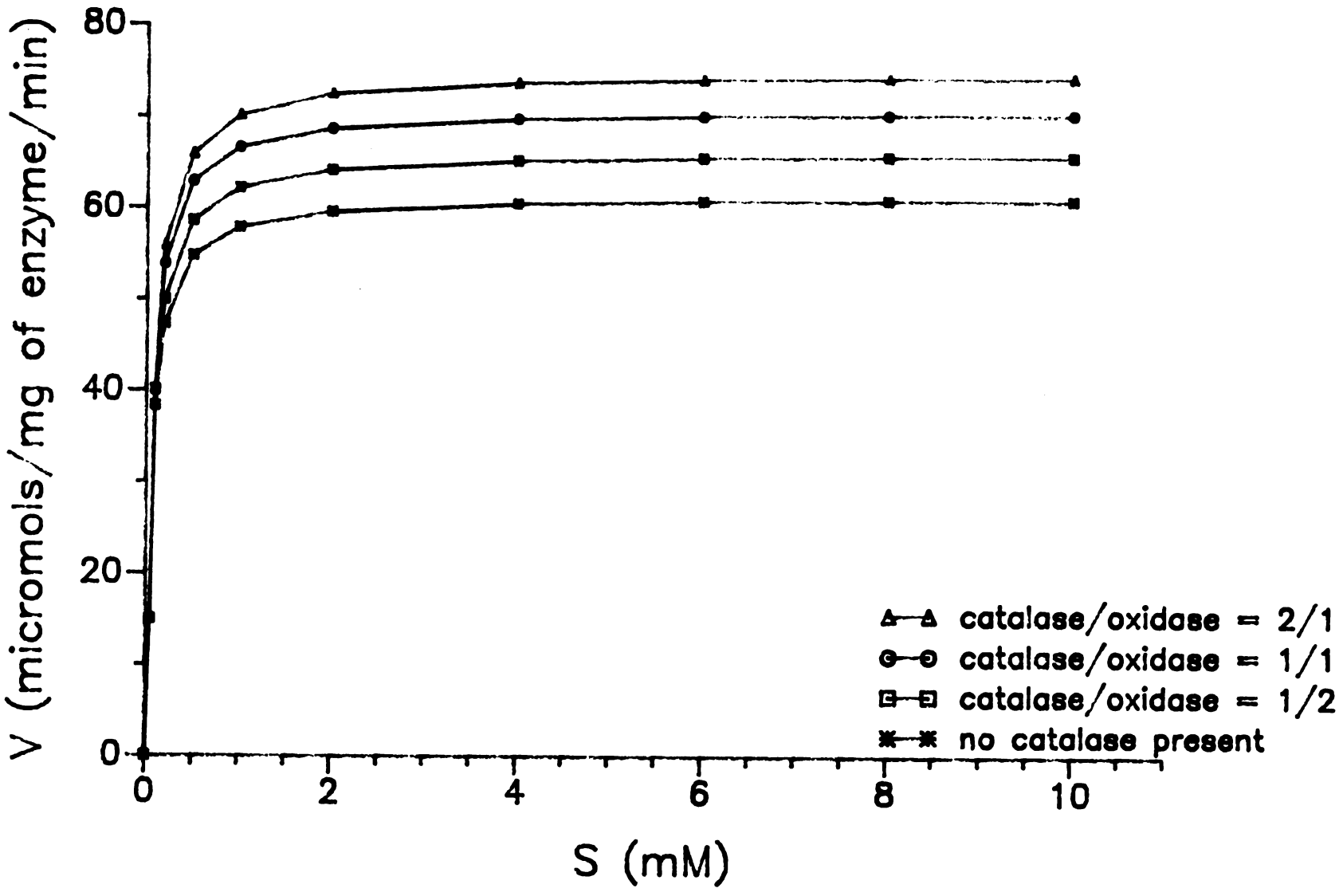

Figure 11– reaction rate vs. substrate conc. for L–lysine ∝–oxidase in the presence of catalase

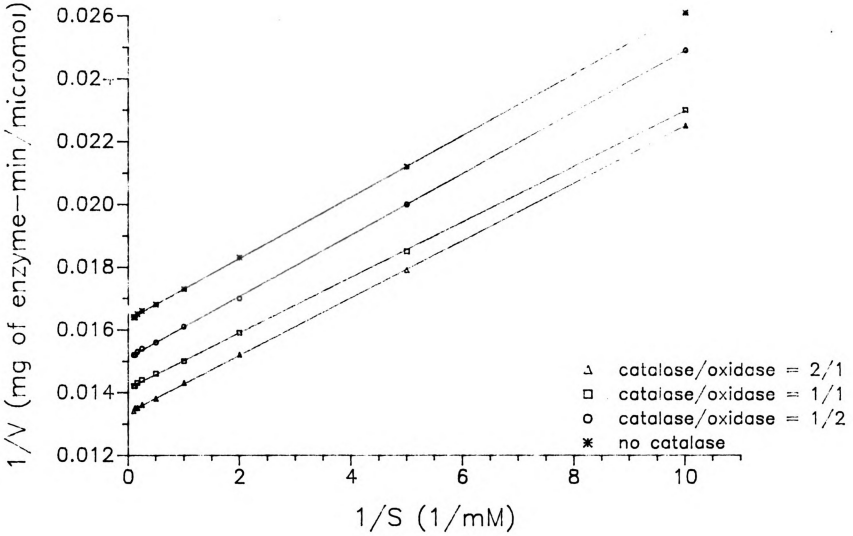

Figure 12– Lineweaver–Burk plots for L–lysine ∝–oxidase in the presence of catalase

catalase:oxidase = 1:2

K_m = 0.065 ± 0.012 mM

V_{max} = 66.2 ± 2.3 μmols/mg-min

catalase:oxidase = 1:1

K_m = 0.063 ± 0.014 mM

V_{max} = 70.8 ± 1.8 μmols/mg-min

catalase:oxidase = 2:1

K_m = 0.062 ± 0.011 mM

V_{max} = 74.9 ± 1.6 μmols/mg-min

It is seen that K_m is independent of the amount of catalase present but that the apparent maximum velocity increases with increasing proportions of catalase. This may be explained by recalling the lysine α-oxidase reaction:

$$\text{L-Lysine} + O_2 + H_2O \rightarrow H_2O_2 + \text{other products} \qquad (21)$$

The hydrogen peroxide produced by this reaction is hydrolyzed into hydrogen and oxygen by catalase. This produces more oxygen which may be limiting for reaction (21). Therefore, the action of catalase on H_2O_2 can cause an increase in the rate of reaction by withdrawing a product and supplying a reactant. This may serve to improve reactor performance by eliminating some reactant diffusion-limitations.

With the kinetics of the enzymes in free solution known, the next step in the experimental program was to immobilize the enzyme within the hollow fiber reactor. These experiments are descibed in the next chapter.

CHAPTER 5

ENZYME RETENTION

Introduction

An important consideration in the design of hollow fiber reactors (HFRs) is the technique used to immobilize the enzymes onto the hollow fiber. Backflush loading was chosen as the most efficient method for achieving high enzyme concentrations in HFRs. Compared to static loading, it is a more rapid method and allows for higher immobilized enzyme concentrations [20]. Since the enzymes are entrapped in the pores of the fiber and are not chemically cross-linked or bound to the support, the recovery of enzyme and reuse of fibers is possible.

In the final design of the system being investigated, PA10 fibers were used in the reactor. The experiments described in this chapter were conducted to determine that these fibers were best suited for the co-immobilization of catalase and L-lysine α-oxidase. Polysulfone (PM30) and polyamide (PA10 and PA30) ultrafiltration (UF) fibers were compared. The numbers 10 and 30 specify nominal molecular weight cutoffs of 10,000 and 30,000, respectively. The fibers were evaluated for retention of protein, retention of enzyme activity, and the recoverability of enzyme.

Materials and Methods

All UF fibers were donated by Romicon, Inc.. Folin phenol reagent for the Lowry protein assay was manufactured by Fisher Scientific. The reagents and analytical equipment used for the determination of catalase and oxidase activity were described in the Chapter 3. Enzyme solutions were prepared in 0.1 M potassium phosphate buffer (pH 7.0).

Single Fiber Reactors

Single fiber reactors (SFRs) were prepared using PA10, PA30, and PM30 UF fibers for the experiments described in this and the following chapters. The SFR consisted of a single hollow fiber encased in a glass shell giving a typical shell-and-tube configuration (Figure 13). Shell material was borosilicate glass, 21.5 cm long, 0.8 cm o.d.. The SFR was assembled by pushing 3 cm sleeves of Tygon tubing (3/16 in. i.d.) over the ends of the glass reactor shell. The ultrafiltration fiber was then fed through the shell. Male and female Luer fittings were then slid onto both ends of the fiber, and the female fittings were pushed into the Tygon sleeves. A sealant that consisted of a mixture of an epoxy resin and curing agent (Dow Chemical Co., Inc.) was applied to the inside of the female Luer fitting, and the male/female connections were made. Three days were allowed for the epoxy to cure.

The SFRs were cleaned and sanitized by the method to be discussed in Chapter 6. Between the cleaning process and the enzyme loading, the SFRs were checked for leakage by pressurizing the tube-side to 15 psig with air from a syringe and checking for escaping air bubbles.

Protein and Activity Determination

The amounts (mass) of catalase and lysine α-oxidase in samples were determined by the Lowry method described in Chapter 3. This technique was found to be accurate for the enzymes being studied by preparing solutions of the enzymes and comparing the known values of the concentrations (μg/ml) to the measured ones. For samples that contained both catalase and lysine α-oxidase, gel chromatography was first performed to separate the enzymes before the amount of each was determined.

Activity assays were performed in all experiments to determine whether

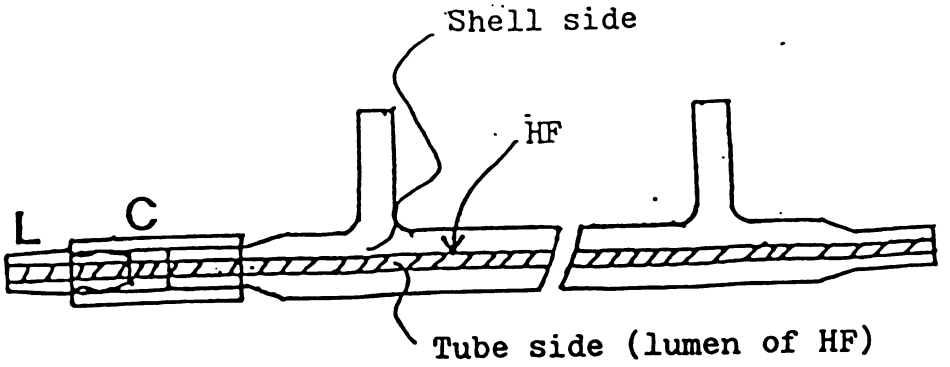

Figure 13: Single Fiber Reactor (SFR) - Shell material is boro-silicate glass, 21.5 cm overall length, 0.8 cm O.D., tapered to 0.5 cm diameter x 1 cm length, end tubes with side tubes 0.5 cm dia. x 1.5 cm length; fittings illustrated on left were applied to both ends of the reactor: L = male and Female Luer lock fittings; C = Tygon tube; HF = Hollow ultrafiltration-fiber. The hollow fiber was retained by a plug of epoxy potting resin (Dow Chemical) between the Luer fittings and the hollow fiber.

backflush loading and ultrafiltration had any negative effects on the enzyme reactivity. The activity of catalase in samples was determined by the rate of reaction at a hydrogen peroxide concentration of 30 mM as described in Chapter 3. These reaction rates were determined relative to the catalase stock solution. L-lysine α-oxidase activity in samples was measured by the method described in Chapter 3 and was compared to the activity of the stock solution.

Enzyme activity was measured in units of μmols of substrate reacted per minute per mg of enzyme. The total activity in an experimental solution was found by multiplying the measured activity by the mass of enzyme in the sample.

Experimental Procedure

The experiments described in this section were conducted to determine which fiber performed best for the co-immobilization of catalase and lysine α-oxidase. In all experiments the SFR system was flushed with buffer before enzyme loading. A syringe containing approximately 15 ml of enzyme was mounted on a syringe pump (Sage Instruments, Model 341A) and attached to one of the shell-side ports of the SFR. The pump was turned on with the SFR held in a vertical position to help eliminate the formation of air bubbles and was allowed to operate until the shell-side of the reactor was filled with enzyme solution. After clamping the SFR in a horizontal position, the remaining shell-side port and one of the tube-side ports were closed creating the backflush loop. Backflush effluent from the remaining tube-side outlet was collected in sample tubes. After enzyme loading, the reactor was drained, and the tube-side was rinsed with buffer. Approximately 20 ml of buffer was then forced through the fiber in ultrafiltration mode (Chapter 2). The ultrafiltrate was collected in four

4.0 ml fractions. The backflush effluent and ultrafiltrate fractions were analyzed for both protein content and enzyme activity.

It was believed that the best way to obtain a desirable enzyme distribution on the fiber of both catalase and lysine α-oxidase was to load one enzyme solution that contained an appropriate mixture of both enzymes. Since the Lowry method could not distinguish the two proteins, and because the retention of the enzymes could not be assumed to be additive, it was necessary to separate the catalase from the oxidase in the backflush effluents and ultrafiltrate fractions for individual analysis. Gel chromatography was chosen as the method of separation. The chromatography column was prepared before the experiment by pouring an Agarose A-0.5m (Bio-Rad, 100-200 mesh) slurry into a column (2.5 X 50 cm.) half filled with buffer, allowing the gel to settle, and washing afterwards with several column volumes of 0.1 M potassium phosphate buffer of pH 7.0. After developing the column with buffer, the sample was added to the top, with care being taken not to disturb the exposed gel surface. Since the catalase has a molecular weight of approximately 250,000, over double that of oxidase, it elutes from the column first. The eluent from the column was separated by a fraction collector (Isco, Cygnet model) into 100 3.0 ml samples. The absorbance of these samples were measured at 280 nm to determine which ones contained protein [41]. It was found that the samples separated into three protein peaks. Samples within these peaks were then assayed for total protein concentration and enzyme activity by the methods discussed previously. The first two peaks, which overlapped, contained catalase indicating that there might be two different isomers of catalase in the stock solution. The final peak, which was distinct, contained L-lysine α-oxidase.

Results

Material and activity balances around the fibers were used to determine the loss of enzyme due to loading on the fibers. The amount lost, L, was calculated according to the following equation [42]:

$$L = C_0V_0 - (C_BV_B + C_FV_F) \quad (22)$$

where C_0 is the concentration of enzyme in the stock solution; V_0 is the volume of the enzyme stock solution; C_B is the concentration or activity of enzyme in the backflush loading effluent; V_B is the volume of the backflush effluent; C_F is the concentration or activity of protein in the ultrafiltrate; and V_F is the volume of the ultrafiltrate. Comparing loss of activity with loss of enzyme protein permitted assessment of enzyme inactivation on the fibers.

Catalase Retention in PM30 Fibers

Fifteen ml of a solution containing 50 units of catalase in buffer was prepared for backflush loading. The enzyme solution was loaded in the manner discussed above, and the effluent and ultrafiltrate were assayed. It was found that the fiber retained approximately 90% of the protein loaded. However, no protein was found in the ultrafiltrate indicating that this enzyme could not be recovered from the fiber for reuse by ultrafiltration. Further studies were carried out with the catalase/PM30 fiber by loading the enzyme and filling the lumen of the SFR with a 30.0 mM solution of hydrogen peroxide. After 2.0 hours, the reactor was drained and the solution was assayed for hydrogen peroxide. It was found that no detectable conversion of H_2O_2 took place in the SFR. This result led to the conclusion that the PM fiber interacted with catalase in a way to

completely inactivate the enzyme. Therefore, this type of fiber could not be used for the system under investigation.

Enzyme Retention in PA Fibers

Because experiments showed that the PM30 fiber was not suitable for the immobilization of either of the enzymes, studies were conducted to determine the ability of the PA fibers to entrap catalase and lysine α-oxidase. Results for the PA30 fibers showed that 80.3% of the catalase and 85.7% of the oxidase in the enzyme stock solutions that were backflushed onto the fiber were detected in the backflush effluent. This indicated that the effective pore size of the fiber was too large for the enzymes, and only a minimal amount of the proteins was retained.

PA10 fibers were then tested for their ability to retain the enzymes. Fifteen ml of an enzyme solution containing 50 units of catalase was backflush loaded. The effluent was assayed and it was found that it contained 15.9% of the total amount of the catalase that was loaded and that the enzyme was 100% active. Buffer was then flushed through the system in ultrafiltration mode. Almost complete recovery of the catalase was accomplished, and the enzyme in the ultrafiltrate was 100% active. Similar results were obtained using L-lysine α-oxidase; the fiber retained 80.3% of the enzyme that was loaded, and the lysine α-oxidase in the backflush effluent and the ultrafiltrate displayed no loss in activity. Additional experiments determined that a particular fiber's ability to entrap the enzymes increased with successive loadings. Approximately 86% of either enzyme that was loaded could be retained in a well conditioned PA10 fiber.

The final experiments conducted in this section involved the co-immobilization of lysine α-oxidase and catalase onto a PA10 hollow fiber.

Ten ml of a solution containing 50.0 units of both enzymes was backflush loaded onto the fiber, and the effluent was collected. After loading, buffer was pumped through the fiber in ultrafiltration mode resulting in four 4.0 ml fractions. In order to determine the total amount of protein in the ultrafiltrate these fractions were combined, and both this solution and the backflush effluent were passed through a gel chromatography column in the manner described earlier. Because the separation resulted in diluting the samples beyond the concentration range that could be determined accurately by the Lowry method, the samples were first spiked with 30 μg/ml of the appropriate enzyme. This "spiking" method was determined to be accurate by testing it on known concentrations of both enzymes.

It was found that 86.3% of the catalase and 82.8% of the oxidase were retained by the PA10 fiber. These experiments were repeated using catalase to lysine α-oxidase ratios of 1:2 and 2:1. Approximately the same percentage of the enzymes was retained for all cases regardless of the loading ratio. Because of the time-consuming nature of gel chromatography, these numbers were generally assumed for the remainder of the experiments conducted, but were checked periodically.

From the experiments conducted in this chapter, it was determined that the PA10 fibers would be used for all remaining experiments due to this fiber's compatibility with and ability to retain the enzymes being studied. With the selection of the appropriate fiber type, the performance of an immobilized enzyme reactor could be investigated.

CHAPTER 6

REACTOR OPERATION

Introduction

The objective of the experiments described in this chapter was to determine the optimum conditions needed in the reactor system to maximize the amount of lysine converted. PA10 single fiber reactors described in Chapter 2 were used. Manufacturer's specifications list fiber dimensions at 1.118 mm inner diameter, 2.007 mm outer diameter, and an inner membrane thickness between 0.1 and 1.0 μm. Two different reactors were used to evaluate the effects of reactor length on conversion. One SFR had an effective length of 21.5 cm and a surface area of 7.55 cm^2, while the other reactor's length and area were 44.0 cm and 15.45 cm^2, respectively.

The SFR was installed in a laboratory reactor system (Figure 14). The fluid conducting elements of the system consisted of Tygon tubing (3/16 inch i.d.) with polyethylene T and quick-disconnect connectors at the junctions. All tubing was wrapped with foam insulation. Valves at the junctions were adjusted to determine the circulation pattern. Both the reservoir and the reactor were held at 37°C in a shaker water bath (Lab Line,Inc., Model 3540).

Before and after each use, the SFR was cleaned and sanitized according to manufacturer's instructions. Cleaning consisted of three cycles: an acid cycle (pH 2-3, 0.045 M H_3PO_4, 0.10 M KH_2PO_4), a base cycle (1% NaOH), and a sanitizing cycle (200 ppm NaOCl). The protocol for each cycle was as follows: 1) pumping approximately two reactor volumes of the appropriate liquid through the lumen to the outlet port, 2) pumping through the shell-side to the shell outlet port, 3) ultrafiltering and recirculating several reactor volumes (P1, P4,and recycle open, see Figure 14). Cleaning usually

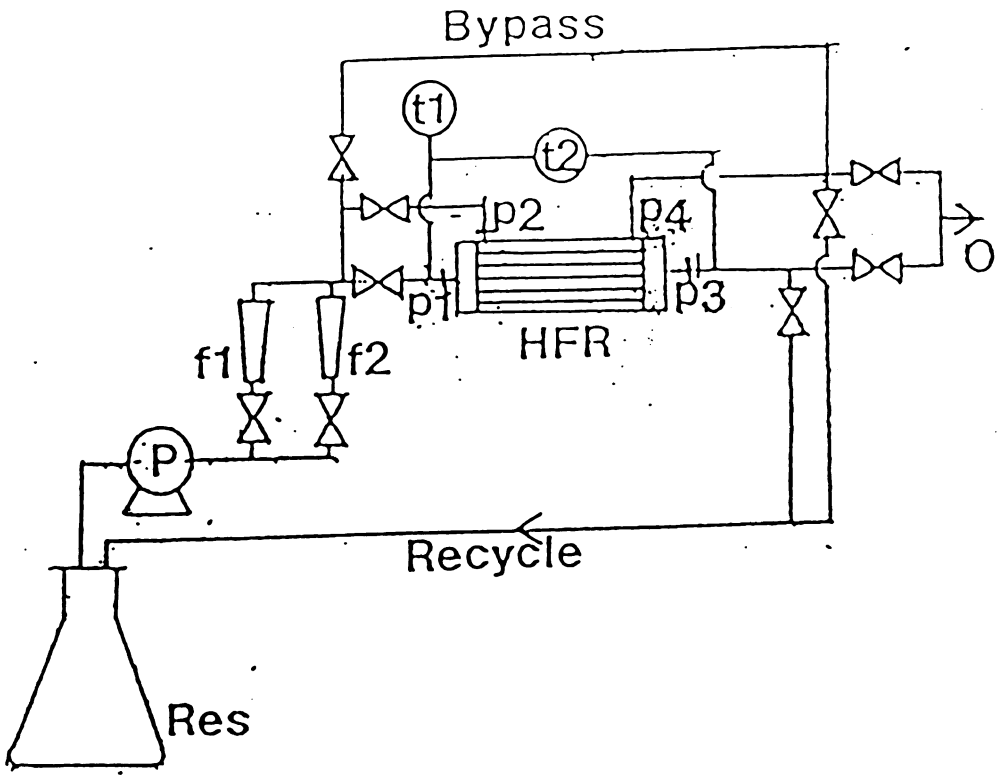

Figure 14: Hollow Fiber Reactor System (HFR)- Res = Reservoir flask, P = Gear or Peristaltic pump (Cole Palmer model# 7520-25 unified drive; Cole Palmer #7520-25 head); f1, f2 = flowmeters (Cole Palmer #FM044-40 and #FM102-5); p1 = lumen side inlet port; p2 = shell side inlet port; p3 = lumen outlet port; p4 = shell side outlet port; t1 = 15 psig pressure transducer (Omega #PX142-015G5V); t2 = 5 psi differential pressure transducer (Omega #PX142-005D5V); O = Outlet sample port; X = Tubing clamps - stops flow (from [41]).

included backflushing acid and sanitizing solutions (P2 and P3 open). After each cycle, all loops of the system were flushed with approximately two system volumes of distilled water.

During reactor experiments, the shell-side of the system was closed. The reservoir contained 120 ml of a 0.2 mM lysine solution. With the recycle loop opened, the solution was pumped from the reservoir through the fiber lumen. To collect samples, the recycle loop was closed and the sample port was opened.

After an experimental run was completed, the exact flow rate was determined by timing the collection of liquid in a graduated cylinder. The samples were then assayed for lysine content by the spectrophotometric technique described in Chapter 3. It was discovered that the samples from the reactor system contained unidentified foreign particles that caused light scattering during the spectrophotometric analysis. It was therefore necessary to filter the samples before assaying; membrane filters (0.2μm) of cellulose acetate were used. The samples were forced through the filters by a syringe, and the filtrate was free of particles and could be assayed with the spectrophotometric method without interference. Volume losses associated with the filtration step were accounted for in the calculation of lysine concentration in the samples collected during reactor operation.

Factorial Design

The SFR reactor operation was studied using a 2^4 factorial design. This design used the conversion of lysine after four hours as the observed response. The design matrix is represented in Table 7. Four operating parameters were evaluated for their effects on conversion; flow rate,

reactor length, the number of units of oxidase loaded, and the catalase/oxidase loading ratio.

Yates's algorithm (Chapter 2) was applied to the results of the experiments after they had been arranged in standard order. These calculations for the reactor system data are shown in Table 8. Column y contains the percent of lysine converted for each experiment, and the remainder of the matrix columns were obtained in the manner described in Chapter 2. The estimate column represents the estimate of the effect of the variables on the conversion of lysine. The first estimate is the grand average of all the observations. The remaining effects are identified by locating the plus signs in the design matrix. Thus, in the third row a plus sign occurs only in the oxidase column, so that the effect in that row is the lysine α-oxidase effect. In the seventh row, plus signs occur in both the oxidase and catalase columns, so that the effect in that row is the interaction between these variables.

From the algorithm, it is seen that each of the variables being studied has a significant effect on the observed response of the reactor system. It is also seen that the major variable interactions are between the amount of catalase and oxidase used and between the reactor length and amount of lysine α-oxidase loaded. In order to determine the optimum operating conditions, a more detailed investigation on the effect of the variables on lysine conversion was conducted.

Operating Charateristics

Effect of Flow Rate

In order to determine the effect of flow rate on the conversion of lysine, all other variables were held constant. The 21.5 cm long reactor was used with 40 units of lysine α-oxidase and no catalase loaded on the

Table 7
Design Matrix for SFR Experiments

Experiment #	A	B	C	D	Variable	-	+
1	-	-	-	-	**A** flow rate (ml/min)	3.0	9.0
2	+	-	-	-	**B** oxidase (units)	15	30
3	-	+	-	-	**C** catalase/oxidase	0	2/1
4	+	+	-	-	**D** reactor length (cm)	21.5	44.0
5	-	-	+	-			
6	+	-	+	-			
7	-	+	+	-			
8	+	+	+	-			
9	-	-	-	+			
10	+	-	-	+			
11	-	+	-	+			
12	+	+	-	+			
13	-	-	+	+			
14	+	-	+	+			
15	-	+	+	+			
16	+	+	+	+			

Table 8
Yate's Algorithm for the SFR Experiments

Expt. #	% conversion y	(1)	(2)	(3)	(4)	Divisor	Esti-mate	I.d.
1	14.54	37.75	76.5	172.96	364.4	16	22.77	ave
2	23.21	38.75	96.5	191.42	67.0	8.0	8.44	A
3	15.08	41.93	86.9	32.52	40.04	8.0	5.01	B
4	23.67	54.53	105.0	34.98	-3.94	8.0	-0.49	AB
5	17.25	36.83	12.26	13.60	38.46	8.0	4.80	C
6	24.68	49.63	15.26	26.44	-7.94	8.0	-0.99	AC
7	23.35	40.65	20.46	-0.40	22.46	8.0	2.81	BC
8	31.18	64.31	14.52	-3.54	-3.14	8.0	-0.39	ABC
9	13.40	8.67	1.0	19.96	18.46	8.0	2.31	D
10	23.43	8.59	12.60	18.50	2.46	8.0	0.31	AD
11	19.46	7.43	12.80	-2.0	12.84	8.0	1.60	BD
12	30.03	7.83	23.66	-5.94	-3.14	8.0	-0.39	ABD
13	15.71	10.03	-0.80	11.6	-1.46	8.0	-0.18	CD
14	24.94	10.43	0.40	10.86	-3.94	8.0	-0.50	ACD
15	29.51	9.23	0.40	1.20	-0.74	8.0	-0.09	BCD
16	34.80	5.29	-3.94	-4.34	-5.54	8.0	-0.69	ABCD

hollow fiber. The flow rate was adjusted by changing the setting on the pump and was measured by timing the collection of liquid in a graduated cylinder both before and after an experimental run. Samples were taken every thirty minutes and were assayed for lysine content. The results of these studies are shown in Figures 15 and 16. For the single fiber reactor, a flow rate change from 3 to 9 ml/min gave an increase from 12% to 22% in lysine conversion. The conversion leveled off at 22% despite further increases in flow.

The Effect of L-lysine α-oxidase

For the experiments described in this section, the flow rate was kept constant at 9 ml/min, a reactor length of 21.5 cm was used, and no catalase was present. The amount of lysine α-oxidase that was loaded on the fiber was varied from 15 to 60 units. The results of this investigation are shown in Figure 17. It is seen that the amount of lysine converted reached an optimum level when 30 units of L-lysine α-oxidase was loaded. Additional enzyme had no effect on the conversion of lysine. This corresponds to an optimum loading of 3.97 units/cm^2, which was verified in experiments using the longer reactor.

The Effect of Catalase

Initial studies of SFR performance were conducted by Paula McMahon [43]. In these studies, large discrepencies were observed in the amount of lysine conversion expected and that obtained in the SFR. This was suspected to be due to the deficiency of oxygen within the hollow fiber walls which may occur as the reaction proceeds. The reaction therefore may become oxygen limited. In addition to eliminating the cytotoxic effect of hydrogen peroxide in blood, it was thought that the addition of catalase

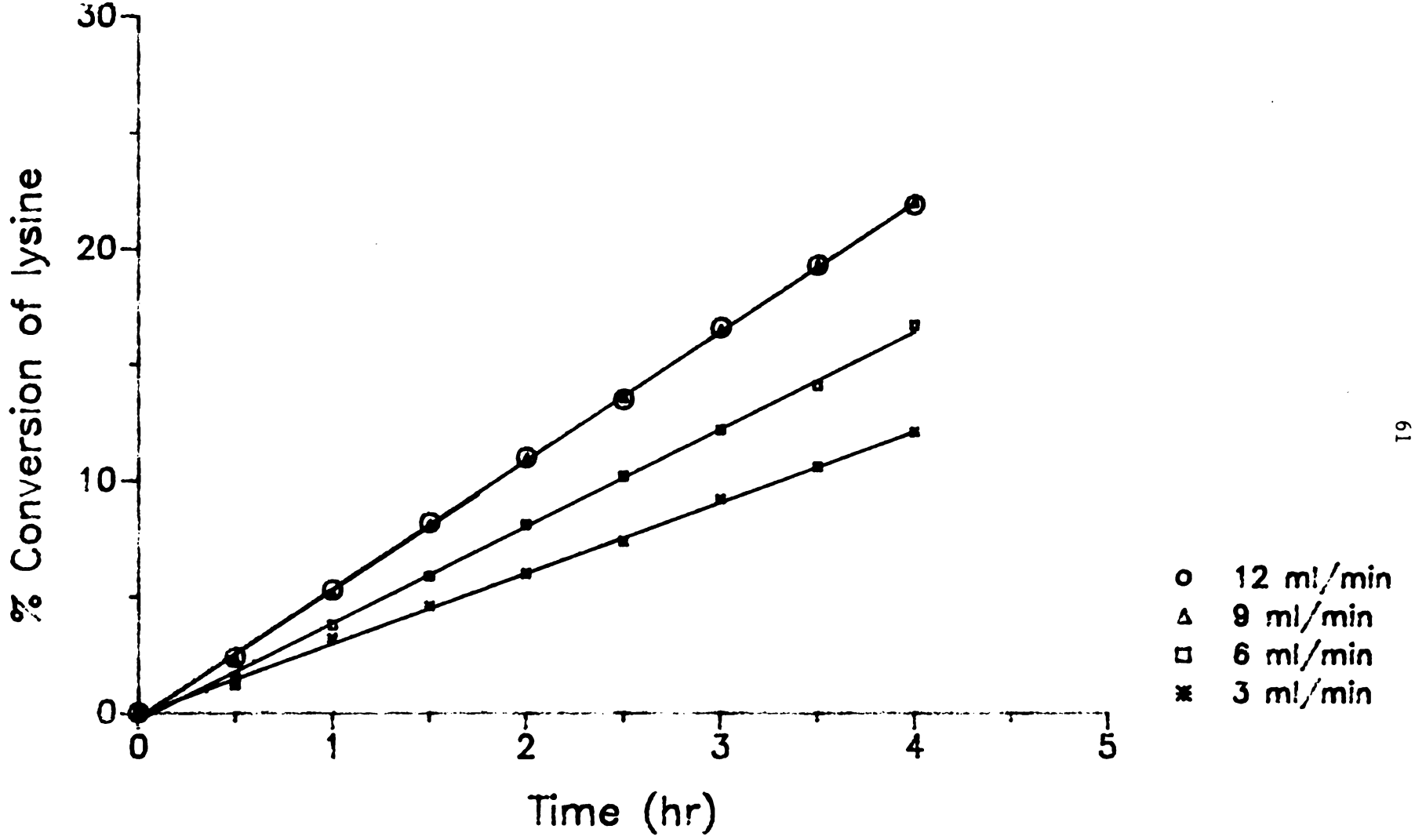

Figure 15– % conversion of lysine vs. time for various flow rates .

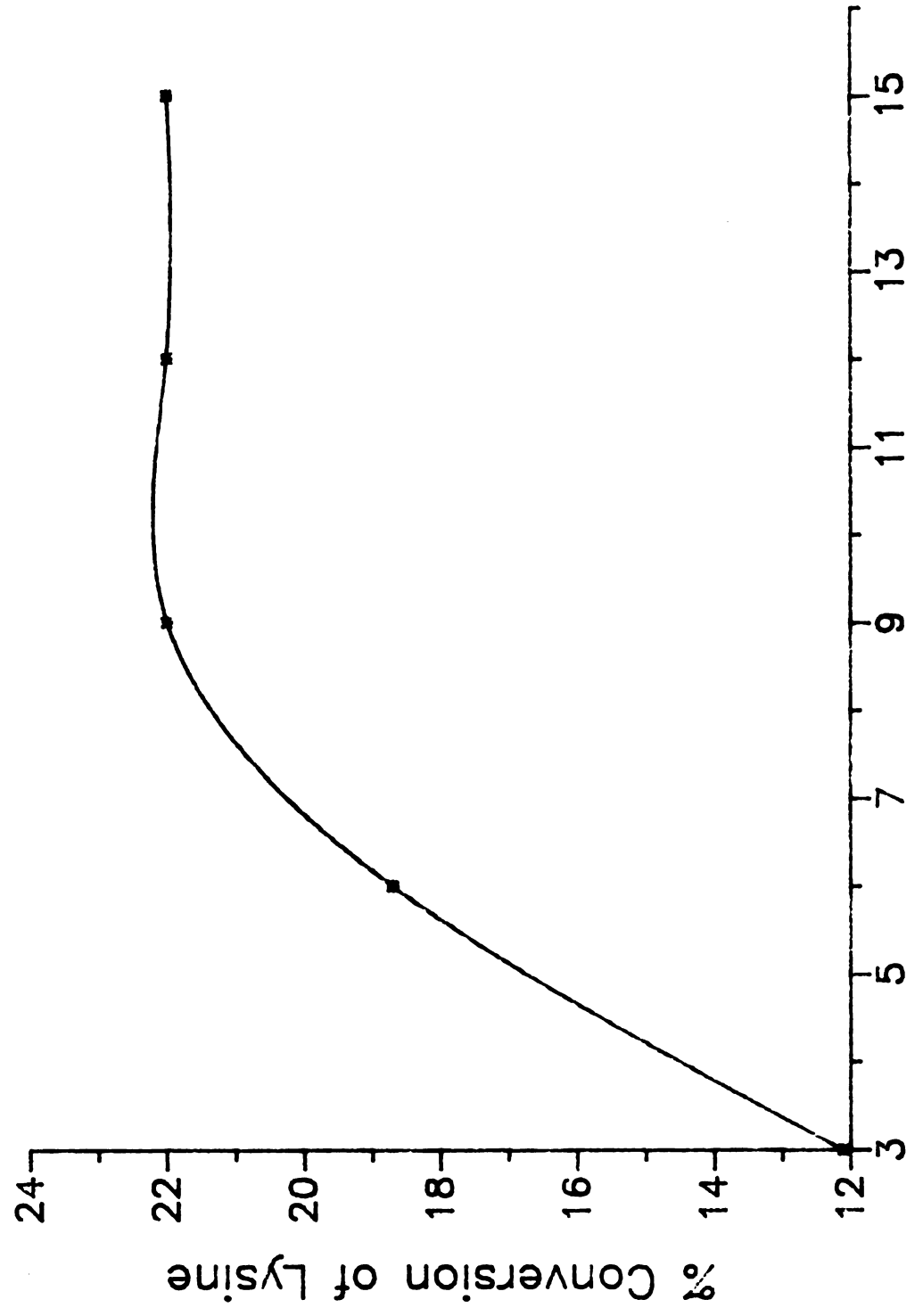

Figure 16– % conversion of lysine vs. flow rate (40 units of oxidase, no catalase)

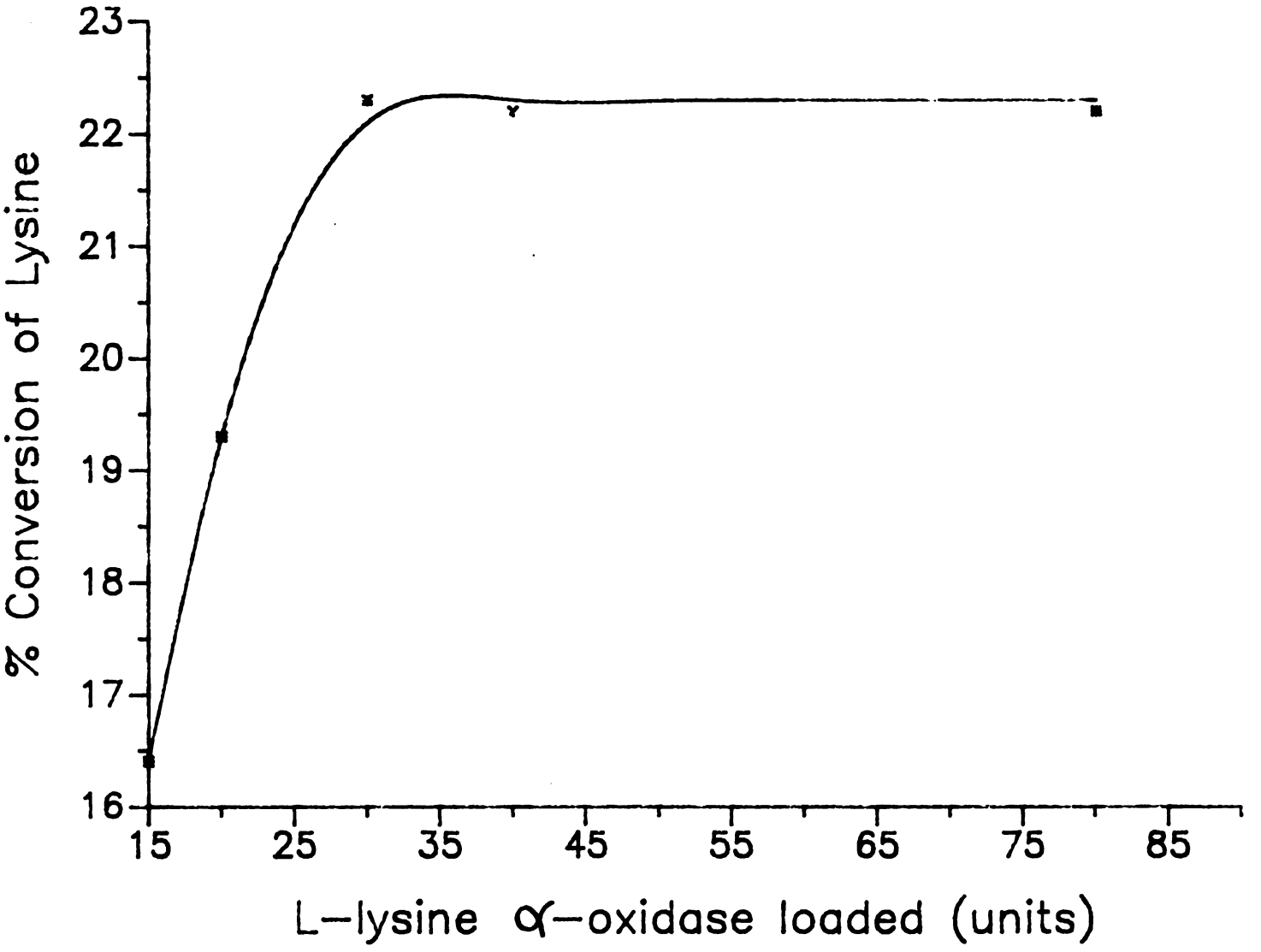

Figure 17- % conversion of lysine vs. units of L-lysine α-oxidase loaded (9 ml/min, no catalase)

could also affect the amount of lysine converted by removing one of the products (H_2O_2)
and providing oxygen for further consumption. This effect was described in more detail in Chapter 4. For the experiments conducted in this section, a reactor of length 21.5 cm, the optimal lysine α-oxidase loading of 3.97 units/cm^2, and a flow rate of 9 ml/min were used. The ratio of catalase to oxidase was adjusted by altering the relative concentration of the enzymes in the stock solution that was backflush loaded on the SFR. This ratio was varied from 0.5:1 to 4:1 (unit basis). Results of this study are shown in Figure 18. An increase in catalase caused an increase in the efficiency of the reactor until the optimum ratio of 2.5:1 was reached. It appears that too much catalase can cause an inhibitory effect that lowers the conversion of lysine. This could be due to a "crowding" effect which is explained later in this chapter.

Optimum Operating Conditions

The experiments conducted in this section were used to determine the optimum operating conditions for the single fiber reactor. To summarize the results described above, the optimum flow rate, lysine α-oxidase loading, and catalase to oxidase loading ratio were found to be 9.0 ml/min, 3.97 units/cm^2, and 2.5:1, respectively. In addition, the use of a longer fiber (44.0 cm) gave increased conversions over the 21.5 cm reactor. At optimum conditions, the 44.0 cm reactor converted 34.8% of the lysine in four hours as compared to 31.8% for the shorter reactor. These optimum operating conditions were used as a basis for reactor scale-up to be described in Chapter 7.

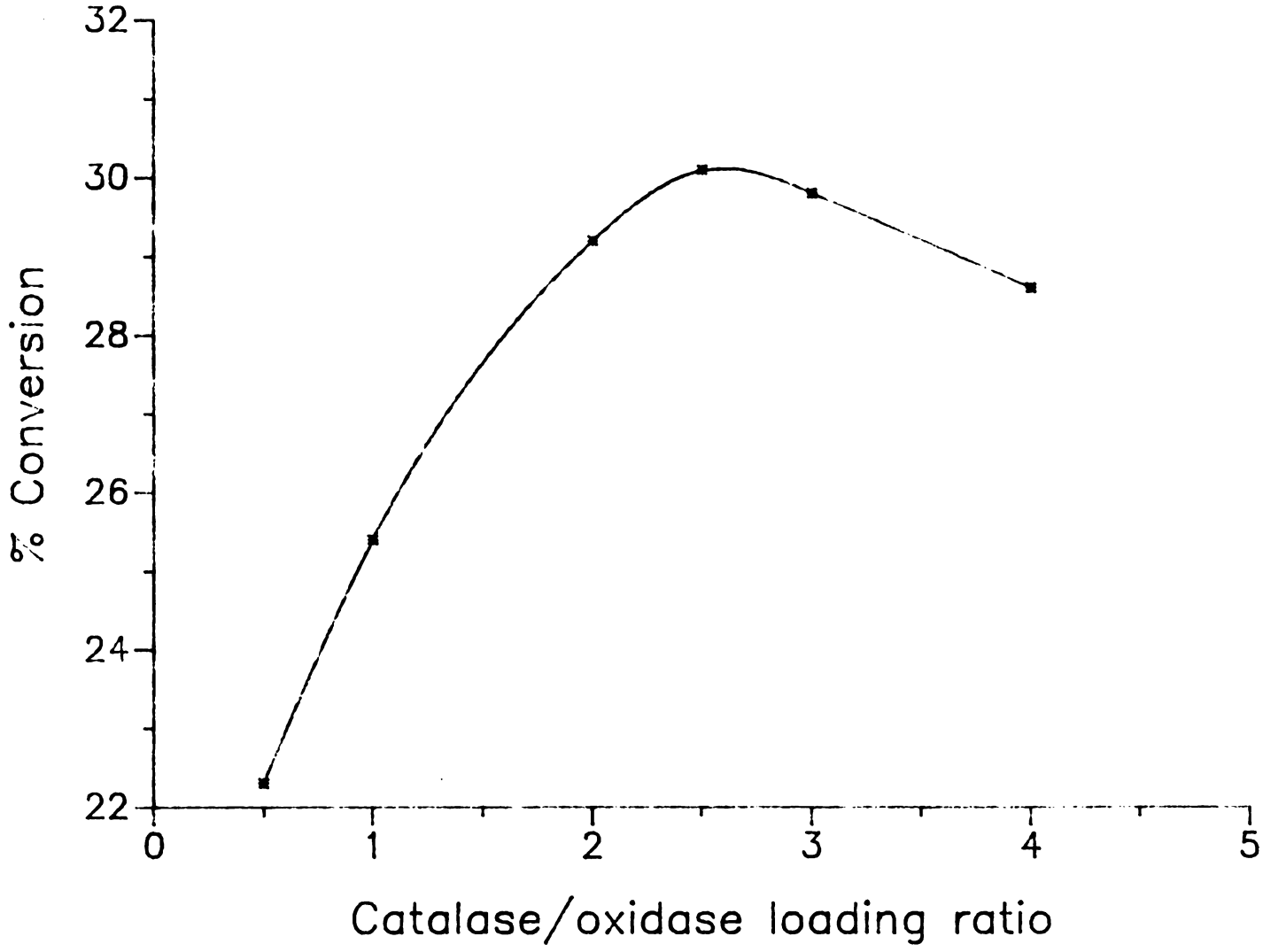

Figure 18– % conversion of lysine vs. the catalase to lysine ∝–oxidase loading ratio (flow rate = 9 ml/min, 30 units of oxidase loaded on fiber)

Enzyme Stability

In order for a hollow fiber reactor cartridge to have practical applications in medical treatments, extended storage of the cartridge with the loaded enzyme must be possible. The retention of lysine α-oxidase activity upon immobilization in the fiber was evaluated. Two storage procedures were tested; 1) storage in reactor with 0.2 mM lysine solution in the lumen, and 2) storage without the lysine solution. The reactors were operated under optimum conditions after storage, and the conversion of lysine after two hours of operation was determined. After each experiment, the reactor was stored in a refrigerator for five days before its next use. From Figure 19, it is seen that after 30 days, the enzyme retained 82% of its original activity on the fiber that was stored with lysine and 67% of its original activity without lysine.

Enzyme Immobilization and Localization

Localization of enzyme affects the parameters in modelling of immobilized reactor operation. Therefore, the effects of two different lysine solution flow regimes on the distribution of enzyme in the fiber wall were evaluated. In order to accomplish this, L-lysine α-oxidase was labelled with flourescein isothiocyanate dye (Sigma, catalog No. F-7250) in the following manner. A mixture of 200 units of enzyme in 5.0 ml of 0.1 M potassium phosphate buffer (pH 7.0) and 5.0 mg of the dye was shaken by hand for approximately three minutes. The mixture was then centrifuged for three minutes, and the supernatant was poured into a column of agarose beads similar to the gel chromatography column described in Chapter 5. A separation of the fluorescent protein from the inert dye was observed. The yellow dyed protein band eluted from the column first and was collected using a fraction collector (Isco, Cygnet Model). The fractions containing

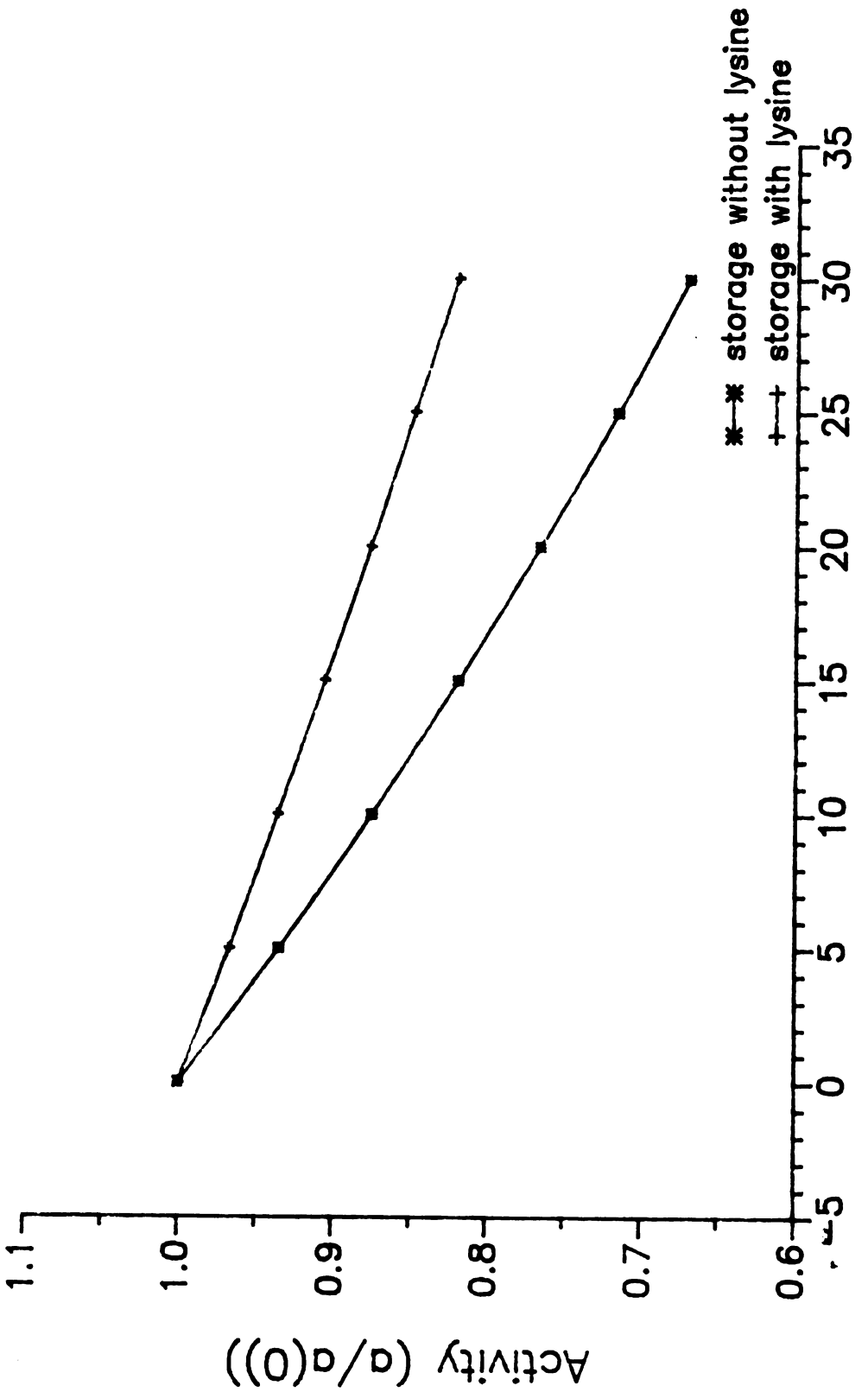

Figure 19— change in relative enzyme activity during storage

the labelled protein were combined to yield approximately 50 ml of protein solution.

The labelling of the enzyme enabled its visualization in the immobilized state under ultraviolet light. Under normal flow conditions (e.g. 9 ml/min flow), no discernable movement of enzyme in either the axial or radial direction of the SFR was detected after four hours of operation. In experiments done with pulsatile flow in the lumen, the amplitude of the pulse was limited due to the eventual radial flux of enzyme in the fiber wall. This set pulse amplitude limits for the experiments described in the following section.

Pulsatile Flow

In normal hollow fiber operation the amount of lysine that can be converted is limited by its rate of diffusion through the hollow fiber wall to the enzyme. Lewis and Middleman [25] reported that diffusion was apparently the dominant mechanism for substrate transport in hollow fiber systems. This is also verified by the modeling results presented later in this chapter. The reactor productivity could be increased in proportion to the increase in the amount of enzyme per unit area of membrane in the reactor if diffusion limitations could be eliminated. This objective could be accomplished by forcing the substrate to flow convectively into the fiber wall.

Recently several investigators have shown that pulsatile flow, or ultrafiltration swing, in a membrane-enzyme reactor may improve the performance of the reactor as compared to the steady flow operation [44-46]. The pulsatile flow process essentially involves the same basic reactor system shown in Figure 14, but two pumps are used to pump feed through the SFR at different flow rates and a third pump is added as a

withdrawal pump. The withdrawal pump guarantees the maintenance of the average flow rate throughout the reactor system. The effect of the higher flow rate half-cycle of the pulsatile flow is to increase the transmembrane pressure drop across the fiber wall. The increase in pressure drop increases substrate transport into the immobilized enzyme region. The second half-cycle at the lower flow rate decreases the pressure drop to allow product to be transported back into the feed stream. The ultrafiltration swing can cause an increase in the conversion of substrate by virtually minimizing limitations in a hollow fiber reactor system.

The schematic representation of the experimental apparatus used to determine the effect of pulsatile flow in the lysine α-oxidase/catalase SFR system is shown in Figure 20. The optimum values of seventy-five units of catalase and 30 units of oxidase were loaded in the hollow fiber. Substrate solution was delivered to the tube-side in two modes. When the reactor was operated without the ultrafiltration swing, only one of the inlet pumps was used to feed the substrate into the reactor. A three-way valve was rotated such that the outlet pump was bypassed, and the reactor effluent was recycled back to the reservoir. For pulsatile operation, the three-way valve was turned towards the outlet pump, and the outlet flow rate was set at 12 ml/min, the mean value of the pulsatile inlet flow rate. A timer (Fisher Scientific, Model CD-4) was used to switch between one inlet pump (set at a flow rate greater than 12 ml/min) and the other (set at a flow rate less than 12 ml/min) periodically to produce a pulsed inlet flow. The concentration of lysine in the reservoir was determined every thirty minutes, and the total conversion of lysine after four hours was compared for reactors operating with and without pulsatile flow.

The results of the pulsatile flow experiments are shown in Table 9 below:

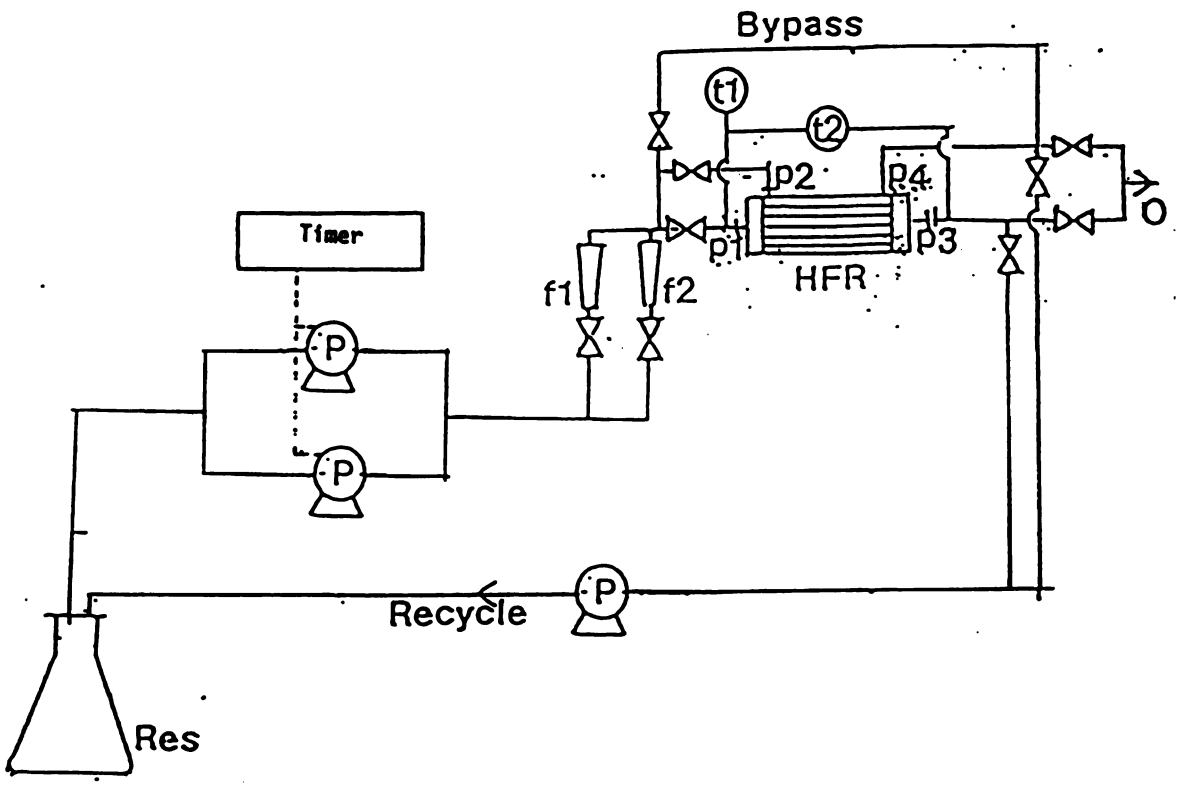

Figure 20: Hollow Fiber Reactor System (HFR) With Pulsatile Flow- Res = Reservoir flask, P = Gear or Peristaltic pump (Cole Palmer model# 7553-00 unified drive; Cole Palmer #7015-20 head); Timer (Chrontrol CD Model); f1, f2 = flowmeters (Cole Palmer #FM044-40 and #FM102-5); p1 = lumen side inlet port; p2 = shell side inlet port; p3 = lumen outlet port; p4 = shell side outlet port; t1 = 15 psig pressure transducer (Omega #PX142-015G5V); t2 = 5 psi differential pressure transducer (Omega #PX142-005D5V); O = Outlet sample port; X = Tubing clamps - stops flow.

Table 9
Results of Pulsatile Flow Experiments

	case 1	case 2	case 3	case 4	case 5
Flow rate Pump 1(ml/min)	12.0	13.5	15.0	16.5	18.0
Flow rate Pump 2(ml/min)	0.0	10.5	9.0	7.5	6.0
Pressure in lumen High flow (psig)	1.25	1.40	1.56	1.71	1.87
Pressure in lumen Low flow (psig)	----	1.09	0.94	0.78	0.62
% conversion of lysine	34.8	36.9	40.0	35.4	22.1

When the two inlet pumps were set at 15 and 9 ml/min, pulsatile flow gave an increase in conversion of 15% over normal flow conditions. Pulsatile flow at a larger amplitude swing, 18 to 6 ml/min, resulted in decreased conversion. The reason for this was due to the leakage of enzyme caused by the transmembrane pressure drop associated with the pulsed flow.

Evaluation of Intrinsic Immobilized Kinetics

One of the more important concerns in the development of a hollow fiber reactor system is the effect that the immobilization has on the intrinsic kinetics of the enzymes. The rate of the reaction occurring in the hollow fiber is represented by:

$$\text{Rate of reaction} = - V_{res} \cdot \frac{dS}{dt} = \frac{E\,(k[e]A)S}{K_m + S} \qquad (23)$$

In this equation, V_{res} is the volume of the reservoir, K_m and $k[e]A$ (= V_{max}) are the intrinsic rate constants in which k is the turnover number, [e] is the amount of enzyme loaded per unit area of fiber, A is the total surface area of the hollow fiber (= $2\pi az$, see Figure 3) S is the substrate concentration in the lumen, and E is the effectiveness factor. The effectiveness factor depends on the generalized modulus, m, defined as [47]:

$$m = \frac{L\, r(S)}{\sqrt{2}} \left[\int_0^S D_s\, r(S)\, dS \right]^{-\frac{1}{2}} \tag{24}$$

where L is the characteristic length, r(S) is the intrinsic reaction rate (= $V_{max}S/(K_m+S)$), and D_s is the diffusivity of substrate.

Moo-Young and Kobayashi [48] have developed a simplified equation for the effectiveness factor in a hollow fiber membrane using a Michaelis-Menten type reaction with no inhibition which avoids the integration and solution of a more complex set of equations:

$$E = \frac{E_0 + \beta_1 E_1}{1 + \beta_1} \tag{25}$$

where

$$E_0 = \begin{cases} 1 & (0 \le m \le 1) \\ 1/m & (m > 1) \end{cases} \tag{26}$$

$$E_1 = \frac{\tanh m}{m} \tag{27}$$

and

$$\beta_1 = K_m / S \tag{28}$$

In deriving these equations, the mass transfer resistance in the membrane has been neglected. The hollow fiber reactor results presented by Waterland [23] that was discussed in Chapter 2 showed that this is a good simplifying assueptiOn. Equations (23-28) may be used in data analysis to evaluate the intrinsic immobilized kinetics of the hollow fiber reactor and the diffusion of lysine within the SFR as follows.

The enzymes were immobilized within the hollow fiber, and a 2.0 mM lysine solution was pumped through the lumen at 9 ml/min. Lysine conversion data were collected over a 48 hr period; the results are shown in Figures 21-23. The Patern computer program (see Appendix) is a subroutine that minimizes a cost function. This subroutine was used in a main program (see Appendix) to take an initial guess for K_m, V_{max}, and D_s and to evaluate the calculated reaction rates at several lysine concentrations from Equations (23-28). The calculated reaction rates were then compared to those obtained experimentally. The program was set up to minimize the sum of the square of the residuals between the observed and calculated reaction rates by adjusting the values of K_m, V_{max}, and D_s; the resulting fit was very good as seen in Figures A1-A3 in the appendix.

Three SFR cases were studied. In case 1, the reactor length was 21.5 cm, the amount of lysine α-oxidase loaded was 3.97 units/cm^2, and the catalase to oxidase ratio was 2.5/1. Case 2 was similar to case 1 except the amount of lysine α-oxidase loaded was 1.98 units/cm^2. Finally, case 3 used a reactor length of 44.0 cm and enzyme loading conditions similar to that of case 1. Cases 1 and 3 represent optimum enzyme loading conditions. The data from these studies are shown graphically in Figures (21-23). This information and the Patern subroutine were used to obtain the following

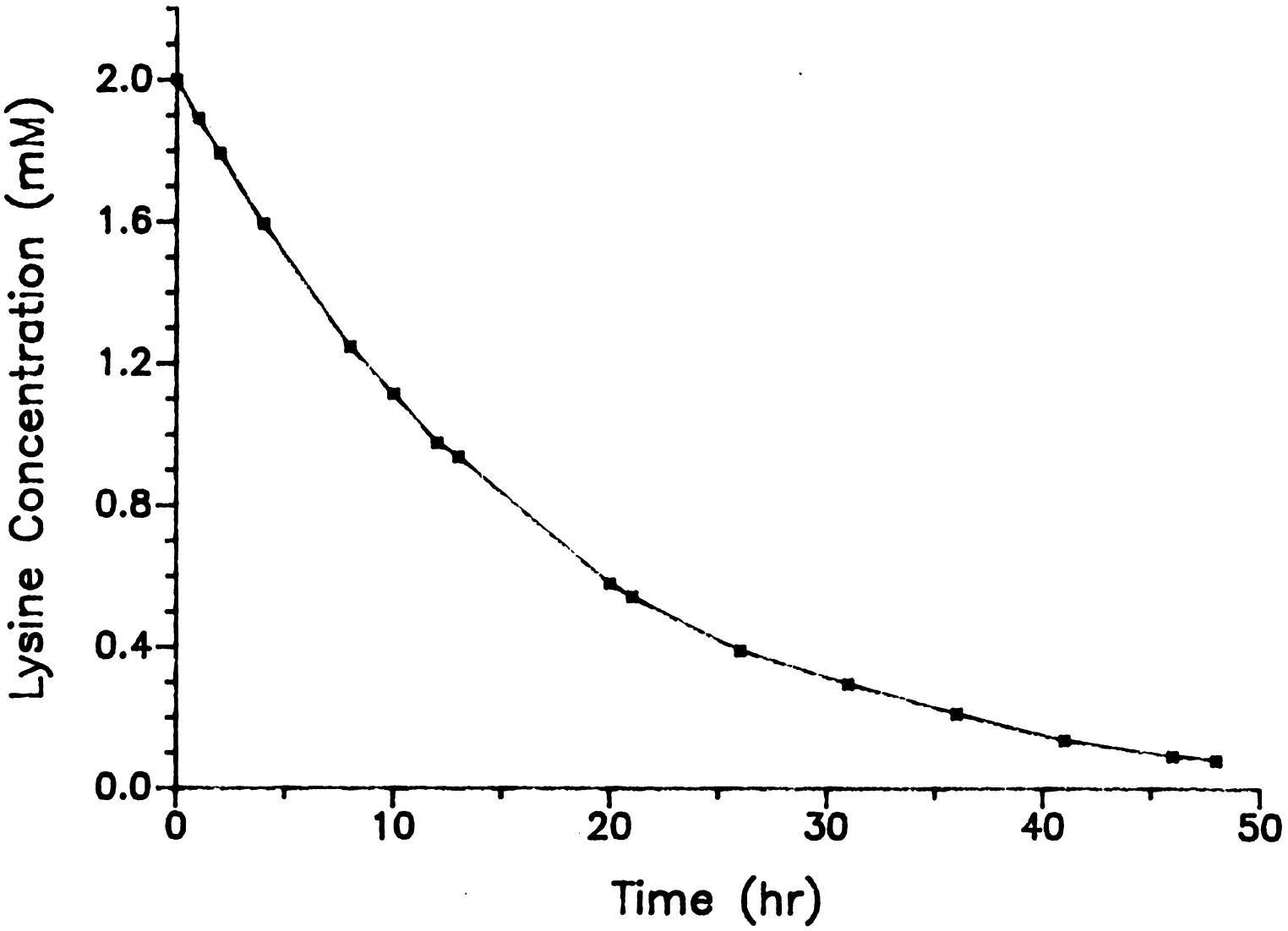

Figure 21— lysine concentration vs. time for case 1;reactor length = 21.5 cm, optimum loading

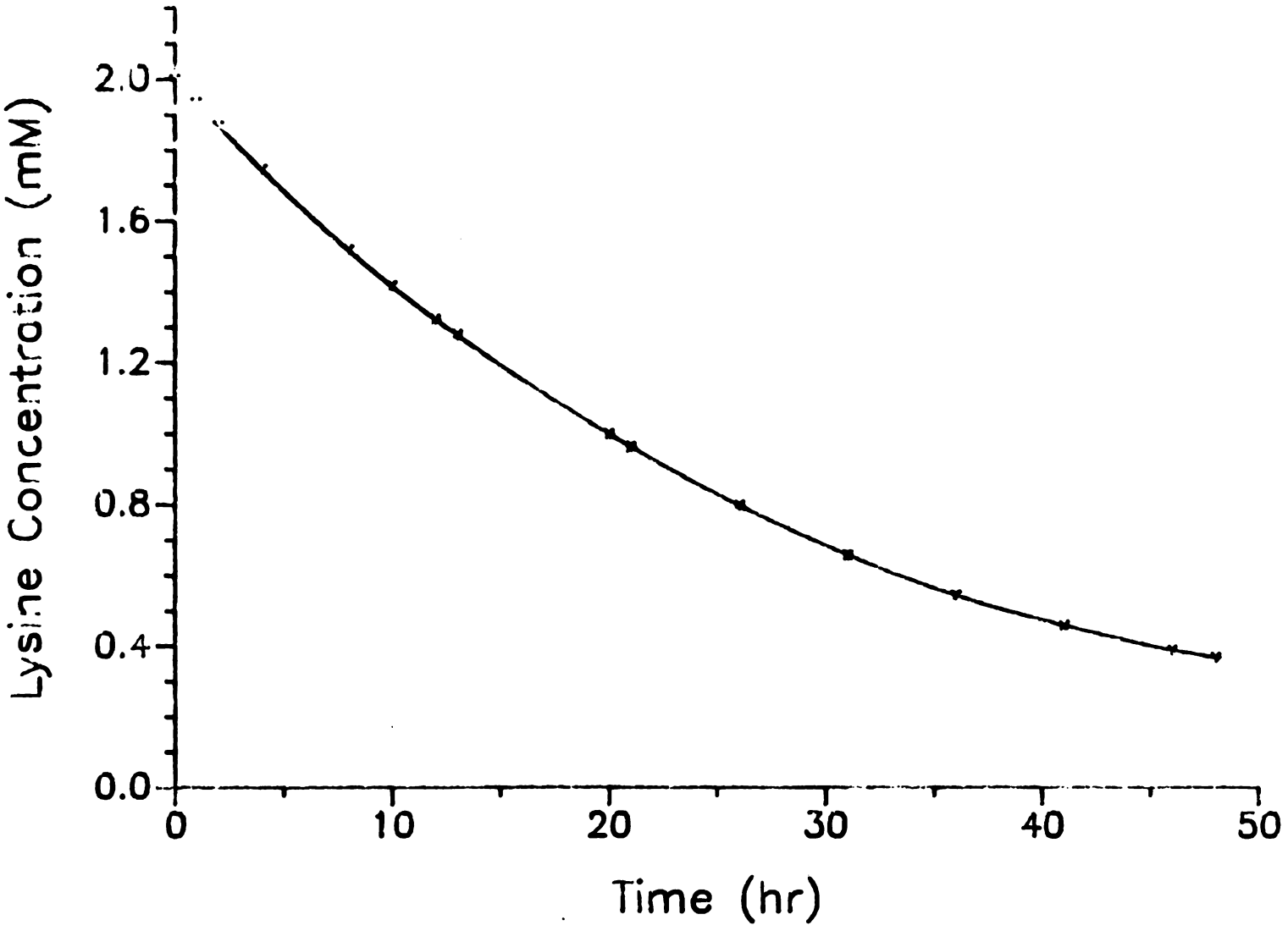

Figure 22– lysine concentration vs. time for case 2;reactor length = 21.5 cm, 50% optimum loading

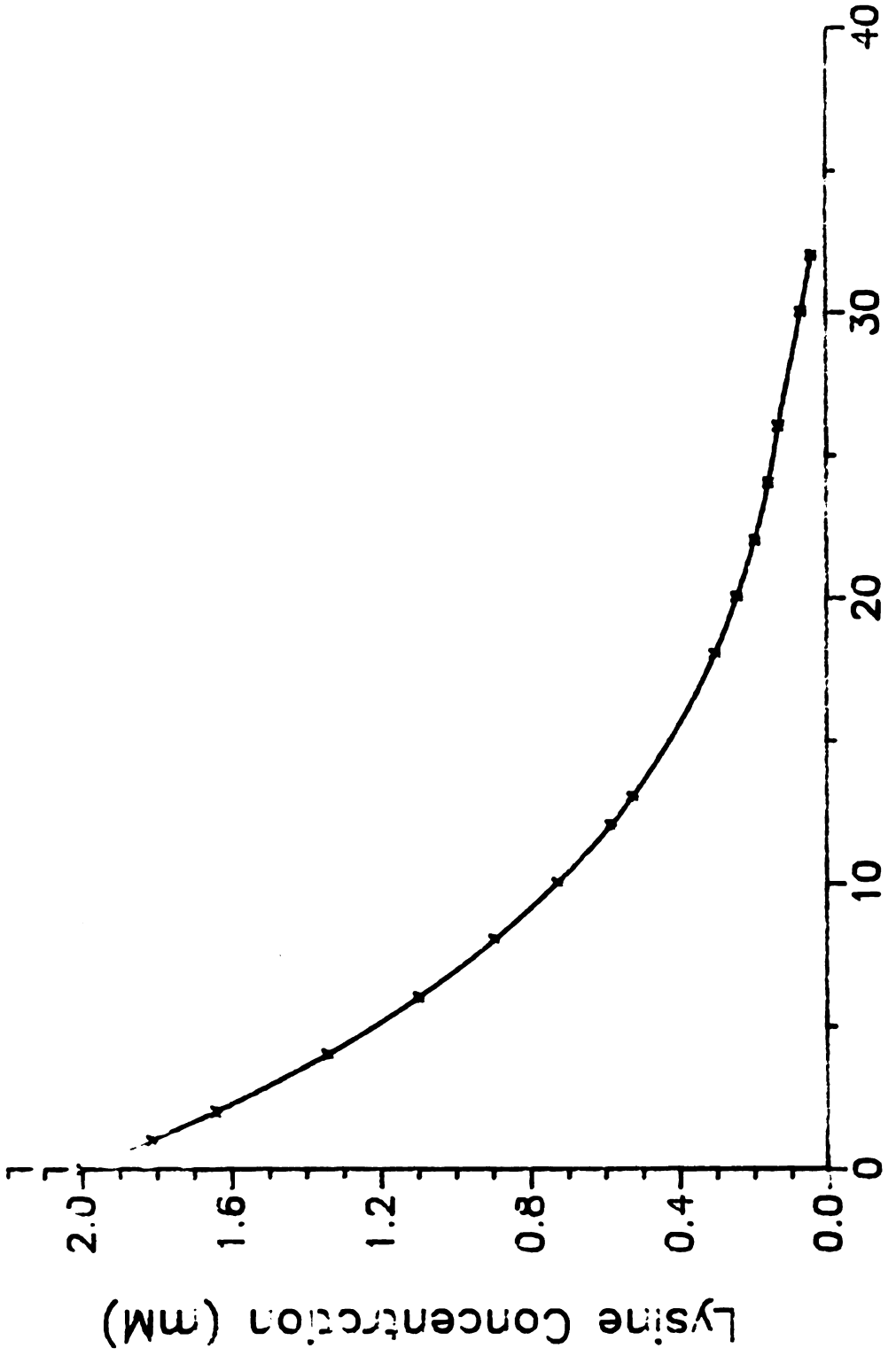

Figure 23– lysine concentration vs. time for case 3;reactor length = 44.0 cm, optimum loading

fitted kinetic results:

Case 1:

$k = 322.23\ min^{-1}$

$K_m = 7.0\ mM$

$D = 1.50 \times 10^{-7}\ cm^2/sec$

Case 2:

$k = 313.61\ min^{-1}$

$K_m = 7.15\ mM$

$D = 1.45 \times 10^{-7}\ cm^2/sec$

Case 3:

$k = 324.83\ min^{-1}$

$K_M = 6.90\ mM$

$D = 1.53 \times 10^{-7}\ cm^2/sec$

It is seen that the results of these experiments are in good agreement with each other. For these three cases, the average values of the kinetic parameters and the diffusivity of lysine could be used in Equations (24-28) to construct an effectiveness factor versus modulus curve (Figure 24). This information could be used in Equation (23) to calculate reaction rates at various lysine concentrations. Figures A1-A3 in the appendix show the comparison of the calculated reaction rates and the reaction rates obtained experimentally.

As discussed in Chapter 4, the k and K_m in free solution for lysine α-oxidase in the presence of catalase are approximately 7100 min^{-1} and 0.06 mM, respectively. The disparity between the immobilized and free solution kinetics may be due to a variety of factors. First, physical entrapment of the enzyme can cause a "crowding" effect which reduces the accessibility

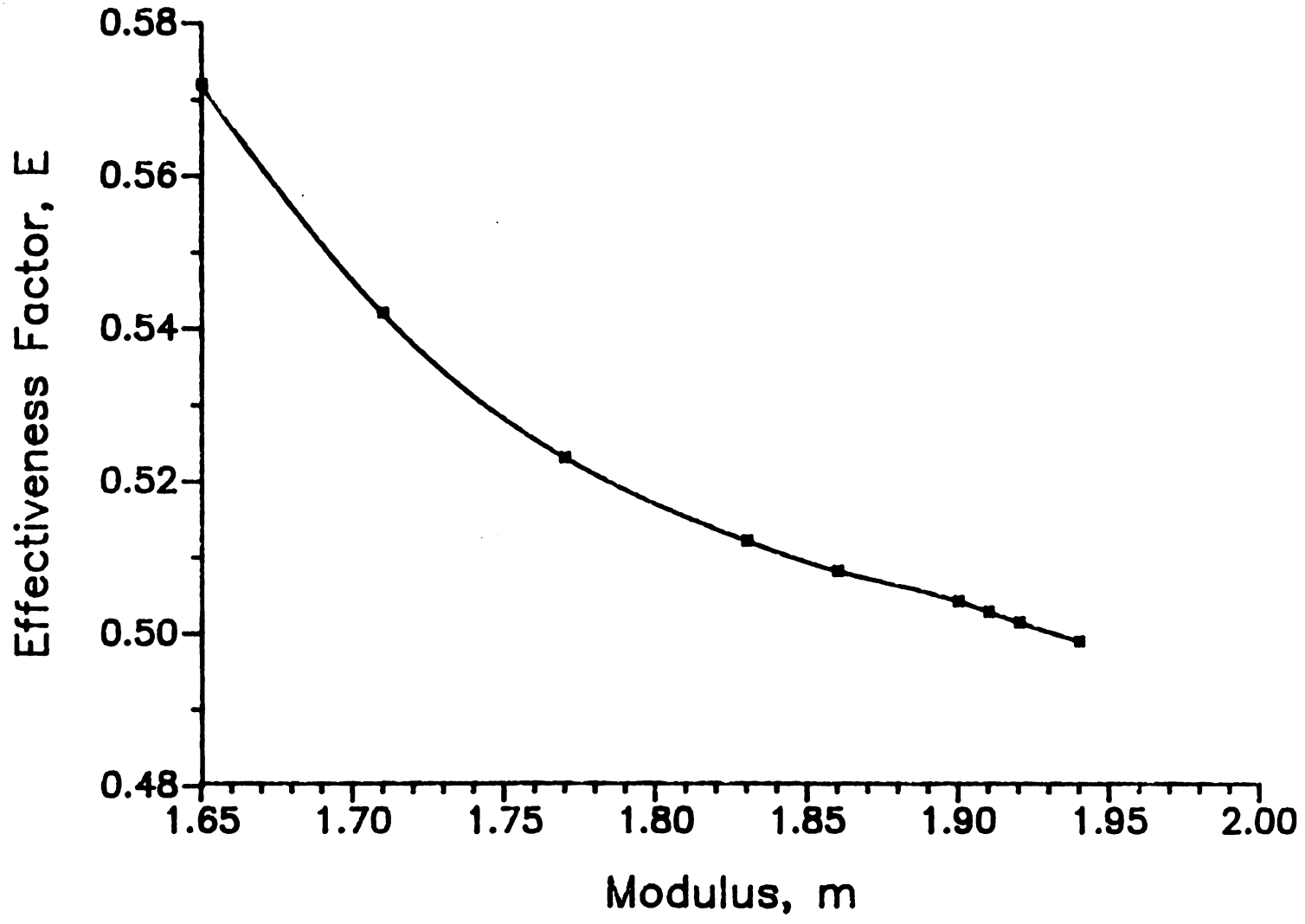

Figure 24— effectiveness factor vs. modulus for SFR(L = 44.0 cm) at optimum loading conditions.

of enzyme to the substrate and would increase K_m. In addition, the decrease in kinetics could be caused by the compaction of protein caused by backflush loading.

The diffusivity of amino acids in free solution has been reported to be on the order of 10^{-6} cm^2/sec [49-51]. The difference between the reported value and the one found from these experiments may be due to an interaction between the positively charged lysine molecule and the polyamide membrane or due to the diffusion of lysine in a polymeric (protein) solution. Work conducted for this thesis did not include the evaluation of the diffusivity of amino acids across the membrane.

In addition to giving important insights into the mode (diffusion-limited, reaction-limited, mixed) of reactor operation, the kinetic parameters may also be used to model the reactor system. The hollow fiber cartridge system can be modelled as a batch reactor in which the feed stream is recycled through the cartridge until a desired conversion is achieved. The rate of lysine conversion in the reactor may be modelled as follows:

$$\text{Rate of lysine conversion} = \frac{V_{res}}{n[e] \cdot A} \cdot \frac{dS}{dt} = -E\left[\frac{k \cdot S}{S + K_m}\right] \qquad (29)$$

where V_{res} is the volume of the reservoir, n is the total number of fibers in the cartridge and the intrinsic immobilized kinetics in the right hand parentheses are multiplied by the effectiveness factor, E, to describe the overall kinetics of the reactor. The enzyme concentration loaded per unit surface area of hollow fiber is represented by the term [e] (mol/cm^2), S is the bulk lumen concentration, and A is the total fiber surface area in

contact with the substrate solution. This expression is rearranged and integrated in the following form:

$$\int_{s_o}^{s} \frac{dS}{-E\left[\frac{k \cdot S}{[s] + K_m}\right]} = \frac{n\,[e]\cdot A}{V_{feed}} \int_0^t dt \qquad (30)$$

The integration is carried out from s_o = 0.2 mM to the final concentration dictated by the desired conversion of lysine, e.g. s = 0.1 mM for 50% conversion or s = 0.05 mM for 75% conversion. The right hand side of the equation, the design time, is a grouping of design variables and constants. Depending on what in the process is fixed and/or known, the remaining variables may be calculated directly from the integrated results using the immobilized intrinsic kinetics of the SFR found as described earlier. The design curve is shown in Figure 25. In constructing this curve, the values of the K_m, k, and D_s that were used were 7.0 mM, 320 min^{-1}, and 1.5 x 10^{-7} cm^2/sec, respectively. From this plot, it is seen that the design time needed to achieve 50% conversion is 0.021. This means that if a cartridge containing 62 fibers in which [e] = 3.63 x 10^{-4} mol/cm^2 and A = 12.59 cm^2 was used, 1,000 ml of plasma could be processed to 50% conversion in 153 minutes.

The experiments conducted in the next chapter were used to determine whether the information obtained from the SFR could be scaled up. If so, the conversions of lysine obtainable in a hollow fiber cartridge could be predicted using the design time data presented above. Similarly, if a given conversion was required for a fixed amount of substrate solution, the design time could also be used to determine the required cartridge surface area, i.e. the number of cartridges needed in parallel.

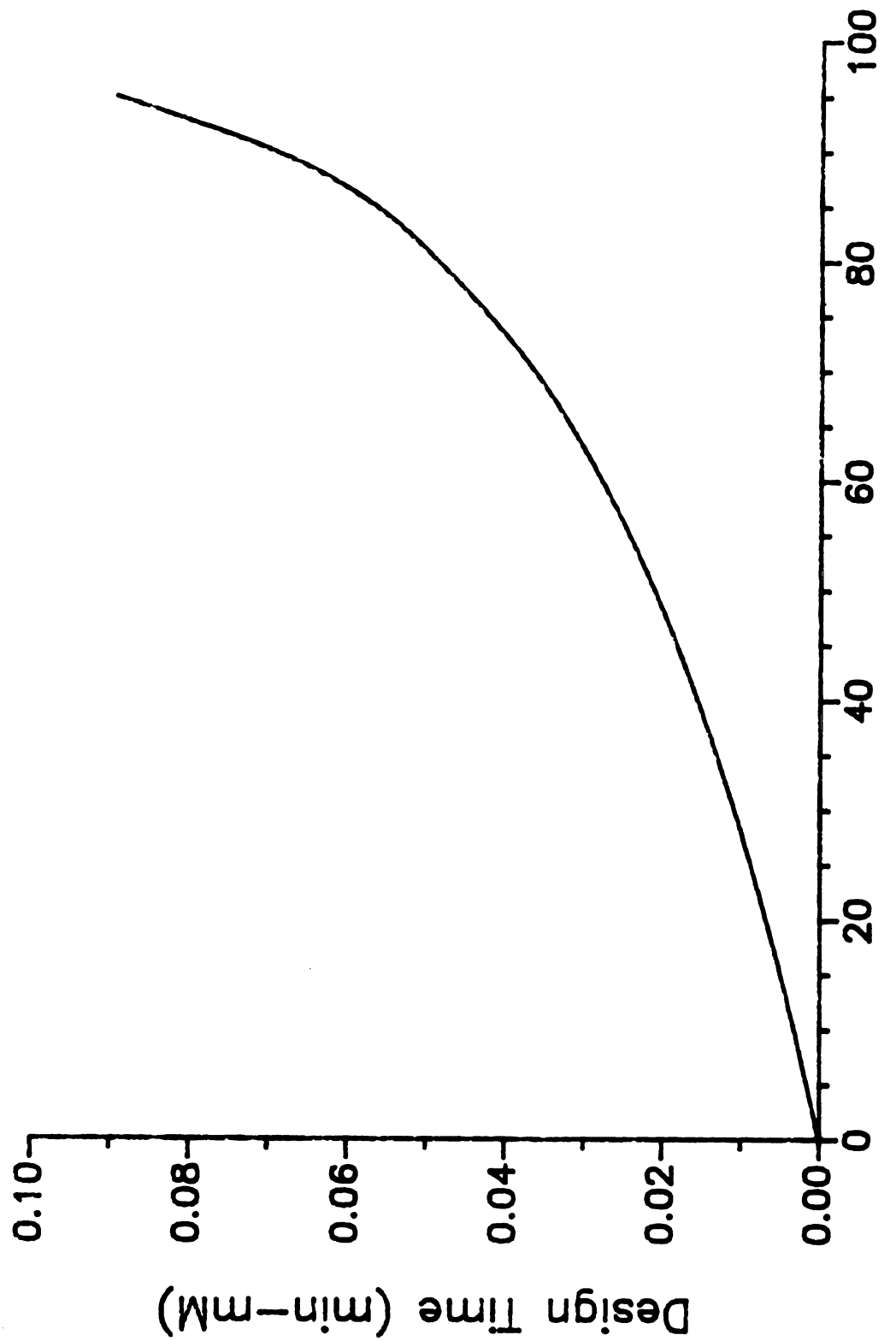

Figure 25– design time vs. % conversion of lysine for the single fiber reactor

CHAPTER 7

SCALE-UP

Motivation

The experiments conducted in the previous chapters were used to obtain important information on the charateristics of a lysine α-oxidase/catalase system within single fiber reactors. However, in order for such a reactor system to have practical applications, a larger hollow fiber cartridge must be used. It was therfore important to determine whether the data obtained for SFRs were consistent with hollow fiber cartridge performance.

A PA10 research cartridge was obtained from Romicon, Inc., and replaced the single fiber reactor in the system shown in Figure 14. The cartridge had a total fiber surface area of 1.1 ft^2 and consisted of 62 hollow fibers arranged in parallel. Cleaning and sanitizing the cartridge was accomplished in the manner described in Chapter 5. The cycles are summarized in the table below:

Table 10
Fiber Cleaning Process

Time	Reagent
30 min	0.7% phosphoric acid solution
15 min	Distilled water
30 min	0.5% potassium hydroxide soln
15 min	Distilled water
20-30 min	200 ppm sodium hypochlorite
15 min	distilled water

Experimental Methods

Backflush loading was used to immobilize the enzyme within the hollow fiber cartridge. The solution for the loading was prepared by mixing 8.5 ml of lysine α-oxidase stock solution, 10.5 ml of catalase stock solution, and 200 ml of 0.1 M potassium phosphate buffer (pH 7.0) in a 250 ml Erlenmeyer flask. This solution was pumped through the cartridge in the backflush mode described in Chapter 4. The effluent was collected in 10 ml fractions. The Lowry method (Chapter 3) was then used to determine the protein concentration of the backflush solution and all the effluent fractions. Results from this assay indicated that 85.4% of the protein loaded was retained by the cartridge. This represents the optimum catalase/oxidase loading ratio and 50% of the optimum amount of lysine α-oxidase loaded per cm^2 of the total fiber surface area in contact with substrate. Half the optimum was used because of the limited supply of enzyme.

The cartridge was placed in a water bath that was kept at a constant 37°C by a submersion heater (Haake E3). One liter of a 0.20 mM lysine solution was also placed in the water bath and kept well mixed by a magnetic stirrer. The lysine solution was pumped through the lumen of the cartridge in recycle mode at a flow rate of 9 ml per minute per fiber in the cartridge. Samples were taken at numerous times and measured for their lysine content using the saccharopine dehydrogenase method described in Chapter 3. A plot of substrate concentration versus time was prepared and is shown in Figure 26. Also shown in this figure is the predicted conversion using data from the SFR and the model described in Chapter 6. It is seen that approximately 190 minutes of operation is required to convert 50% of the lysine whereas the predicted time for 50% conversion is 153 minutes. The main reason that the actual time is longer than the

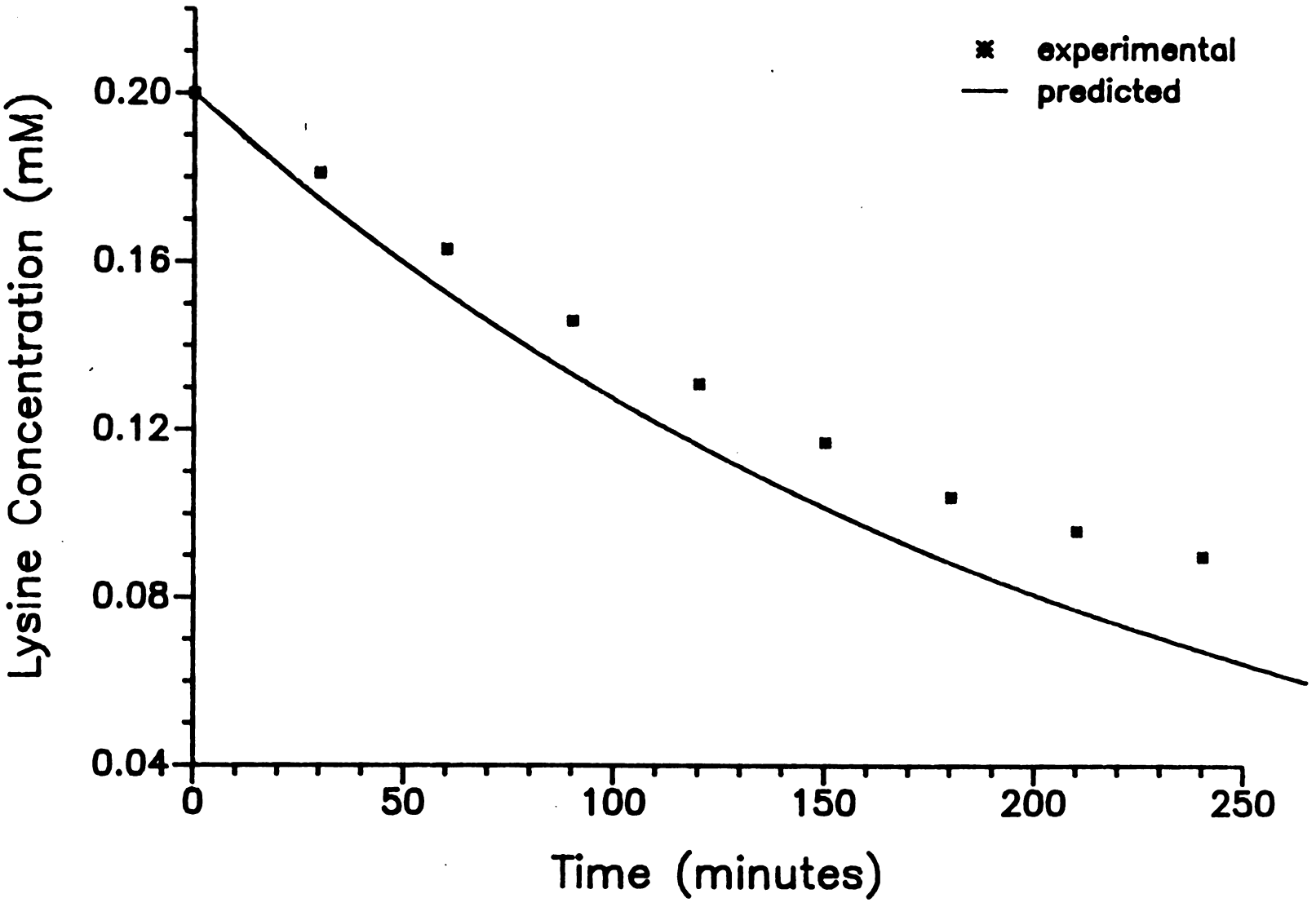

Figure 26– lysine concentration vs. time for the hollow fiber reactor (cartridge)

predicted time may be due to the fact that the model assumes that the operating parameters of each of the fibers in the cartridge are identical. This would be the case if the enzyme was loaded onto the individual fibers, which were then assembled into the cartridge. As described earlier, however, the enzyme solution was backflush loaded onto a cartridge with the fibers already intact. Perfect distribution of enzyme in the fibers of the cartridge is therefore unlikely. Since the amount of L-lysine α-oxidase loaded within a hollow fiber is an important operating parameter (Chapter 6), anything other than perfect distribution can affect the performance of the reactor.

In order to model the hollow fiber cartridge, the immobilized enzyme kinetics were evaluated. One liter of a 10.0 mM lysine solution was pumped through the reactor under the same conditions described above. The reactor was operated for a period of 29 hr. A plot of lysine concentration versus time is shown in Figure 27. As was the case with the single fiber reactor, Equations (23-28) (Chapter 6), along with the Patern subroutine (see Appendix), were used to evaluate the immobilized kinetics for the cartridge. Values for the Michaelis constant (K_m), turnover number (k), and diffusion of lysine (D_s) within the cartridge were found to be 7.02 mM, 275.3 min^{-1}, and 1.49 x 10^{-7} cm^2/sec, respectively. The K_m and D_s for the cartridge are similar to those found for the single fiber reactor (Chapter 6). The lower turnover number may be due to the imperfect enzyme distribution within the cartridge. These values were then used to construct the effectiveness factor versus Thiele modulus curve shown in Figure 28.

With the intrinsic immobilized kinetic constants of lysine α-oxidase within the hollow fiber cartridge known, Equation (30) (Chapter 6) was used to construct the design time curve for the cartridge (Figure 29). From

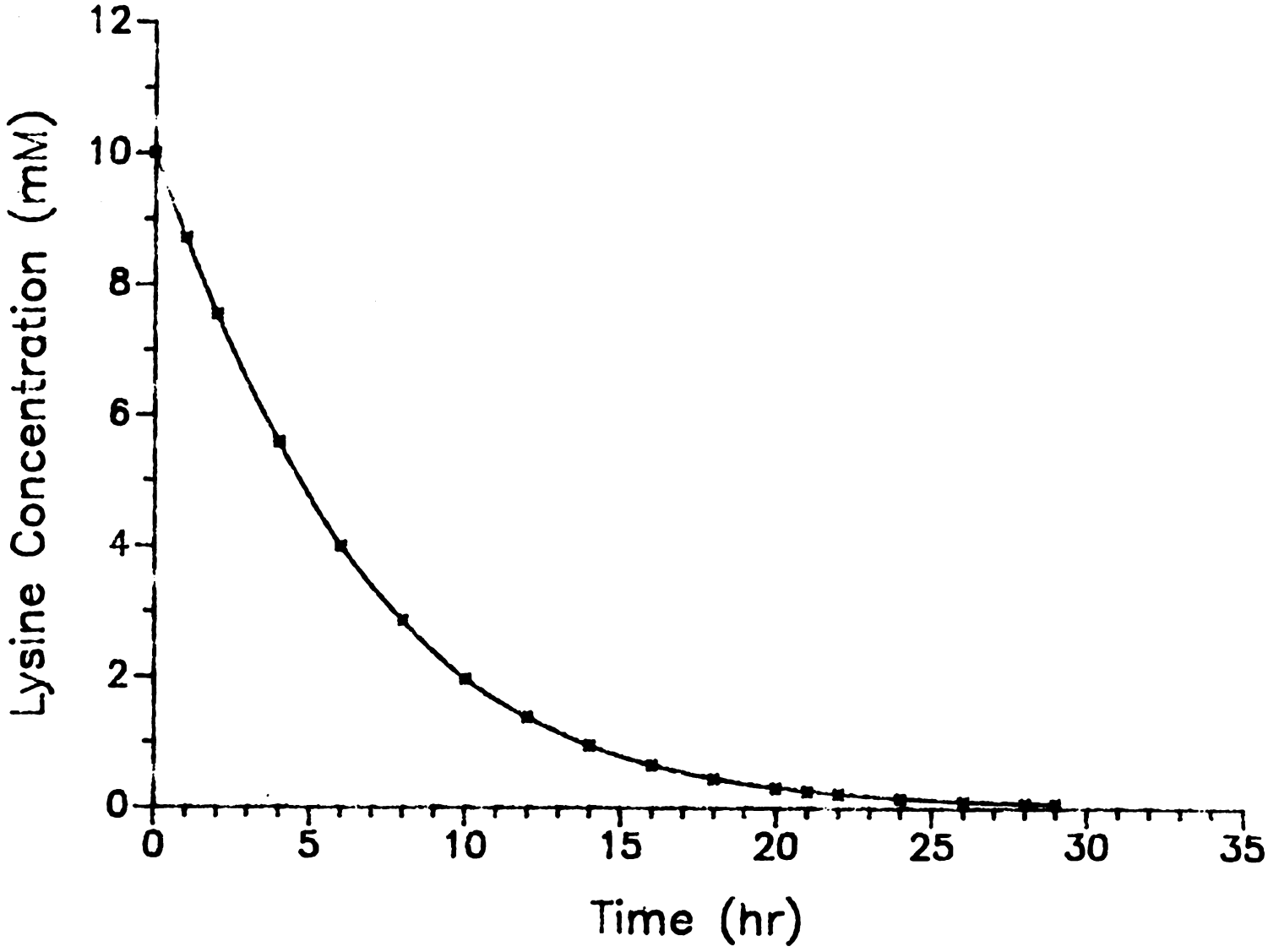

Figure 27— lysine concentration vs. time for the extended use of the hollow fiber cartridge

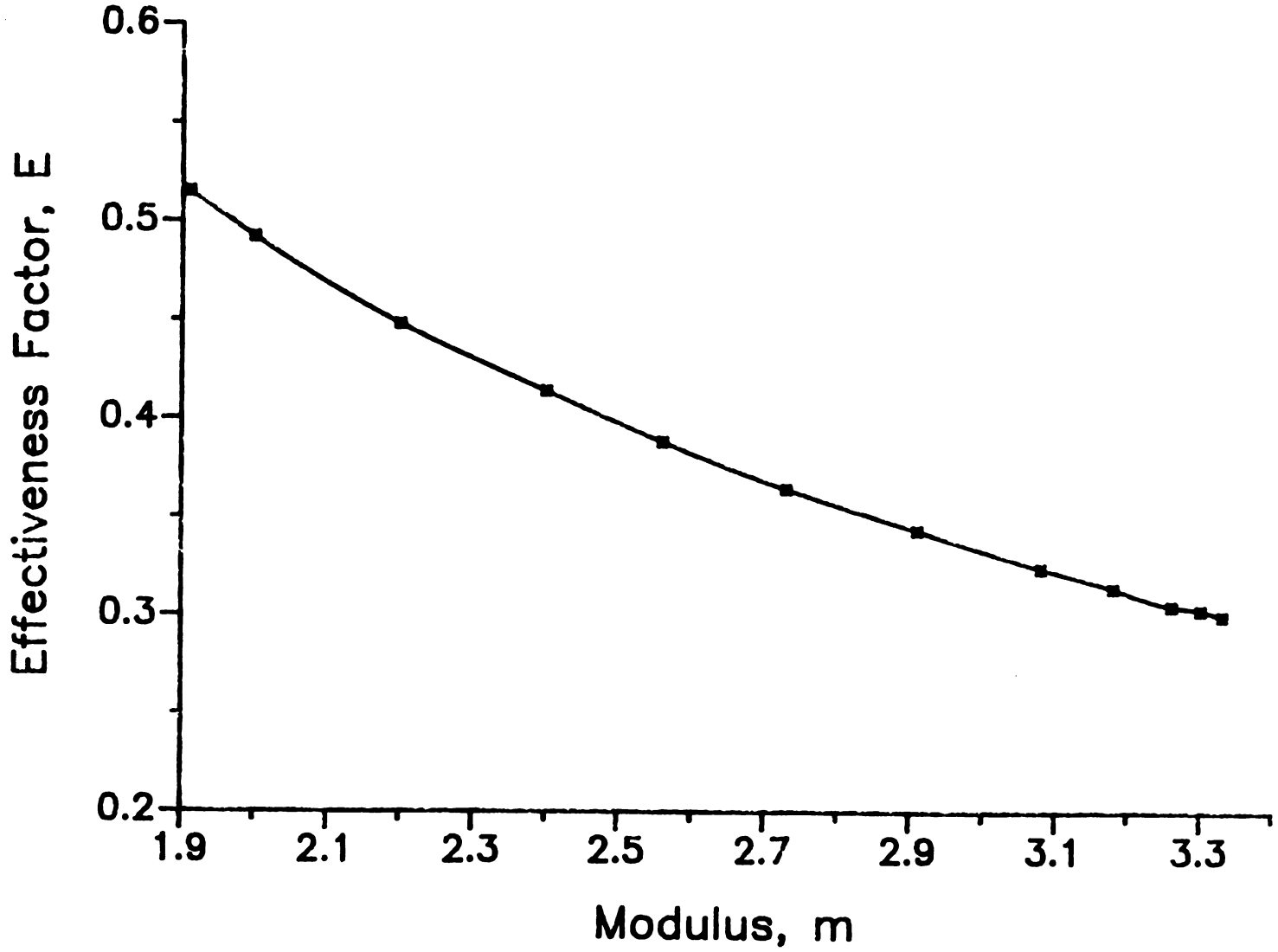

Figure 28– effectiveness factor vs. general modulus for the cartridge

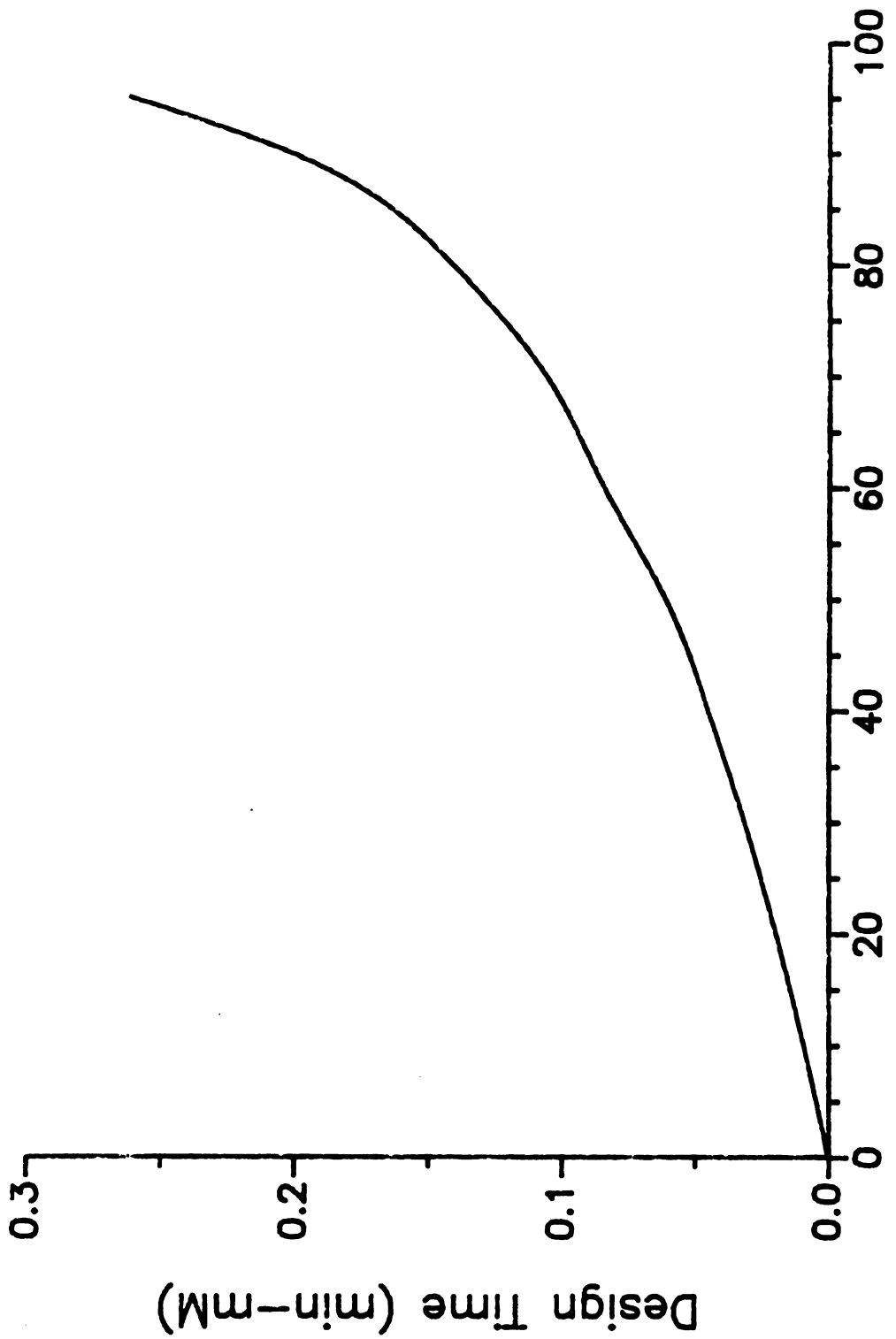

Figure 29— design time vs. % conversion of lysine for the hollow fiber cartridge

this figure, it is seen that the design time to obtain 50% conversion is 0.0601 μmols-min/ml. Therefore, in order to remove 50% of the lysine from 5,000 ml of blood (volume for average adult male) in four hours using devices under the conditions described above, 3.5 cartridges would be required.

As seen from Figure 28, the effectiveness factor for the cartridge in the range of 0.2 mM lysine is approximately 0.30. This means that the reaction within the cartridge is diffusion limited. The effect of pulsatile flow on the conversion of lysine within the hollow fiber cartridge was therefore investigated. The experimental setup was similar to the one in Figure 20 where the cartridge replaced the SFR. Flow rates of 6.0 and 15.0 ml per minute per fiber were used for the two inlet pumps and the outlet pump was adjusted to 12 ml per minute per fiber. Samples were taken every half hour for four hours and measured for lysine concentration using the enzymatic technique described in Chapter 3. Figure 30 shows the conversion of lysine versus time for both the case using normal operation and the case with pulsatile flow. It is seen that after four hours 85.0% of the lysine is converted. Also, with pulsatile flow it took under two hours to reach 55% conversion whereas it took four hours for the same conversion under normal operation. From this information, it can be concluded that the immobilized enzyme reactor/dialyzer would be able to remove almost as much lysine from plasma as injection therapy, and would have the advantage of reuse of the enzymes and no negative immune response from the patient.

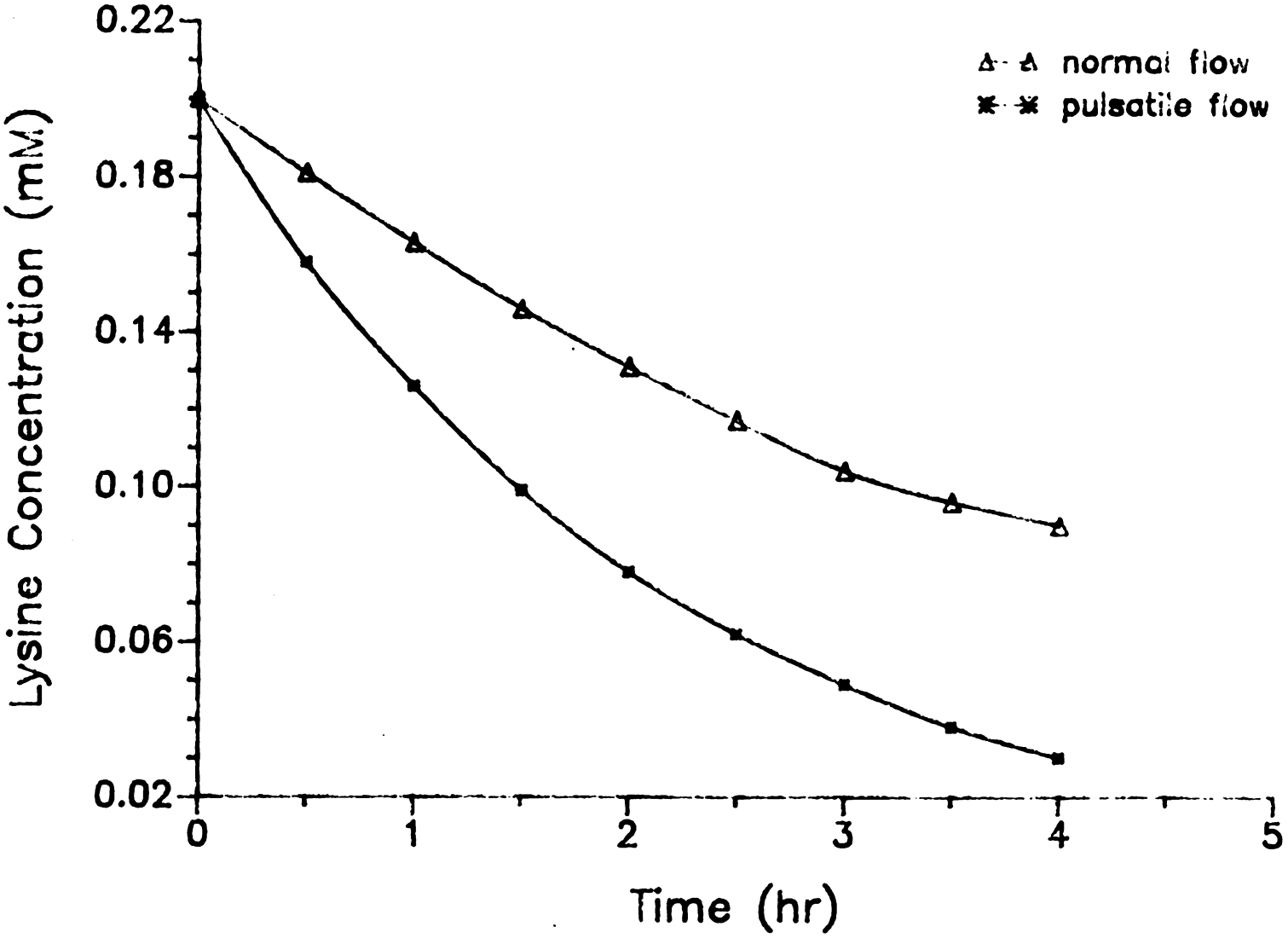

Figure 30– lysine concentration vs. time for the hollow fiber reactor (cartridge)

CHAPTER 8

Conclusions and Recommendations

The overall objective of the research conducted for this thesis was to develop an immobilized enzyme blood dialyzer as a clinical technique for leukemia therapy. An enzyme immobilization technique involving enzyme entrapment in hollow fiber membranes was investigated. The specific problem studied was the possible removal of lysine from the blood of leukemia patients by its conversion with the enzyme L-lysine α-oxidase.

The results of the experiments conducted have shown that enzyme immobilization in hollow fibers provides the capability of retaining and reusing L-lysine α-oxidase and catalase in a reactor system. Several hollow fiber types were evaluated for their compatibility with the enzymes. The polyamide material in the nominal 10,000 molecular weight cut-off range was found to be the most compatible with both enzymes and retained much of the enzyme in an active state during reactor operation. These fibers were obtained from Romicon,Inc..

The kinetics and reactor performance of catalase and lysine α-oxidase have been studied extensively in our laboratory. The reactor configuration used during most of the experiments was the single fiber reactor (SFR) which gave a quantitative understanding of reactor operation.

Enzyme and Reactor Performance

Factorial design logic was used to determine that the important variables that influence the performance of the reactor in converting lysine were flow rate, reactor length, and the amount of both enzymes that were immobilized within the spongy layer of the hollow fiber reactor. Experiments were conducted to find the optimum values for these variables.

These optimum conditions were then used in extended periods of reactor operation (≈ 48 hr) in order to determine the immobilized kinetics of L-lysine α-oxidase in the presence of catalase.

The intrinsic immobilized enzyme kinetics were used in two sets of calculations. In the first group, the design time for both the single fiber reactor and hollow fiber cartridge were determined. The results from this study indicated that fiber surface area was an effective basis for scale-up of the reactor. The second set of experiments were used to calculate the effectiveness factor for the hollow fiber reactor.

Summary of Results

As mentioned in the introduction, this thesis presents initial data for the application of an immobilized enzyme hollow fiber reactor in cancer therapies. The important results include the following:

1) The free solution kinetic parameters of L-lysine α-oxidase were found to be K_m = 0.060 mM and V_{max} = 62.3 μmols/mg-min in the absence of catalase. The K_m and V_{max} values in the presence of a 2/1 ratio of catalase to oxidase were 0.062 mM and 74.9 μmols/mg-min, respectively. No type of inhibition was observed.
2) The polysulfone fibers inactivated catalase during enzyme loading.
3) Polyamide fibers were found to be compatible with both enzymes. Fibers with a molecular weight cutoff of 10,000 retained 85% of the total enzyme that was backflush loaded.
4) Enzyme retention following backflush loading in PA10 fibers was enhanced by repeated use of the fibers.
5) Flow rate, enzyme loading, and reactor length were found to affect conversion of lysine in the SFR. The optimum conditions were determined to be a flow rate of 9 ml/min, 3.97 units of l-lysine α-

oxidase loaded per cm^2 of the fiber's surface area, and a catalase to oxidase loading ratio of 2.5:1. Using a SFR with a length of 44.0 cm, 34.8% of the lysine was converted.

6) L-lysine α-oxidase immobilized in a polyamide SFR retained over 80% of its original activity after 30 days of refrigerated storage. No leakage of enzyme from the fiber wall was noted.

7) At a concentration of lysine equal to that of human plasma (approximately 0.2 mM), the reaction within the spongy layer of the hollow fiber approaches a diffusion controlled regime (Effectiveness factor ≈ 0.65 and 0.3 for the SFR and hollow fiber cartridge, respectively).

8) Pulsatile flow reduced diffusion limitations and gave an increase in conversion of 15% over normal flow conditions.

9) The Michaelis constant (K_m) and the turnover number (k) of immobilized L-lysine α-oxidase were determined to be approximately 7.0 mM and 320 min^{-1}, respectively. The diffusivity of lysine within the lumen of the hollow fiber was found to be 1.5×10^{-7} cm^2/sec.

10) Fiber surface area was used as a basis for scale-up of the reactor. A model using SFR data predicted that 153 minutes of operation would be required to convert 50% of the lysine using a hollow fiber cartridge containing 62 fibers arranged in parallel. The actual time required was 190 minutes.

11) It was found that 85% of the lysine could be converted in four hours by operating the cartridge under pulsatile flow conditions. The ability to remove this much lysine from plasma should have a positive theraputic effect in the treatment of leukemia.

Future Studies

The research program conducted in this thesis consisted of the preliminary set of experiments necessary to develop an understanding of the problems associated with the co-immobilization of an amino acid oxidase and catalase and the conversion of amino acids in hollow fiber reactors. The specific enzyme/amino acid system used was L-lysine α-oxidase and L-lysine, and the results of the study indicated a potential use of an immobilized reactor/dialyzer for the removal of lysine from plasma in cancer therapies.

Before the hollow fiber cartridge discussed in this report could have practical applications, several factors require further investigation. The relatively short residence time in the SFR may not have permitted the development of concentration gradients possible in a longer reactor. As described by Powell [42], the Sherwood numbers in SFRs indicate a lower average mass transfer coefficient in longer fibers. This points to a possible source of error in assuming negligible tube side resistance when scaling up the length of an SFR. When longer reactors are used, experiments should be conducted to determine if mass transfer across the lumen does become a limiting factor. If it does, evaluation of smaller diameter fibers may be desirable.

For the experiments conducted in this thesis, the substrate solution consisted of lysine in buffer. This solution could be considered a Newtonian fluid. However, blood is a complex suspension that is non-Newtonian. Davis and Watson [29] reported that the velocity profile of the solution being pumped through the lumen of the hollow fiber has an effect on the conversion of substrate. Since the velocity profile within the hollow fiber could be different for blood and the buffer, the removal of lysine from whole blood might also be different.

Another factor that might be different in the processing of whole blood is the diffusivity of lysine. It is important to note that in this study, the diffusivity of lysine was treated as a variable that was fitted to experimental data. Future experiments should include permability studies to determine the diffusivity of lysine within the hollow fiber. In addition, the fitted value of the diffusivity of lysine was an order of magnitude less than the reported values of diffusivity of amino acids in free solution. This could be due to an interaction between the positively charged lysine molecule and the polyamide fiber material or due to diffusion through the enzyme solution. The effect of fiber material on the diffusivity of amino acids should also be investigated.

Since blood is a suspension, there may be fouling problems associated with the processing of blood in hollow fiber reactors. Fouling would lead to severe diffusion limitations in the reactor and prevent long term use of the hollow fiber cartridge. Fouling studies should be performed to determine whether steps must be taken to prevent this phenomenon.

Finally, the saccharopine dehydrogenase method for lysine determination described in Chapter 3 was found to be sensitive to the environment of the sample and therefore would probably not be accurate in the determination of lysine in plasma due to the colloidal nature of blood. Other methods for lysine determination should be investigated.

The research conducted so far has given important insights into the potential use of an immobilized enzyme reactor in cancer therapies. It is hoped that future work may be conducted to allow <u>in vivo</u> testing of the hollow fiber device.

APPENDIX

COMPUTER PROGRAMS

The following computer programs were used to determine the intrinsic immobilized kinetic parameters of L-lysine α-oxidase. As described in Chapter 6, three cases were studied. The first two cases used the 21.5 cm long SFR at the optimum and 50% of the optimum enzyme loading conditions, respectively. In the third case the 44.0 cm long SFR was used under optimum conditions. One liter of a 2.0 mM lysine solution was pumped through the lumen of these reactors, and the concentration of lysine in the reservoir was determined at given intervals. The results of these studies were shown in Figures 21-23 of Chapter 6.

The data used to construct these figures were also used to mathematically fit an equation for time (t) as a function of substrate concentration (S). This equation is of the form:

$$t = Vol\ [Q(1) \cdot S + Q(2) \cdot \ln(S)] \qquad \text{(A-1)}$$

where Vol is the volume of the reservoir and Q(1) and Q(2) are constants that fit the data. A correlation coefficient of approximately 0.994 was observed for the fits in all three cases. The derivative of Equation (A-1) with respect to S can be inverted to give the following expression:

$$\frac{dS}{dt} = Vol\left[\frac{S}{Q(1) \cdot S + Q(2)}\right] \qquad \text{(A-2)}$$

Equation (A-2) represents the experimental reaction rate (Rexp). The results for the three cases studied were:

case 1:

Q(1) = 208.33

Q(2) = 833.33

case 2:

Q(1) = 27.30

Q(2) = 1707.20

case 3:

Q(1) = 21,82

Q(2) = 656.25

The computer programs were then established to use the experimentally obtained reaction rates to fit the intrinsic immobilized Michaelis constant, turnover number, and diffusivity of lysine to the given model (Equations (23-28 of Chapter 6). The main program sets the initial values for these parameters and calls both the Patern and Calc subroutines. Patern minimizes a cost function by adjusting the values of the parameters being fitted. Calc uses Equations (23-28) to determine a calculated reaction rate (R) and then defines the cost function to be the sum of the square of the residuals between the calculated and experimental reaction rates. Figures A1 through A3 show the comparison between the calculated and experimental reaction rates for the three cases. It is seen that the greatest disparities occur at the higher lysine concentrations, or small conversions. Even at these concentrations, the largest difference in the calculated reaction rate was less than 8%. This indicates that the model, and therefore the fit parameters, were very accurate in describing the reactor system under investigation.

```
C             THIS FILE IS THE MAIN PROGRAM WHICH INITIATES
C       THE PATERN SEARCH ROUTINE BY CALLING PATERN.  IT ALSO
C       CONTAINS THE INITIAL VALUES OF THE PARAMETERS AND
C       OTHER FORMATTING INSTRUCTIONS FOR PATERN.  THE DATA
C       TO BE FIT BY A TRANSFER FUNCTION ARE THE INPUT (U)
C       AND THE OUTPUT (X) VALUES.
C
C
C
      DIMENSION P(1000), STEP(1000)
C
C     SET INITIAL CONDITIONS AND INITIAL SEARCH PARAMETERS
      P(1) = 6.0
      P(2) = 300.0
      P(3) = 1.5E-7
      STEP(1) = 1
      STEP(2) = 1
      STEP(3) = 0.1E-7
      IO = 2
      NP = 3
C     MPASS = 3
      NRD = 3
C
C     CALL PATERN(NP,P,STEP,NRD,IO,COST)
      CALL PATERN(NP,P,STEP,NRD,IO,COST)
C
      STOP
      END
C
C     THIS FILE IS A PAIR OF SUBROUTINES WRITTEN TO BE
C     COMPATIBLE WITH THE OPTIMIZATION SUBROUTINE PATTERN.
C     THEY SIMULATE A PROCESS USING DISCRETE DIFFERENCE
C     EQUATIONS AND COMPARE THE SIMULATION OUTPUT WITH
C     THE ACTUAL OUTPUT (READ IN THROUGH A DATA FILE),
C     CALCULATING AN ERROR OR A "COST" ASSOCIATED WITH THAT
C     SIMULATION.  PATTERN USES THESE SUBROUTINES ITERATIVELY
C     IN ORDER TO FIND THE OPTIMUM SET OF TRANSFER FUNCTION
C     PARAMETERS TO FIT THE DATA.
C
      SUBROUTINE PROC(P,COST)
      DIMENSION P(1000),STEP(1000)
C
C     INITIALIZE ARRAYS AND DEFINE PARAMETERS
C
C      aKm = P(1)
C      Ek  = P(2)
C      Ds  = P(3)
C      DELT = 1.
      COST = 0.0
C
C     PERFORM SIMULATION AND CALCULATE ERROR
C
      CALL CALC(P,COST)
      RETURN
      END
C
C
C
      SUBROUTINE BOUNDS(P,IOUT)
      DIMENSION P(1000),STEP(1000)
      IOUT = 0
      IF (P(1) .LT. 0.) IOUT = 1
      IF (P(2) .LT. 0.) IOUT = 1
      IF (P(3) .LT. 0.) IOUT = 1
      RETURN
      END
```

```
      SUBROUTINE PATERN(NP,P,STEP,NRD,IO,COST)
C-----THE SIZE OF B1,B2,T,AND S NEED ONLY BE EQUAL TO THE NUMBER OF PAR
      DIMENSION P(1000),STEP(1000),B1(100),B2(100),T(100),S(100)
C-------------------------------------------------------------
C       THE FOLLOWING COMMAND ALLOWS PATERN TO USE AN INTEGER
C       VARIABLE AS THE THIRD PARAMETER P(3).
C
C       NSRC    =3
C       P(NSRC) =       IFIX(P(NSRC))
C-------------------------------------------------------------
C-----STARTING POINT
      L=1
      ICK=2
      ITTER=0
      DO5 I=1,NP
      B1(I)=P(I)
      B2(I)=P(I)
      T(I)=P(I)
  5   S(I)=STEP(I)*10.
C-----INITIAL BOUNDARY CHECK AND COST EVALUATION
      CALL BOUNDS(P,IOUT)
      IF(IOUT.LE.0)GOTO10
                  IF(IO.LE.0)GOTO6
                  WRITE(05,1005)
                  WRITE(05,1000)(J,P(J),J=1,NP)
  6   RETURN
 10   CALL PROC(P,C1)
                  IF(IO.LE.0)GOTO11
                  WRITE(05,1001)ITTER,C1
                  WRITE(05,1000)(J,P(J),J=1,NP)
C--------BEGINNING OF PATTERN SEARCH STRATEGY
 11   DO99 INRD=1,NRD
      DO12 I=1,NP
 12   S(I)=S(I)/10.
C-------------------------------------------------------------
C       S(NSRC) =       1.0001
C-------------------------------------------------------------
                  IF(IO.LE.0)GOTO20
                  WRITE(05,1003)
                  WRITE(05,1000)(J,S(J),J=1,NP)
 20   IFAIL=0.0
C-----PRETURBATION ABOUT T
      DO30 I=1,NP
      IC=0
 21   P(I)=T(I)+S(I)
      IC=IC+1
      CALL BOUNDS(P,IOUT)
      IF(IOUT.GT.0)GOTO23
      CALL PROC(P,C2)
                  L=L+1
                  IF(IO.LT.3)GOTO22
                  WRITE(05,1002)L,C2
                  WRITE(05,1000)(J,P(J),J=1,NP)
 22   IF(C1-C2)23,23,25
 23   IF(IC.GE.2)GOTO24
      S(I)=-S(I)
      GOTO21
 24   IFAIL=IFAIL+1
      P(I)=T(I)
      GOTO30
 25   T(I)=P(I)
      C1=C2
 30   CONTINUE
      IF(IFAIL.LT.NP)GOTO35
      IF(ICK.EQ.2)GOTO90
      IF(ICK.EQ.1)GOTO35
```

```
      CALL PROC(T,C2)
                  L=L+1
                  IF(IO.LT.2)GOTO31
                  WRITE(05,1002)L,C2
                  WRITE(05,1000)(J,T(J),J=1,NP)
 31   IF(C1-C2)32,34,34
 32   ICK=1
      DO33 I=1,NP
      B1(I)=B2(I)
      P(I)=B2(I)
 33   T(I)=B2(I)
      GOTO20
 34   C1=C2
 35   IB1=0
      DO39 I=1,NP
      B2(I)=T(I)
      IF(ABS(B1(I)-B2(I)).LT.1.0E-20)IB1=IB1+1
 39   CONTINUE
      IF(IB1.EQ.NP)GOTO90
      ICK=0
                  ITTER=ITTER+1
                  IF(IO.LT.2)GOTO40
                  WRITE(05,1001)ITTER,C1
                  WRITE(05,1000)(J,T(J),J=1,NP)
C-----ACCELERATION STEP
 40   SJ=1.0
      DO45 II=1,11
      DO42 I=1,NP
      T(I)=B2(I)+SJ*(B2(I)-B1(I))
C-------------------------------------------------------------------
C       IF(I.EQ.NSRC)T(I)=IFIX(T(I))
C-------------------------------------------------------------------
 42   P(I)=T(I)
      SJ=SJ-.1
      CALL BOUNDS(T,IOUT)
      IF(IOUT.LT.1)GOTO46
      IF(II.EQ.11)ICK=1
 45   CONTINUE
 46   DO47 I=1,NP
 47   B1(I)=B2(I)
      GOTO20
 90   DO91 I=1,NP
 91   T(I)=B2(I)
 99   CONTINUE
      DO100 I=1,NP
100   P(I)=T(I)
      COST=C1
                  IF(IO.LE.0)RETURN
                  WRITE(05,1004)L,C1
                  WRITE(05,1000)(J,P(J),J=1,NP)
      RETURN
1000  FORMAT(3(35X,I7,5X,E13.6/))
1001  FORMAT(//1X13HITERATION NO.  ,I5/5X,5HCOST= ,E15.6,20X,
     1   10HPARAMETERS)
1002  FORMAT(10X3HNO.,I4, 8X5HCOST=,E15.6)
1003  FORMAT(/1X28HSTEP SIZE FOR EACH PARAMETER   )
1004  FORMAT(1H113HANSWERS AFTER ,I3,2X,23HFUNCTIONAL EVALUATIONS   //
     1   5X5HCOST=,E15.6,20X,18HOPTIMAL PARAMETERS  )
1005  FORMAT(1H135HINITIAL PARAMETERS OUT OF BOUNDS        )
      END
```

```
C
C
      SUBROUTINE CALC(P,COST)
C
C     Determine inhibited enzyme reaction Thiele modulus from
C     Kinetic and diffusion parameters and determine effectiveness factor
C     from Moo-Young and Kobayashi approximation.  Use of this model
C     to predict reaction rates for various concentrations of lysine.
C
      DIMENSION Q(10),P(100)
      open (60,file='rate.dat.',status='old')
C     INITIALIZE VALUES; Q(1) and Q(2) are parameters that fit the
C     experimental data and EO is the micromoles of enzyme loaded.
      Q(1) = 208.33
      Q(2) = 833.33
      EKM = P(1)
      EK = P(2)
      DS = P(3)
      VOL = 1000.
      EO = 0.004464
      VMAX = EK*EO
      COST = 0.0
C     READ DATA AND CALCULATE MODULUS AND EFFECTIVENESS FACTOR
      DO50J=1,24
      READ (60,*) S
C     CALCULATE GENERAL MODULUS
            L = 0.1
            B = EKM/S
            X = ((S*L)/(S+EKM))*(VMAX/(120*DS))**0.5
            Y = (VOL*(S+EKM*ALOG(EKM/(EKM+S)))**0.5
            TM = X/Y
            IF (TM.GE.0.AND.TM.LE.1)THEN
              E = 1.0
            ELSE
              E = 1/TM
            END IF
      EFF = (E + B*TANH(TM)/TM)/(1+B)
      R =(EFF*VMAX*S)/(S+EKM)
      REXP = VOL*(S/(Q(1)*S+Q(2)))
      COST = COST + ABS((R-REXP)**2)
50    CONTINUE
      CLOSE (60)
      RETURN
      END
```

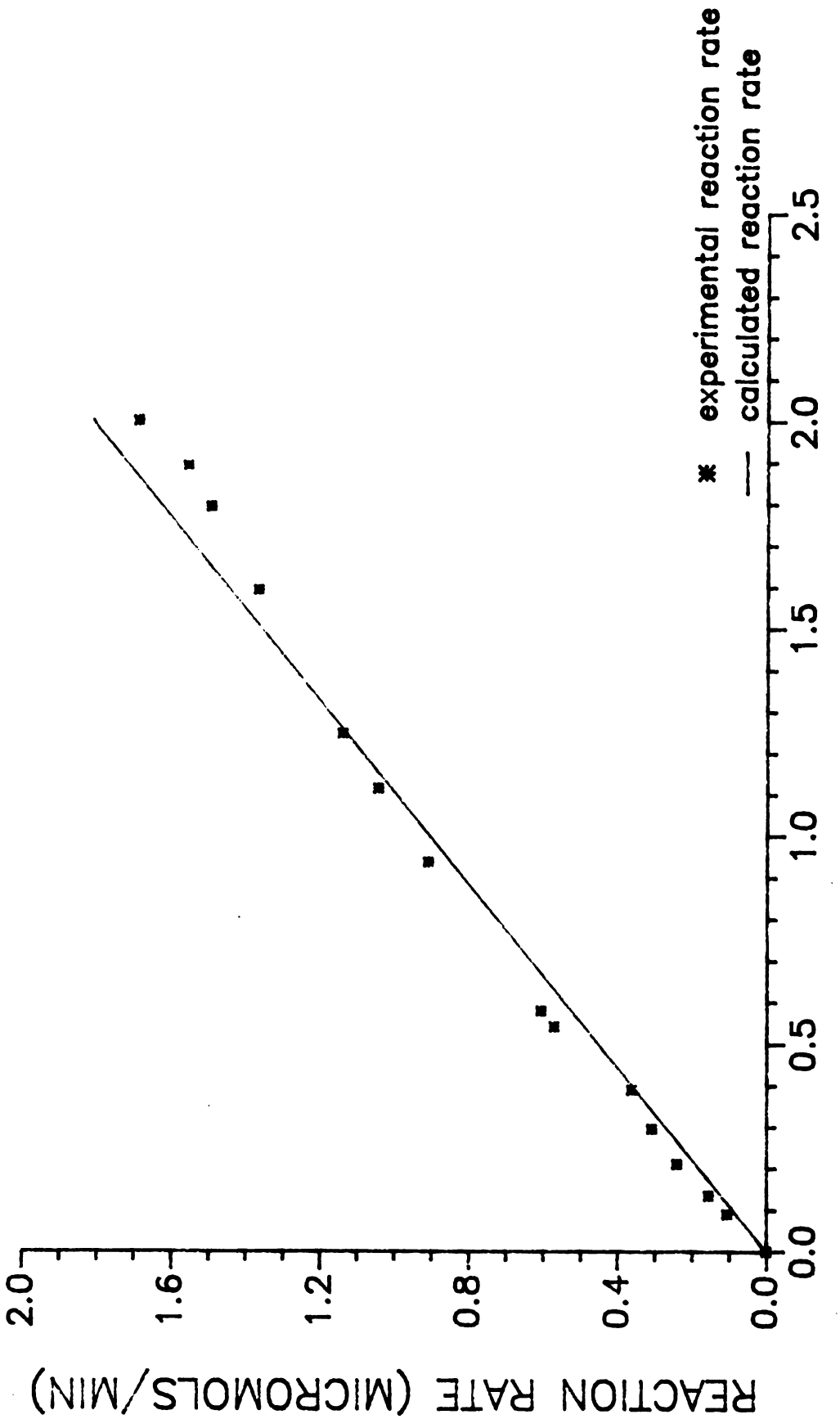

Figure A1— reaction rate vs. substrate concentration for case 1 (Chapter 6)

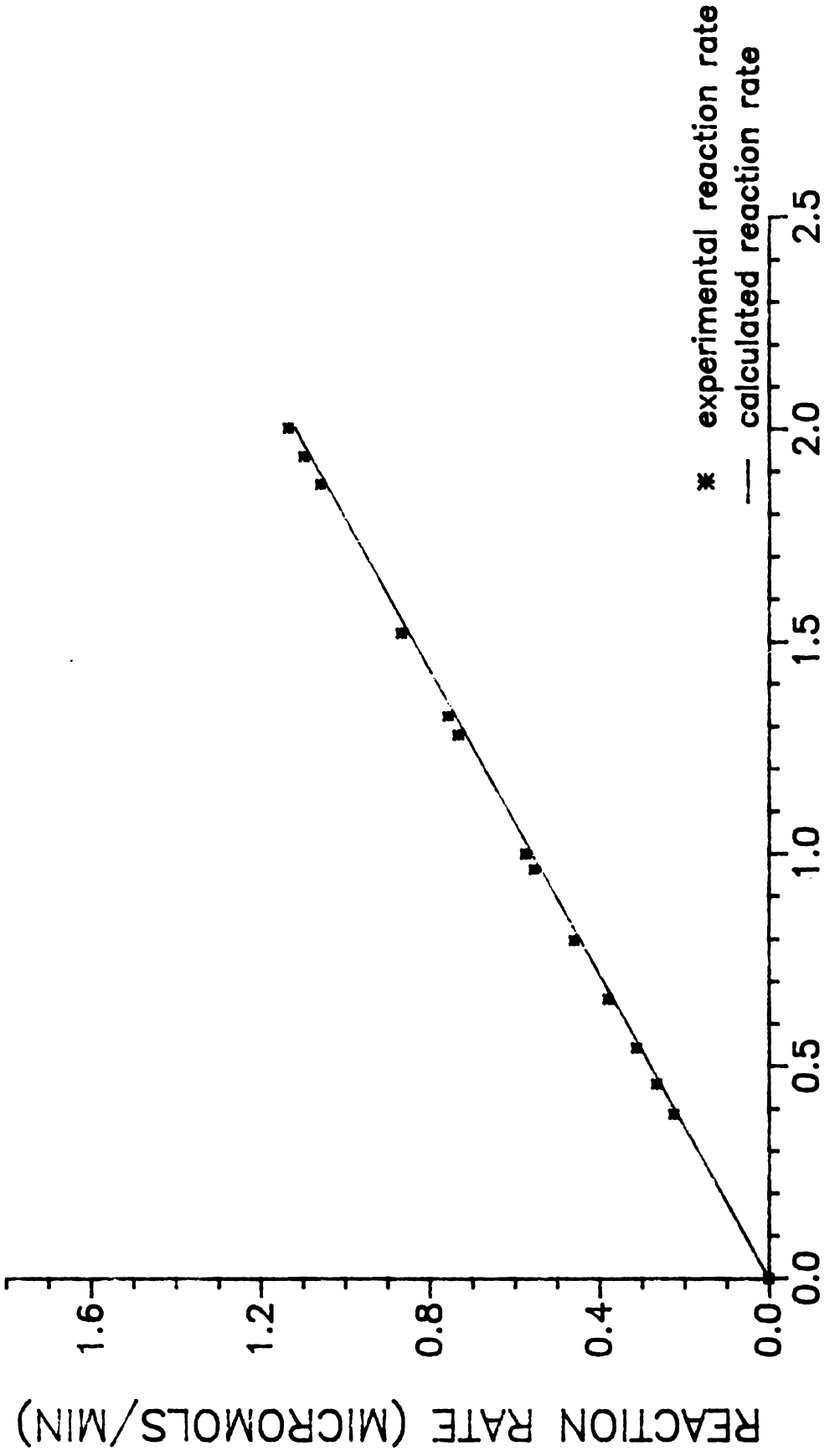

Figure A2— reaction rate vs. substrate concentration for case 2 (Chapter 6)

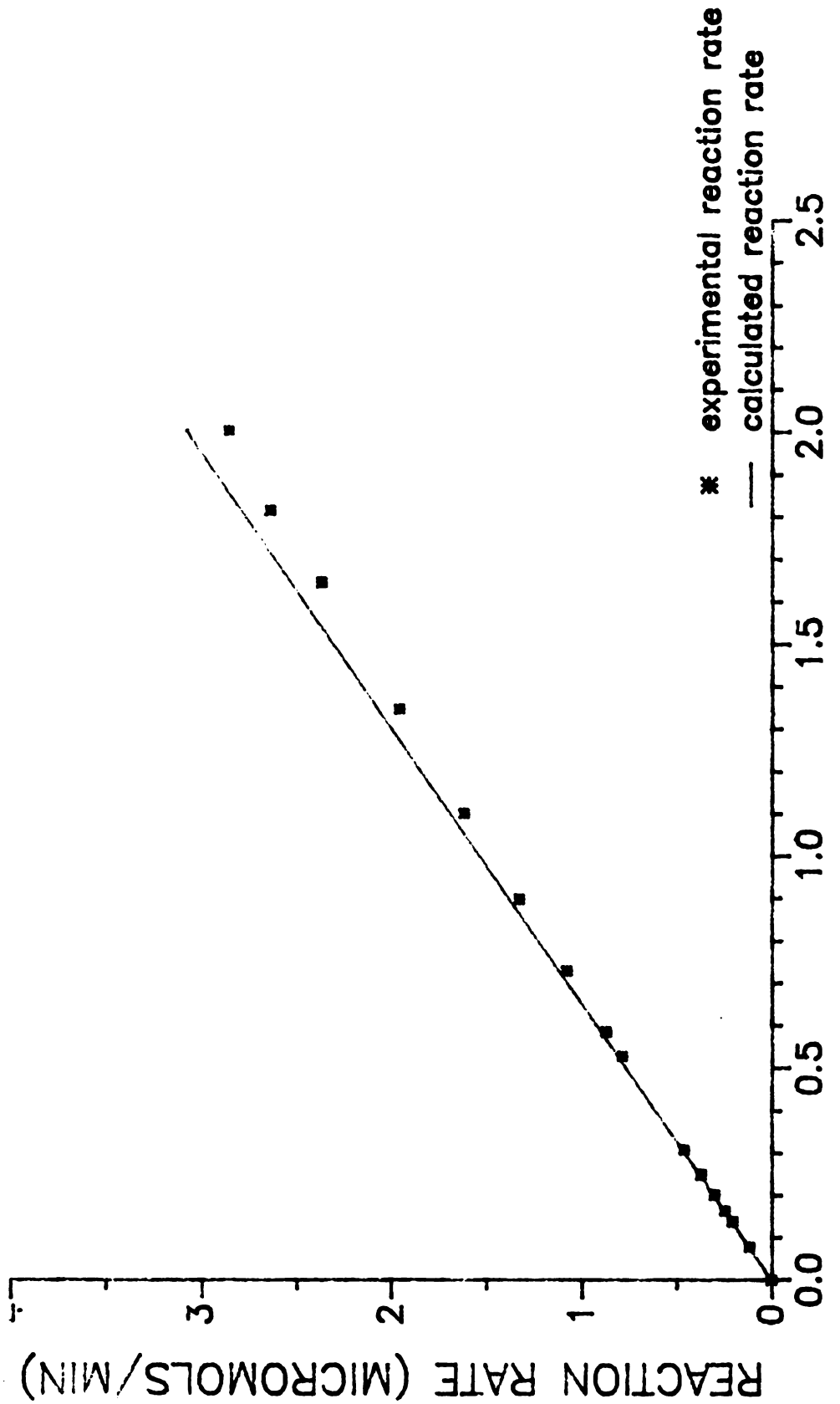

Figure A3— reaction rate vs. substrate concentration for case 3 (Chapter 6)

LIST OF REFERENCES

List of References

1. Freese, E.G., J. Gerson, H. Taber, H.J. Rhaese, and E. Freese, Mutat. Res., 4, 517 (1967).

2. Dimitrov, N.V., J. Hansz. M.A. Toth, and B. Bartolotta, Blood, 38, 638 (1971).

3. Regan, J.D., N. Vodopick, S. Takeda, W.H. Lee, and F.M. Faulcon, Science, 163, 1452 (1969).

4. Horowitz, B., B.K. Madras, A. Meister, L.J. Old, E.A. Bovse, and E. Stockert, Science, 160, 533 (1968).

5. Kreis, W. and C. Hession, Cancer Res., 33, 1866 (1973).

6. Weinberg, A. and Y. Becker, Exptl. Cell Res., 60, 470 (1970).

7. Iyer, G.Y.N., J. Lab. Clin. Med., 54, 229 (1959).

8. McMenamy, R.H., C.C. Lund, G.J. Neville, and D.F.H. Wallach, J. Clin. Invest., 39, 1675 (1960).

9. McMenamy, R.H., C.C. Lund, and D.F.H. Wallach, J. Clin. Invest., 39, 1688 (1960).

10. Kusakabe H., K. Kodama, A. Kuninaka, H. Yoshino, and K. Soda, Agric. Biol. Chem., 44, 387 (1980).

11. Sugimura, T., S.M. Birnbaum, M. Winitz, and J.P. Greenstein, Arch. Biochem. Biophys., 81, 439 (1959).

12. Abell, C.W., W.J. Stith, and D.S. Hodgins, Cancer Res., 32, 285 (1972).

13. Abell, C.W., D.S. Hodgins, and W.J. Stith, Cancer Res., 33, 2529 (1973).

14. Greenfield, R.S. and D. Wellner, Cancer Res., 37, 2523 (1977).

15. Adamson, R.H. and S. Fabro, Cancer Chemother. Res., 32, 2114 (1972).

16. Private communication, Dr. M. Zile, Department of Food Science and Human Nutrition, Michigan State University.

17. Kodama, K., H. Kusakabe, A. Kuninaka, H. Yoshino, H. Misono, and K. Soda, J. Biol. Chem., 255, 976 (1980).

18. Machida, H., H. Kusakabe, K. Kodama, Y. Midorikawa, A. Kuninaka, H. Misono, and K. Soda, Agric. Biol. Chem., 43, 337 (1979).

19. Waterland, L.R., C.R Robertson, and S. Michaels, Chem. Eng. Commun., 2, 37 (1975).

20. Breslau, B.R. and B.M. Kilcullen, pp. 179-190, in Enzyme Engineering, Vol 3, E.K. Pye and H.H. Weetall, eds., Plenum Press, NY, 1978.

21. Chambers, R.P., W. Cohen, and W.H. Baricos, Methods in Enzymology XLIV: Immobilized Enzymes, 291 (1976).

22. Kleinstreuer, C. and T. Poweigha, Advances in Biochemical Engineering/Biotechnology, 30, 91 (1984).

23. Waterland, L.R., S. Michaels, and C.R Robertson, AIChE J., 20, 50 (1974).

24. Kim, S.S. and D.O. Cooney, Chem. Eng. Sci., 31, 289 (1976).

25. Lewis, W. and S. Middleman, AIChE J., 20, 1012 (1974).

26. Webster, I.A. and M.L. Shuler, Biotechnol. Bioeng., 23, 447 (1981).

27. Webster, I.A. and M.L. Shuler, Biotechnol. Bioeng., 20, 1541 (1978).

28. Webster, I.A., M.L. Shuler, and P.R. Rony, Biotechnol. Bioeng., 21, 447 (1979).

29. Davis, M.E. and L. Watson, Biotechnol. Bioeng., 27, 182 (1985).

30. Chambers, R.P., W. Cohen, and W.H. Baricos, Methods in Enzymology XLIV: Immobilized Enzymes, 291 (1976).

31. Box, G.E.P., W.G. Hunter, and J.S. Hunter, Chapter 10, in Statistics for Experimenters, Wiley and Sons, NY, 1978.

32. Lowry, O.H., N.J. Rosebriogh, A.L. Farr, and R.J. Randall, J. Biol. Chem., 193, 265 (1951).

33. Nakatani, Y., M. Fujioka, and K. Higashino, Anal. Biochem., 49, 225 (1972).

34. Nakatani, Y. and M. Fujioka, Eur. J. Biochem., 16, 180 (1970).

35. Ogawa, H., and M. Fujioka, J. Biol. Chem., 253 (1978).

36. Chance, B. and D. Herbert, Biochem. J., 46, 402 (1950).

37. Stryer, L., Chapter 6, in Biochemistry, W,H. Freeman and Company, NY, 1981.

38. Bailey, J.E., and D.F. Olis, pp 105, Biochemical Engineering Fundamentals, second ed., McGraw-Hill Book Company, NY, 1986.

39. Wilkinson, G.N., Biochem. J., 80, 324 (1961).

40. Abe, K., N. Makino, and F.K. Anan, J. Biochem., 85, 473 (1979).

41. Goodwin, T.W. and R.A. Morton, Biochem. J.,40, 628 (1946).

42. Powell, A., M.S. Thesis, Michigan State University, 1988.

43. Personal communication, P. McMahon, M.S. student in Department of Chemical Engineering, Michigan State University.

44. Kim, I.H. and H.N. Chang, AIChE J., 29, 910 (1983).

45. Kim, I.H. and H.N. Chang, AIChE J., 29, 645 (1983).

46. Park, T.H., I.H. Kim, and H.N. Chang, Biotechnol. Bioeng., 27, 1185 (1985).

47. Bischoff, K.B., AIChE J., 11, 351 (1965).

48. Moo-Young, M. and T. Kobayashi, Canadian J. Chem. Eng., 50, 162 (1972).

49. Cohn, E.J. and J.T. Edsall, PP 410-412, in Proteins, Amino Acids, and Peptides as Ions and Dipolar Ions, Reinhold Publishing Corporation, NY, 1943.

50. Polson, A., Biochem. J., 31, 1903 (1937).

51. Annetts, M., Biochem. J., 30, 1807 (1936).

General References

Beers, R.F. and I.W. Sizer, J. Biol. Chem., 195, 133 (1952).

Grunwald, J. and T.M.S. Chang, Int. J. Art. Organs, 4, 82 (1981).

Hardisty, R.M. and P.J. Weatherall, Blood and Its Disorders, Blackwell Scientific Publications, Oxford, 1974.

Herbert, D. and J. Pinsent, Biochem. J., 43, 193 (1948).

Kleinstreuer, C. and S.S. Agarwal, Biotechnol. Bioeng., 28, 1233 (1986).

Knob, R., M.S. Thesis, Michigan State University, 1988.

Kusakabe H., K. Kodama, H. Machida, and A. Kuninaka, Agric. Biol. Chem., 43, 1983 (1979).

Kusakabe H., K. Kodama, A. Kuninaka, H. Yoshino, and K. Soda, Agric. Biol. Chem., 43, 2531 (1979).

Kusakabe H., K. Kodama, A. Kuninaka, H. Yoshino, K. Soda, and M. Sugi, Agric. Biol. Chem., 43, 1371 (1979).

Kusakabe H., K. Kodama, A. Kuninaka, H. Yoshino, and K. Soda, Agric. Biol. Chem., 43, 1749 (1979).

Poznansky, M.J., and T.M.S. Chang, Biochim. Biophys. Acta., 334, 103 (1974).

Rinderknecht, H., Nature, 193, 167 (1962).

Shu, C.D. and T.M.S. Chang, Int. J. Art. Organs, 4, 82 (1981).

Soda, K., Anal. Biochem., 25, 228 (1968).

Soda, K., H. Misona, and T. Yamamoto, Biochemistry, 7, 4102 (1968).

Webster, I.H. and M.L. Shuler, Biotehnol. Bioeng., 21, 1725 (1979).

Webster, I.H. and M.L. Shuler, Tech. Biotecnol., 31, 226 (1981).